Fault Estimation Algorithms: Design and Verification

by

Jinya Su

A doctoral thesis submitted in partial fulfilment of the requirements for the award of the degree of Doctor of Philosophy (PhD) of Loughborough University

July 2016

Control and Reliability Group,
Department of Aeronautical and Automotive Engineering,
Loughborough University, Loughborough,
Leicestershire, UK, LE11 3TU

I dedicate this thesis to my loving parents...

Acknowledgements

I would like to express my deepest gratitude to my supervisor, Prof. Wen-Hua Chen for his constant support in the past years. Firstly, he helped me secure a precious Ph.D position with full studentship. Secondly, he gave me tremendous freedom to pursue a wide range of meaningful research topics and has been training me to be an independent researcher. Thirdly, he offered me a precious Research Associate position in the fourth year, as a consequence, I can concentrate on writing up the thesis and doing amazing research in intelligent vehicle. Last but not the least, as a researcher, his achievements in disturbance observer based control, model predictive control and aeronautical applications always inspire me to move forward.

I would also like to express my deepest gratitude to my co-supervisor, Prof. Baibing Li, for his constant help and supervision during my whole research process. Firstly, his technical support guided me into the field of filtering. Secondly, his timely and periodical encouragement helped me gain courage. Thirdly, he devoted much time and effort to helping me revise and polish papers. His conscientious attitude towards research is a lifelong treasure to cherish.

I am grateful to Dr Sarah Dunnett, who has been monitoring my research progress, evaluating my work, and giving me timely feedback on an annual basis in the past years. She is also kind to be my internal examiner. My gratefulness also goes to Prof. Zi-Qiang Lang, Chair of Complex Systems Analysis and Design in Sheffield University, who kindly acts as my external examiner.

My sincere gratitude goes to Prof. Shihua Li and Dr. Jun Yang in my home university (Southeast University, Nanjing, China) who have guided me into the control area. I do learn a lot from both of them! I am grateful to all of the members of Centre for Autonomous Systems who make it a wonderful place for research. Especially, thank Dr. Cunjia Liu, for his frequent help in my daily life. Beyond that, he also gave me much help in understanding engineering concepts. Our discussion is always inspiring.

I must thank my parents for their endless love and constant support in the past 26 years. I know both of you are very proud of your son. Finally, all the gratitude to my love, Meng Meng, for all the laughter and tears and every single moment we have ever had and will surely have. You have my word.

Jinya Su

July, 2016

Abstract

The research in this thesis is undertaken by observing that modern systems are becoming more and more complex and safety-critical due to the increasing requirements on system smartness and autonomy, and as a result health monitoring system needs to be developed to meet the requirements on system safety and reliability.

The state-of-the-art approaches to monitoring system status are model based Fault Diagnosis (FD) systems, which can fuse the advantages of system physical modelling and sensors' characteristics. A number of model based FD approaches have been proposed. The conventional residual based approaches by monitoring system output estimation errors, however, may have certain limitations such as complex diagnosis logic for fault isolation, less sensitiveness to system faults and high computation load. More importantly, little attention has been paid to the problem of fault diagnosis system verification which answers the question that under what condition (i.e., level of uncertainties) a fault diagnosis system is valid.

To this end, this thesis investigates the design and verification of fault diagnosis algorithms. It first highlights the differences between two popular FD approaches (i.e., residual based and fault estimation based) through a case study. On this basis, a set of uncertainty estimation algorithms are proposed to generate fault estimates according to different specifications after interpreting the FD problem as an uncertainty estimation problem. Then FD algorithm verification and threshold selection are investigated considering that there are always some mismatches between the real plant and the mathematical model used for FD observer design. Reachability analysis is drawn to evaluate the effect of uncertainties and faults such that it can be quantitatively verified under what condition a FD algorithm is valid.

First the proposed fault estimation algorithms in this thesis, on the one hand, extend the existing approaches by pooling the available prior information such that performance can be enhanced, and on the other hand relax the existence condition and reduce the computation load by exploiting the reduced order observer structure. Second, the proposed framework for fault diagnosis system verification bridges the gap between academia and industry since on the one hand a given FD algorithm can be verified under what condition it is effective, and on the other hand different FD algorithms can be compared and selected for different application scenarios.

It should be highlighted that although the algorithm design and verification are for fault diagnosis systems, they can also be applied for other systems such as disturbance rejection control system among many others.

CONTENTS

Statement of Originality

The contributions of this thesis are threefold: 1. a comparison analysis between residual based and fault estimation based FD approaches is made both qualitatively and quantitatively; 2. several fault estimation algorithms are proposed for different systems according to different requirements; 3. a new perspective to the problem of FD system verification and robust threshold selection is provided. The novelty of the thesis is supported by the following publications:

In Chapter 2, literature reviews on FD algorithms and uncertainty estimation algorithms are conducted. A comparison analysis is drawn between residual based and fault estimation based FD algorithms, which partially gives the motivations of the research in this thesis. The aforementioned results have been published in (note: name in **bold**: the author of the thesis; "*": the corresponding author):

1. **Jinya Su***, Wen-Hua Chen, and Baibing Li. "Disturbance observer based fault diagnosis", *Proceeding of IEEE 33rd Chinese Control Conference (CCC)*, pp. 3024–3029, Nanjing, China, 2014.

2. **Jinya Su***, Wen-Hua Chen, and Baibing Li. "High order disturbance observer design for linear and nonlinear systems", *Proceeding of IEEE International Conference on Information and Automation (ICIA)*, pp. 1893–1898, Lijiang, China, 2015.

In Chapter 3, the properties of a unified Kalman filter are investigated including existence, optimality and asymptotic stability. The results are then applied to the problem of simultaneous input and state estimation. The aforementioned results have been published in:

3. **Jinya Su**, Baibing Li* and Wen-Hua Chen, "On existence, optimality and asymptotic stability of the Kalman filter with partially observed inputs", *Automatica*, 53, 149–154, 2015.

4. **Jinya Su**, Baibing Li* and Wen-Hua Chen, "Simultaneous state and unknown input estimation with partial information on the unknown inputs", *System Science & Control Engineering*, 3(1), pp. 445–452, 2015.

In Chapter 4, a reduced-order disturbance observer is proposed to unify the existing results on disturbance observer design for discrete-time linear systems with a slowly time-varying disturbance model. The result has been summarized in:

5. **Jinya Su***, Wen-Hua Chen, Further results on "Reduced order disturbance observer for discrete-time linear systems", *Tentatively submitted to Automatica.*

In Chapter 5, a reduced-order disturbance observer is further designed for discrete-time atlinear stochastic system where no explicit disturbance model is assumed. The result has been published in:

6. **Jinya Su**, Baibing Li*, Wen-Hua Chen and Jun Yang, "Reduced-order disturbance observer design for discrete-time linear stochastic systems", *Transactions of the Institute of Measurement and Control*, 38(6), pp. 657–664, 2016.

In Chapter 6, the relationship between time-domain and frequency-domain disturbance observer is rigorously established. On this basis, a functional disturbance observer is proposed using the technique of state functional observer. The result has been published in:

7. **Jinya Su***, Wen-Hua Chen and Jun Yang "On relationship between time-domain and frequency-domain disturbance observers and its applications", *ASME Journal of Dynamic Systems Measurement and Control*, 138(9), 2016.

In Chapter 7, the model based FD system verification and robust threshold selection problem is investigated using the technique of reachability analysis. The actuator and sensor fault diagnosis problem for a direct current motor system is used to evaluate its effectiveness. The result has been summarized in:

8. **Jinya Su***, Wen-Hua Chen, "Fault diagnosis system verification and robust threshold selection using reachability analysis", *IEEE Transactions on Systems, Man and Cybernetics: Systems*, under review.

In Chapter 8, a comparison analysis between residual based and fault estimation based fault diagnosis algorithms is made using a case study of sensor fault diagnosis for vehicle lateral dynamics based on the results in Chapter 7. The result has been published in

9. **Jinya Su***, Wen-Hua Chen, "Fault diagnosis for vehicle lateral dynamics with robust threshold", *2016 IEEE International Conference on Industrial Technology (ICIT2016)*, pp. 1777–1782, 2016. (received IEEE-IES Student Paper Travel Award)

10. **Jinya Su***, Wen-Hua Chen, "Model-based fault diagnosis algorithms verification and their comparison analysis", *tentatively submitted to IET Control Theory and Applications.*

Some other publications that are not included into this thesis can be found in Appendix B, where a complete publication list is provided.

NOMENCLATURE

DOB Disturbance OBserver

DOS Dedicated Observer Scheme

EHGSO Extended High-Gain State Observer

EKF Extended Kalman Filter

ESO Extended State Observer

FD Fault Diagnosis

FIS Fault Indicating Signal

FODOB Full Order Disturbance OBserver

FSDOB full measurable state based DOB

KF Kalman Filter

MMSE Minimum Mean Square Error

MVUE Minimum Variance Unbiased Estimation

NDOB Nonlinear Disturbance OBserver

PIO Proportional Integral Observer

RODOB Reduced Order Disturbance OBservers

SFO State Functional Observer

SISE Simultaneous Input and State Estimation

SISO Single Input Single Output

UAV Unmanned Aerial Vehicles

UIF Unknown Input Filtering

UIO Unknown Input Observer

UKF Unscented Kalman Filter

ULF Unknown Linear Filter

UMVF Unbiased Minimum-Variance Filter

LIST OF SYMBOLS

Some frequently used notations in this thesis are as follows:

ΔA: Uncertain part of matrix A

$A^{1/2}$: Square root of nonnegative definite matrix A

λ, ω: Characteristic value and vector of A such that $A\omega = \lambda\omega$

$A \geq B$: $A - B$ is non-negative definite

$|A|$ or $det(A)$: Determinant of matrix A

$adj(A)$: Adjacent matrix of matrix A

$A^{\perp}$: An orthogonal complement of A

A^{+}: Moore-Penrose Pseudo-inverse of A

rank(A): Rank of A

tr(A): Trace of A

O: Zero matrix of appropriate dimension

I: Identity matrix of appropriate dimension

zeros(m,n): Zero matrix of dimension $m \times n$

$\oplus, \otimes$: Set-based addition and multiplication

List of Figures

Chapter 1

INTRODUCTION

1.1 Overview

Safety and reliability is attracting more and more attention in practical engineering, especially for safety-critical systems such as aeronautical systems, automotive engineering among many others. In such areas, a minor fault regardless of actuator, sensor or system plant fault, if not being detected and handled in due time, may result in unpredictable consequences–the loss of properties or even personnels. Consequently, much effort has been paid to fault diagnosis[1]; the basic philosophy of which is redundancy including hardware redundancy and analytical redundancy [5].

Hardware redundancy is a commonly used approach in industry (especially in aerospace systems, such as fly-by-wire and hydraulic systems in aircraft). However, this approach may result in additional cost and extra weight. With the rapid development of control theory and constant improvement of computation power in conjunction with the new requirements on fault diagnosis system (such as fault isolation, fault severity information), analytical redundancy (especially, model based fault diagnosis approaches) is drawing increasing attention in both academia and industry since its first appearance in 1970s [5]. The classical model based fault diagnosis approaches perform fault diagnosis through monitoring the output estimation errors or their functions (also termed residuals and consequently this approach is termed residual based fault diagnosis hereafter). This approach, however, requires multiple observers to achieve fault isolation and can not easily/directly obtain fault amplitude information (see, [6] and the references therein).

To this end, a lot of attention has been paid to fault estimation based diagnosis approach, where the system faults are treated as system unknown inputs and input estimation algorithms can be used to estimate the unknown inputs and consequently system faults. The research in this thesis falls into this category. To this

[1] Alternative names are available for fault diagnosis such as "fault detection and isolation", "health monitoring" among others. But they mainly denote a mechanism that can detect the presence of faults and isolate what types of faults have occurred.

end, a comparison analysis between residual based and fault estimation based fault diagnosis approaches is first made in terms of fault diagnosis logic and computation complexity.

Then a number of uncertainty estimation algorithms are proposed for the purpose of fault estimation according to different system specifications and requirements. Specifically, for discrete-time systems, according to whether the full state information is required (directly or indirectly) in derivation of disturbance estimates, full order disturbance observer and reduced-order disturbance observer are proposed respectively. In full order disturbance observer design, all the system states are needed directly or indirectly to derive the disturbance estimate; whereas in reduced-order disturbance observer design, only partial system states are required consequently leading to lower observer order. In the aforementioned approaches, different types of prior information on disturbances can be pooled into disturbance observer design, thus improving the system estimation performance. Following this line of thought, attention is turned to continuous-time domain. The relationship between time-domain disturbance observer and frequency-domain disturbance observer is rigorously established, based on which a new reduced-order disturbance observer in time-domain is proposed using the technique of state functional observer.

In model based fault diagnosis, the first step is fault diagnosis observer design to generate fault indicating signals (e.g., residuals in the residual based approaches, fault estimates in the fault estimation based approaches); the next step is threshold selection to evaluate the fault indicating signals. In practical engineering, however, uncertainties (e.g., parameter uncertainties, external disturbance, noises among many others) are inevitable. As a result, there are always some mismatches between the actual plant and the mathematical model used for fault diagnosis observer design. This phenomenon will pose two challenges for model based fault diagnosis. On the one hand, it is challenging to verify a fault diagnosis algorithm, i.e., answering the question that under what condition (e.g., level of uncertainties) a given fault diagnosis algorithm is valid. On the other hand, it is hard to choose an appropriate threshold to evaluate the fault indicating signals such that false alarm rate and missed detection rate are kept at a low level.

The rest of the thesis therefore focuses on these two challenges. They are formulated as the reachability analysis problem for uncertain systems. The basic philosophy of the proposed approach is to quantitatively evaluate the effect of uncertainties and faults on fault indicating signals. Two practical illustrating examples including actuator and sensor fault diagnosis for a direct motor system, and sensor fault diagnosis for vehicle lateral dynamics are presented to demonstrate the main idea

of the proposed approach. Particularly, a quantitative comparison between residual based and fault estimation based fault diagnosis approaches is further drawn based on the newly proposed approach.

1.2 Outlines

This thesis aims at: (i) comparing residual based and fault estimation based fault diagnosis approaches both qualitatively and quantitatively; (ii) proposing a set of uncertainty estimation algorithms for the purpose of fault estimation according to different requirements; (iii) providing a new perspective to the problem of fault diagnosis system verification and robust threshold selection.

The outlines of the remaining thesis and their relationships are shown in Fig. 1.1, where detailed descriptions are also given as follows:

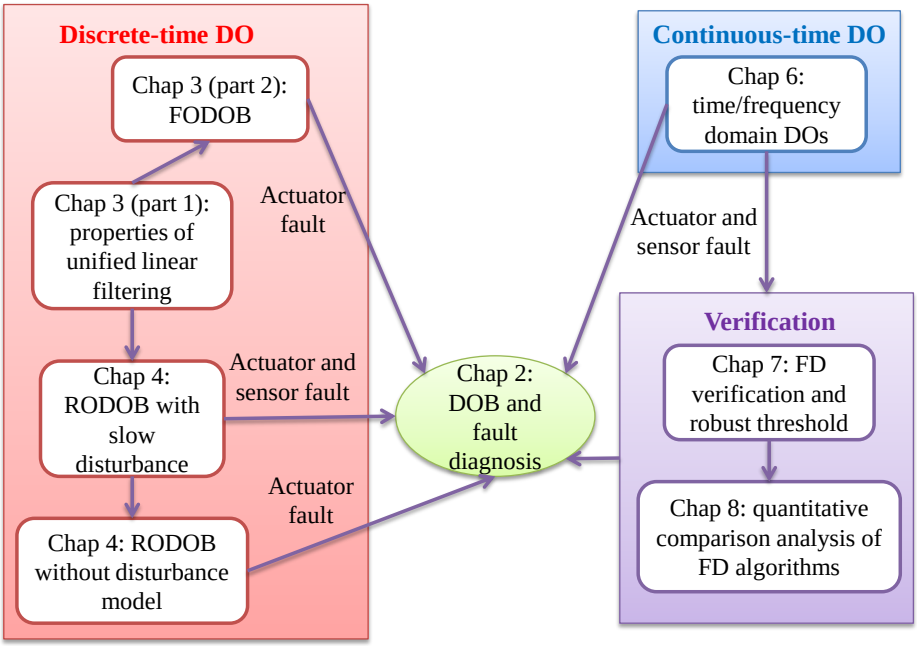

Figure 1.1. Illustration of the thesis's outline.

- Chapter 2 provides a literature review on the topics related to this thesis and presents the research motivations. The fault diagnosis algorithms are fist reviewed [6]. The existing disturbance observer algorithms are then reviewed and categorized in terms of the levels of state information used in derivation of disturbance estimate [7]. Finally, a comparison analysis between the residual based and fault estimation based fault diagnosis approaches is made to partially present the motivations of the research in this thesis.

- In Chapter 3, the properties of a unified Kalman filter (accommodating the classical Kalman filter and Unknown Input Observer as its special cases) are investigated including existence, optimality and asymptotic stability [8]. The results in this Chapter provide a unified result on linear filtering. The results are then applied to the problem of simultaneous state and input estimation, resulting in Full Order Disturbance OBserver (FODOB) design [9].

- In Chapter 4, a Reduced-Order Disturbance OBserver (RODOB) is designed for discrete-time linear systems where a slowly time-varying disturbance model is assumed using the technique of state functional observer. The results can unify the existing full order disturbance observers and reduced order disturbance observers for linear systems with certain particular disturbance assumption. More importantly, an easy-to-verify existence condition is proposed.

- In Chapter 5, a RODOB algorithm is designed for discrete-time linear stochastic systems where no explicit disturbance model is assumed [9]. In comparison with the results in Chapter 4, the results in this Chapter provide a better disturbance estimation performance when poor prior disturbance information is available.

- In Chapter 6, the relationship between time-domain DOB and frequency-domain DOB is systematically established. On this basis, a new type of reduced-order disturbance observer in time-domain is proposed, resulting in Functional Disturbance OBserver (FDOB) [10].

- In Chapter 7, the problem of fault diagnosis system verification and robust threshold selection is investigated using the technique of reachability analysis. The actuator and sensor fault diagnosis for a direct current motor is chosen as a case study to demonstrate the main idea of the proposed approach.

- In Chapter 8, the proposed system verification and robust threshold selection approach is applied to the sensor fault diagnosis problem for vehicle lateral dynamics [11]. Particularly, a quantitative comparison analysis between conventional residual based and fault estimation based fault diagnosis approach is made using the newly proposed approach in Chapter 7.

- Chapter 9 concludes the thesis with some discussions and future perspectives.

Chapter 2

LITERATURE REVIEW AND MOTIVATIONS

In this Chapter, *literature reviews are conducted on fault diagnosis algorithms and disturbance estimation algorithms.* Then *a comparison study is made between residual based and fault estimation based fault diagnosis algorithms. Some of the motivations of the thesis are also highlighted through the comparison analysis results.* The layout of this Chapter is illustrated in Fig. 2.1.

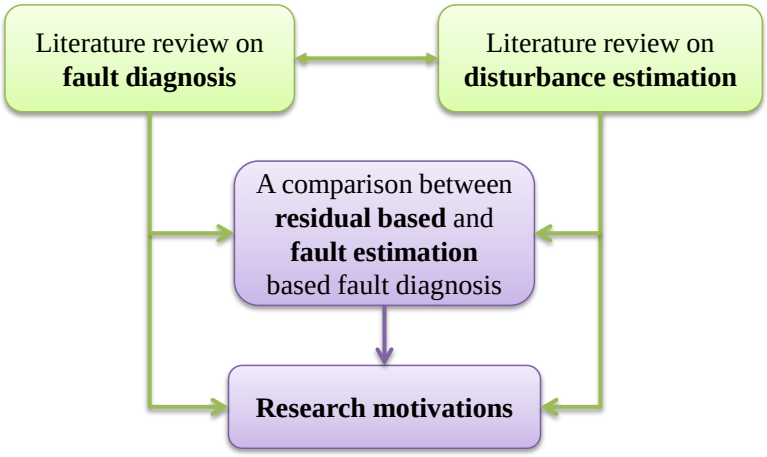

Figure 2.1. Illustration of the structure of this Chapter: literature review and motivations.

2.1 Fault diagnosis

In this section, a literature review is undertaken on fault diagnosis systems including their necessity, categories, evaluation and related challenges.

2.1.1 Necessity of FD algorithms

Safety and reliability is an important issue in practical engineering. It has been reported in [12] that the petrochemical industry alone incurs an estimated 20 billion in losses every year due to process failures. Moreover, safety and reliability appears especially vital beyond monetary losses in safety-critical systems such as aeronautical systems, automotive systems among many others [13,14]. In such areas a minor fault regardless of actuator, sensor or plant component fault, if not being detected and handled in time, may result in unpredictable consequences–the loss of properties or even personnels. It has also been reported in [15] which focused on the study of Unmanned Aerial Vehicles (UAV) reliability that about 80 percentage of flight incidents regarding UAV are due to the faults which have an adverse effect on propulsion, flight control surfaces or sensors. Interested readers can refer to recent review papers [13, 14, 16] for further information.

2.1.2 Existing FD algorithms

Hardware redundancy VS Analytical redundancy

To this end, a wide range of fault diagnosis methodologies have been proposed in the past more than four decades, whose goal is to identify the presence of faults (i.e., fault detection) and then isolate what type of fault has occurred when a fault is detected (i.e., fault isolation). The existing FD methods can be generally categorized into hardware redundancy and analytical redundancy [13]. The basic idea of hardware redundancy is to produce duplicative signals generated by various additional hardware, such as measurements of a signal by multiple sensors with the same function and then detect the presence of fault by cross checks, consistency checks, voting mechanisms, and built-in test technique of varying sophistication [17]. Although this method is almost the standard industrial practice and provides high level of robustness and good performance in the aerospace industry, it is sometimes criticized that this method may result in additional cost and extra weight. As a result, it may not be an appropriate solution for small autonomous systems due to the additional weight brought by redundant hardware [13], [14].

The analytical redundancy approach has received increasing attention since its first appearance in the late 1970s [5]. This approach does not require additional hardware but relies on the mathematical models of the concerned system in conjunction with observer design (or artificial intelligence techniques for data driven fault diagnosis). The basic idea of analytical redundancy approach is to generate a residual signal based on the system model and observer techniques, which under

ideal condition is sensitive to system faults but insensitive to uncertainties, disturbances and faults of no interest. The principles of hardware redundancy and analytical redundancy are shown in Fig. 2.2,

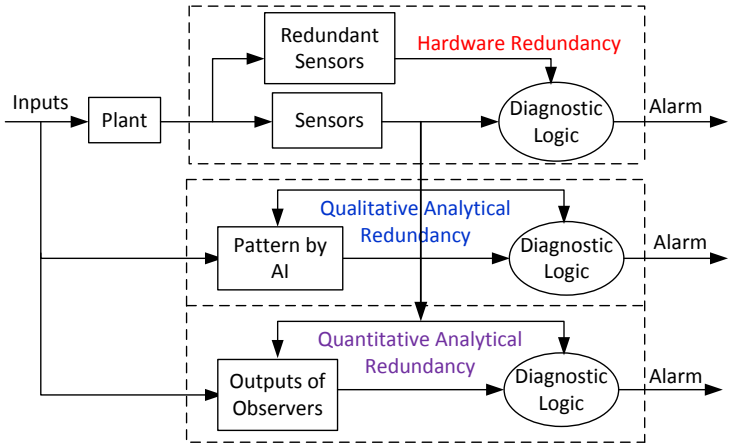

Figure 2.2. Conceptual comparisons between hardware redundancy and analytical redundancy based fault diagnosis approaches.

The analytical redundancy approach can be further categorised into qualitative methods and quantitative methods. In qualitative methods, the normal behaviour and faulty behaviours of the system under consideration are first learned using large amount of history data and represented using feature vectors. Then the fault detection and isolation problem can be transformed into classification problem, as such different artificial intelligence (AI) techniques [14] such as Support Vector Machine (SVM) [18], artificial neural network techniques [19] can be drawn to achieve the classification task. The quantitative methods such as observer based methods generate a residual signal based on the explicitly mathematical models of the plant under consideration. Quantitative FD method includes state observer (fault detection filters [5], [20], unknown input observer [21]), disturbance observer [6], parameter estimation [22] based approaches. While the observer/filter based approaches can be further divided into deterministic approaches and stochastic approaches according to different physical models that are used to describe the systems under consideration.

It is simple and convenient to generate a residual signal by comparing the estimated system outputs with the measured system outputs. For deterministic linear systems, Luenberger observer [23] can be applied for state estimation and consequently residual generation. In the presence of weak non-linearities, Extended Luenberger Observer [24] by linearising the non-linear model around the operating point can be applied. However, this approach can lead to the loss of estimation accuracy due to the neglect of high-order non-linear terms, especially for highly

non-linear systems. As a result, non-linear state estimation methods such as adaptive observers [25], [26], high-gain observers [27], [28], sliding mode observer [29], [30] can be applied for certain types of non-linear systems for the purpose of residual generation.

It is well known that Kalman Filter (KF) is an optimal state filter for discrete-time linear systems with process and sensor uncertainties/noises following Gaussian distributions [31]. As a result, if the linear systems are modelled in a stochastic way, KF can be applied for fault detection. In this approach, the innovation (i.e., the difference between measured output and predicted output) should be white noise with zero mean and known covariance in fault-free conditions. As a result, one can detect the presence of faults by a simple statistical testing of the mean and variance of the innovation signal.

It should be noted that in KF, some conservative assumptions are made on the systems, for example the process is linear, input noise and measurement noise must be Gaussian distributions, and the distribution parameters are also known as a prior. When these assumptions are violated in practical engineering, the state estimation performance may degrade. To handle fault diagnosis for nonlinear systems, the variants of KF have also been applied such as Extended Kalman Filter (EKF) [32], Unscented Kalman Filter (UKF) [33]. In addition, sequential Monte Carlo also known as particle filter (PF) [32, 34] has also been applied for the fault detection when the system is highly non-linear and non-Gaussian.

2.1.3 Evaluation of FD algorithms

The evaluation of FD algorithms can be determined by the following metrics: 1. detection time–detect the presence of faults as early as possible; 2. fault isolation–determine what type of fault has occurred and its location; 3. fault information–the severity of the fault; 4. robustness–work effectively in the presence of uncertainties and disturbances (keep the missed detection rate and false alarm rate at a low level); 5. complexity and computation load–the FD method should be easy to implement and require relatively low computation load.

2.1.4 Threshold generation

In fault diagnosis system, after residuals are generated, a residual evaluation process is needed to transform the meanings of residuals into a Boolean decision function–normal or faulty. When choosing the threshold, a compromise is usually made between minimizing missed detection rate and false alarm rate. The simplest ap-

proach is to set a constant threshold, which can decide whether a fault has occurred or not by detecting whether a residual exceeds the threshold. Generally speaking, a fixed threshold can be designed which should ensure a good trade-off between false alarm rate and missed detection rate. However, how to select the constant threshold is quite a challenging issue and may result in poor performance (high false alarm rate or high missed detection rate) if not being chosen properly due to the presence of uncertainties and noises.

To this end, much effort has been paid to threshold selection, which can achieve a so-called passive robustness in comparison with active robustness obtained by uncertainties elimination and decoupling techniques [35,36]. The principle of passive robustness is to propagate the effect of uncertainties on residuals and threshold simultaneously. However, an appropriate threshold is never an easy task due to the presence of uncertainties [37]. The basic principle of the existing threshold selection approaches is to calculate the states' envelop in the presence of uncertainties and perform consistency checking between measurement output and predicted output envelop for the purpose of fault detection.

According to the different methods used for state envelop calculation, they can be further divided into three categories. The first category is referred to simulation based approach [37], in which the envelope of states or outputs can be obtained based on a finite (possibly large) number of different linear models selected from a continuum of models corresponding to each possible value of the parameters. Although large numbers of different models are performed on fairly fine grids for uncertain parameters or Monte Carlo parameter sampling, it is still possible to miss the model corresponding to the most critical parameter combination. In addition, the parameter space girding method is highly computationally demanding, especially in face of parametric uncertainties with high dimension. The second category is optimization based approach [35,38], in which the upper bound and lower bound of state envelop in each time step can be obtained by solving a constrained optimization problem where the constraint can accommodate parameter uncertainties, initial state uncertainties, input and output uncertainties. However, due to the complexity of the optimisation at each step, this method may be subject to high computation problem especially for multiple parameter uncertainties [38,39]. Besides, few algorithms can guarantee global optimization for generic optimization problems. These limitations constrain its application.

The third category is set-membership based approaches [40], which calculate the possible state or output intervals by taking system uncertainties into account. In [40], the effect of parameter uncertainties and input uncertainties are lumped as

additive uncertainties represented by bounded variables. Then system outputs are explicitly computed based on interval arithmetic. However, the bounded variables have to be pre-determined empirically or numerically, which is not an easy task since the effect of parameter uncertainties is related to the amplitude of unmeasurable and time-varying state variables. In [41] and [42], for one kind of Single Input Single Output (SISO) linear system in observer canonical form, the effect of parameter uncertainties on residuals is amplified through triangle inequality. This method may result in conservative result (i.e., larger residual interval or even useless results) when multiple parameter uncertainties exist.

As one kind of set-membership based approach, interval observer is receiving more and more attention recently [43–47]. In [43], a non-linear continuous-time system is first approximated by an interval quasi-Linear Parameter Varying (qLPV) system using interval analysis. Then based on cooperativity theory, two point observers are obtained to estimate the lower and upper bound of state vector. As a result, a set containing the actual value of the residual can be obtained. This method has much potential since the system matrix uncertainties, input and sensor uncertainties are represented by intervals which have been taken into account in point observer design. In addition, the existence of interval observer is discussed in [45–47]. [45] shows that for linear time-invariant systems with bounded additive disturbances, the existence of an exponentially stable interval observer is that the linear systems are exponentially stable. It is further shown in [46] that for non-linear system with measurement uncertainties one can design an interval observer by partial exact linearisation and another linear change of coordinates. Later, this result has been extended to nonlinear time-varying systems in [47]. The method in [45] has been used for fault detection of an electrical drive. However, it has been pointed out in [46] that the issue of existence of observer gain for the two point observer is not yet clearly established even for linear systems, since the observer gain should not only guarantee the error system matrix is Hurwitz, but also cooperative (all the off-diagonal term is non-negative). Another problem is that in the presence of system parameter uncertainties, two bounded function should be available to cover the effect of parameter uncertainties, which is not an easy task due to the time-varying and unknown property of state variables.

To this end, part of the thesis is devoted to designing an appropriate threshold for model based fault diagnosis systems in the presence of uncertainties.

2.1.5 Necessity of FD verification

Observer based fault diagnosis system is a kind of model based FD approaches, which produces fault-indicating signals using system models, inputs and outputs. As one kind of model based FD algorithm, observer-based FD system has a relatively high demand on the accuracy of system models.

Large numbers of observer based FD algorithms have been proposed in the past more than four decades. However, these algorithms from the academic community have not been fully accepted by the industry end-users [14]. That is because not enough attention has been paid to the verification and validation of those methods. Since in real applications, the mathematical model used for observer based fault diagnosis algorithm design may not be consistent with the real plant due to assumptions made for simplified representations of the dynamic systems, the presence of system uncertainties, input noise, sensor noise, external disturbances among many others. As a result, to bridge the ever-widening gap between the academic community and industry application it becomes more and more urgent to demonstrate whether the proposed FD algorithms can still work effectively in real applications when multiple uncertainties appear.

Consequently, part of the thesis is devoted to the verification problem of model based fault diagnosis algorithms. The problem of threshold selection and system verification is transformed into reachable set calculation for uncertain systems. And reachability analysis tool is applied, which is detailed in Chapter 7.

2.2 Disturbance estimation algorithms

In this section, disturbance estimation algorithms are reviewed and categorized, which can be applied for the purpose of fault estimation.

Since 1970s, due to the increasing requirements on control accuracy and robustness, many effective disturbance estimation techniques have been developed, such as Unknown Input Observer (UIO) [48], Extended State Observer (ESO) [49], and Disturbance OBserver (DOB) [1,50]. Among these approaches, DOB and ESO are most extensively investigated. Consequently, these algorithms will be briefly reviewed. Frequency-domain DOB is first introduced, followed by time-domain DOBs.

2.2.1 Frequency-domain algorithms

The frequency-domain DOB [1, 51] was originally motivated by the unmeasurable disturbance estimation and rejection to achieve a better control performance. And it usually handles linear systems in transfer function form. Suppose that the transfer

function of the system under consideration is $G(s)$ with $G_n(s)$ being its nominal part. The basic idea of frequency-domain DOB in [1] is to obtain disturbance estimate by filtering (through a low pass filter $Q(s)$) the difference between control input and the calculated input using the inverse model of nominal plant $G_n(s)$. The basic diagram in [52] with some modification from [53] is given in Fig. 2.3, where $Q(s)$ is designed

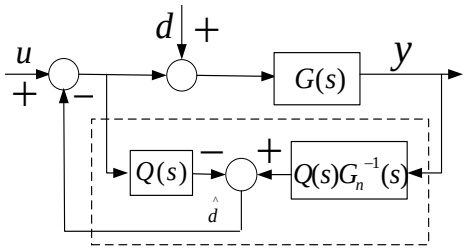

Figure 2.3. The diagram of Q-filter based DOB in [1].

as a low-pass filter with unity gain (for the purpose of nearly constant disturbance estimate) and the relative degree of $Q(s)$ is no less than that of the nominal plant $G_n(s)$ such that $Q(s)G_n^{-1}(s)$ is implementable (see, [1, 52] among many others).

The frequency-domain DOB has multiple merits including being concept-simple and suitable with standard transfer function analysis tools. The disadvantages, as highlighted in [4], are that they can only be applied to a class of linear systems and not easy to deal with transient performance. To this end, a large number of state-space based time-domain algorithms have also been proposed.

2.2.2 Time-domain algorithms

A lot of time-domain disturbance estimation algorithms have been proposed (see recent books [51, 54] and survey papers [55, 56] for a relatively complete list). It is not the objective to give a complete review of the existing results, but some typical DOBs (or related to the research in this thesis) are presented.

A new perspective to categorize the existing DOBs in time-domain is provided. Based on the availability of the state information in derivation of disturbance estimates, the existing time-domain algorithms can be broadly classified into three categories: (a) full measurable state based approaches [50, 57] (termed FSDOB); (b) full state estimation based algorithms [2, 49, 58, 59] (termed FODOB) and (c) reduced-order state function estimation based algorithms [4, 60, 61] (termed RODOB).

FSDOB: In FSDOB algorithms, the disturbance estimate is obtained under the assumption that all the system states are directly measurable. The FSDOBs mainly concern disturbance estimation for nonlinear systems. The original idea of Nonlinear

Disturbance OBserver (NDOB) is proposed in [50] for the purpose of slowly time-varying disturbance estimation (in the case of fast time-varying disturbance, the disturbance estimation performance will degrade and further development should be done).

Consider a nonlinear system with disturbance,

$$\dot{x} = f(x) + g_1(x)u + g_2(x)d, \tag{2.2.1}$$

where $x \in R^n, u \in R^m, d \in R^q$, $f(x), g_1(x), g_2(x)$ are known nonlinear functions, u is the control input and d denotes the lumped system disturbance, which may include parameter uncertainties, external disturbances and system faults.

Then a NDOB was proposed in [50], given by

$$\begin{cases} \dot{z} = -l(x)g_2(x)z - l(x)[g_2(x)p(x) + f(x) + g_1(x)u], \\ \hat{d} = z + p(x), \end{cases} \tag{2.2.2}$$

where $z \in R^q$ is the internal state of the nonlinear observer, and $p(x)$ is the nonlinear function to be designed. The nonlinear disturbance observer gain $l(x)$ is determined by

$$l(x) = \frac{\partial p(x)}{\partial x} \tag{2.2.3}$$

It has been shown in [50] that the NDOB asymptotically estimates the disturbance if the observer gain $l(x)$ is chosen such that

$$\dot{e}_d = -l(x)g_2(x)e_d, \tag{2.2.4}$$

is asymptotically stable regardless of x, where $e_d = d - \hat{d}$ is the disturbance estimation error. The detailed selection of $p(x)$ and consequently $l(x)$ is referred to [50].

To relax the assumption of slowly time-varying disturbance, NDOB is further extended to the case of exogenous disturbance in [62]. Suppose the disturbances are generated by a linear model [1]

$$\dot{\xi} = W\xi, \ d = V\xi, \tag{2.2.5}$$

then a NDOB for estimating exogenous disturbance (2.2.5) is proposed in [62] and

[1] This linear model can accommodate several common disturbances in practical engineering such as constant, ramp, sinusoidal disturbances (see, [10] for further details.)

depicted by

$$\begin{cases} \dot{z} = [W - l(x)g_2(x)V]z + Wp(x) - l(x)[g_2(x)Vp(x) + f(x) + g_1(x)u], \\ \hat{\xi} = z + p(x),\ \hat{d} = V\hat{\xi}. \end{cases} \tag{2.2.6}$$

It has been shown in [62] that the NDOB (2.2.6) can exponentially estimate the disturbance if the nonlinear observer gain $l(x)$ is designed such that $\dot{e}_\xi = [W - l(x)g_2(x)V]e_\xi$ is asymptotically stable.

Recently, a NDOB estimating disturbances in polynomial form $d(t) = d_0 + d_1 t + \cdots + d_q t^q$ has been proposed in [57], which can estimate high order disturbances with lower observer order.

FODOB: In FODOB, the disturbance estimates are obtained by simultaneously estimating both the system states and disturbances. The classical extended state observer (ESO) [49], unknown input observer (UIO) [48, 63] are typical examples of FODOB for continuous time linear systems. Proportional Integral Observer (PIO) based disturbance observer [58], Simultaneous Input and State Estimation (SISE) based on Minimum Variance Unbiased Estimation (MVUE) technique [2] are typical examples of FODOB for discrete-time linear systems. While the Extended High-Gain State Observer (EHGSO) in [64] is a typical example of FODOB for nonlinear systems. The UIO proposed in [63] is taken as an example. Consider a linear system, given by

$$\begin{cases} \dot{x} = Ax + Bu + Dd, \\ y = Cx, \end{cases} \tag{2.2.7}$$

where the disturbances d are of multiple dimension and each element is supposed to satisfy (2.2.5). An extended system including the state dynamics (2.2.7) and disturbance dynamic (2.2.5) can be obtained as follows:

$$\begin{cases} \begin{bmatrix} \dot{x} \\ \dot{\xi} \end{bmatrix} = \begin{bmatrix} A & DV \\ O & W \end{bmatrix} \begin{bmatrix} x \\ \xi \end{bmatrix} + \begin{bmatrix} B \\ 0 \end{bmatrix} u, \\ y = \begin{bmatrix} C & O \end{bmatrix} \begin{bmatrix} x \\ \xi \end{bmatrix}. \end{cases}$$

Then the classical state observer technique can be used to estimate the extended states and consequently disturbance estimates can be obtained.

RODOB: In RODOB design, not all the states are needed in derivation of disturbance estimate. The results in [4] and [61] are typical examples of RODOB for continuous time linear systems and discrete-time linear systems respectively. The RODOB structure of [61] is shown as an example. Consider the linear system (2.2.7),

two types of RODOB are discussed in [61], given by

$$\begin{cases} \dot{z} = Fz + Ly + TBu + TD\hat{d}, \\ \hat{d} = \gamma(Wy - Nz). \end{cases} \tag{2.2.8}$$

and

$$\begin{cases} \dot{z} = Fz + Ly + TBu + TD\hat{d}, \\ \dot{\hat{d}} = \rho(Wy - Nz). \end{cases} \tag{2.2.9}$$

Under some existence condition in [61], the RODOs (2.2.8) and (2.2.9) can estimate the disturbance d where only a state linear function Tx rather than all the state x is estimated. As a result, as long as the matrix T has a full row rank under the existence condition, the existence condition of RODOB will be relaxed compared with that of FODOB where all the states are estimated in derivation of disturbance estimate.

2.3 Motivations: residual VS fault estimation

In this section, a simulation comparison analysis between the conventional residual based and fault estimation based fault diagnosis approaches is drawn, which partially presents the motivations of the research in this thesis, i.e., fault estimation algorithms: design and verification.

To this end, a motor system in state space model (see, Appendix A.1) serves as a case study for the simulation comparison analysis. The linear system with both actuator and sensor faults (the position sensor fault is not taken into account since it is not detectable through theoretical analysis) can be represented by the following system (2.3.1):

$$\begin{cases} \dot{x} = Ax + Bu + Dy_d + \Gamma\Gamma_d + Ef_a, \\ y = Cx + Sf_s \end{cases} \tag{2.3.1}$$

where y_d is the reference signal, Γ_d is the external unknown load, f_a and $E = B$ denote actuator fault and its distribution matrix, while f_s and S denote sensor fault and its distribution matrix, where S is given by

$$S = \begin{bmatrix} 0 & 1 & 0 & 0 \\ 0 & 0 & 1 & 0 \end{bmatrix}^T.$$

It should be noted that system (2.3.1) is not the motor model but the model for the purpose of observer design, where y_d is deliberately modelled into Eq. (2.3.1) to ease controller design.

2.3.1 Residual based approach

In residual based fault diagnosis, a bank of observers are usually designed to achieve fault isolation. There are generally two types of a bank of observers, i.e. the dedicated observer scheme (DOS) and the generalized observer scheme (GOS) [14, 65]. The high-level philosophy of them are the same. A DOS is a bank of observers driven by only one sensor output and consequently only sensitive to one sensor fault. While in the GOS scheme, the bank of observers are driven by all outputs but one and consequently sensitive to all faults except one. The mathematical description of the DOS is as follows: a bank of observers are firstly designed for system (2.3.1) as follows:

$$\begin{cases} \dot{\hat{x}}_i = A\hat{x}_i + Bu + Dy_d + \Gamma\Gamma_d + K_{oi}(y_i - \hat{y}_i), \\ \hat{y}_i = C_i\hat{x} \end{cases} \tag{2.3.2}$$

where K_{oi} is the observer gain matrix to be designed and y_i is the measurement for ith observer with its corresponding distribution matrix C_i; C_i is the combinations of the rows of C depending on different measurements used in i^{th} observer.

Combing (2.3.1) and (2.3.2), one can obtain the output estimation error $e_{yi} = y_i - C_i\hat{x}_i$, given by

$$e_{yi} = S_i f_s + C_i e_{xi}$$

where e_{xi} denotes the state estimation error $e_{xi} = x - \hat{x}_i$, which is governed by

$$\dot{e}_{xi} = (A - K_{oi}C_i)e_{xi} + Ef_a - K_{oi}S_i f_s$$

Then residuals r_is are usually defined as the function of output estimation error e_{yi}, such as the 2-norm of e_{yi}, i.e., $r_i = ||e_{yi}|| = \sqrt{e_{yi}^T e_{yi}}$.

The structure of the DOS and GOS for fault diagnosis is illustrated in Fig. 2.4.

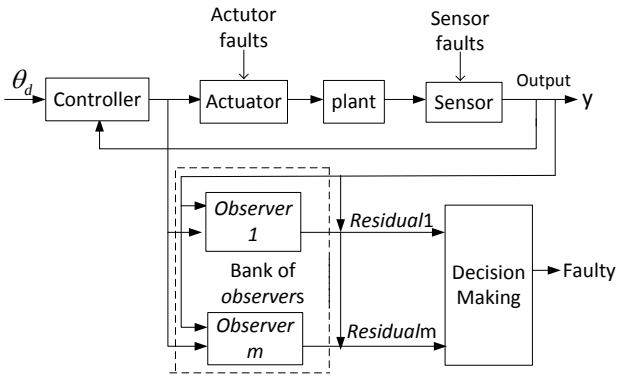

Figure 2.4. The diagram of residual based fault diagnosis.

2.3.2 Fault estimation based approach

In fault estimation based approach, the fault diagnosis is achieved by directly approximating faults. Its diagnosis logic is as follows: when the faults are approximately obtained, one can directly tell whether a fault has occurred or not and where the faults come from (which actuator, sensor) by checking the non-zero component of fault estimates. The diagram of fault estimation based approach is shown in Fig. 2.5.

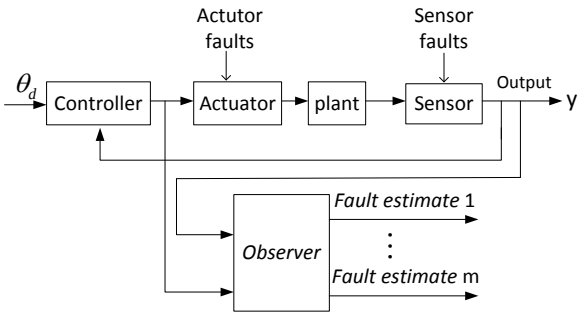

Figure 2.5. The diagram of fault estimation based approach.

To obtain fault estimates for the linear systems (2.3.1), the extended state observer [66] is used, which estimates the faults by augmenting the faults as additional states. Let $\bar{x} = (x, f_s, f_a)$ and suppose the faults are slowly time-varying, then system (2.3.1) can be equivalently represented by the following extended system equation,

$$\begin{cases} \dot{\bar{x}} = \bar{A}\bar{x} + \bar{B}u + \bar{D}y_d + \bar{\Gamma}\Gamma_d, \\ \bar{y} = \bar{C}\bar{x} \end{cases} \tag{2.3.3}$$

where $\bar{A} = \begin{bmatrix} A & 0 & E \\ 0 & 0 & 0 \end{bmatrix}$, $\bar{B} = \begin{bmatrix} B \\ 0 \end{bmatrix}$, $\bar{D} = \begin{bmatrix} D \\ 0 \end{bmatrix}$, $\bar{\Gamma} = \begin{bmatrix} \Gamma \\ 0 \end{bmatrix}$ and $\bar{C} = \begin{bmatrix} C & S & 0 \end{bmatrix}$.
Then for system (2.3.3), a state observer can be designed as

$$\begin{cases} \dot{\hat{\bar{x}}} = \bar{A}\hat{\bar{x}} + \bar{B}u + \bar{D}y_d + \bar{\Gamma}\Gamma_d + \bar{K}_o(\bar{y} - \hat{\bar{y}}), \\ \hat{\bar{y}} = \bar{C}\hat{\bar{x}} \end{cases} \tag{2.3.4}$$

where the gain matrix $\bar{K}_o$ is the observer gain matrix to be designed. When the extended state $\bar{x}$ is obtained, one can approximately obtain f_s and f_a, which will serve as the fault indicating signals.

2.3.3 Simulation comparison study

Simulation studies are performed to compare the performance of the aforementioned approaches. The control parameters in Eq. (A.1.3) are designed as $k_\theta = 2.5, k_e = 0.35, k_\omega = 3.6, k_i = 5.8$. The observer gains K_{oi} in Eq. (2.3.2) and $\bar{K}_o$ in Eq. (2.3.4) are designed based on pole assignment technique (i.e., "place" in Matlab), where the poles for K_{oi} are $-10 \pm 4i, -20 \pm 4i$ and the poles for $\bar{K}_o$ are $-10 \pm 4i, -20 \pm 4i, -4, -5$. The position, velocity and current sensor noises are supposed to be Gaussian distributions with zero mean and variance amplitude of 0.01, 0.02 and 0.01. The reference output θ_d and load Γ_d are shown in Fig. 2.6 (a).

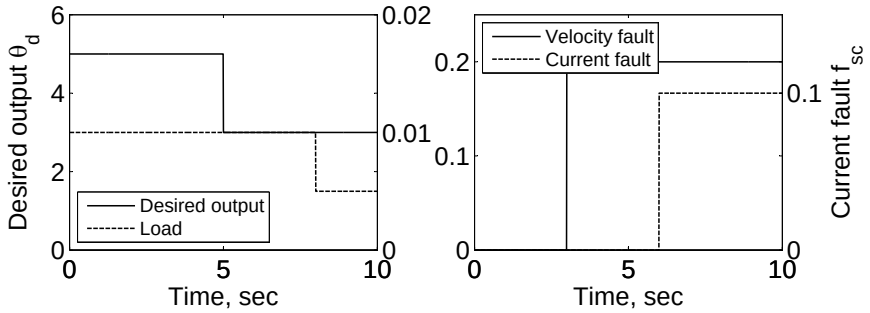

Figure 2.6. The simulation profiles: (a) reference output and load; (b) sensor faults.

Case 1: Both velocity sensor fault f_{sv} and current sensor fault f_{sc} occur. The profile for simulation study is shown in Fig. (b) of Fig. 2.6.

For the residual based approach, the concept of GOS is used for the purpose of sensor fault isolation. The residual is defined as the 2-norm of output estimation error, where the residual r_1 is designed to be only sensitive to velocity sensor fault and residual r_2 is only sensitive to current sensor fault. The dynamics of residuals r_1 and r_2 of the residual based approach are depicted in Fig. 2.7, while the fault estimates of fault estimation based approach are shown in Fig. 2.8.

Comparing the results of residual based approach Fig. 2.7 and fault estimation based approach Fig. 2.8, one can see that both methods can effectively detect the presence of current sensor fault, since in the presence of current sensor fault there exists a substantial change in the residual r_2 and current fault estimation. However, regarding the velocity sensor fault, only fault estimation based approach can effectively detect the presence of fault and residual based approach fails to achieve this goal, since a threshold is not easy to be chosen to tell the residual under normal case and faulty case apart. The reason in detail is shown as follows.

Self-correction: One can see from Fig. 2.7 that in the presence of velocity

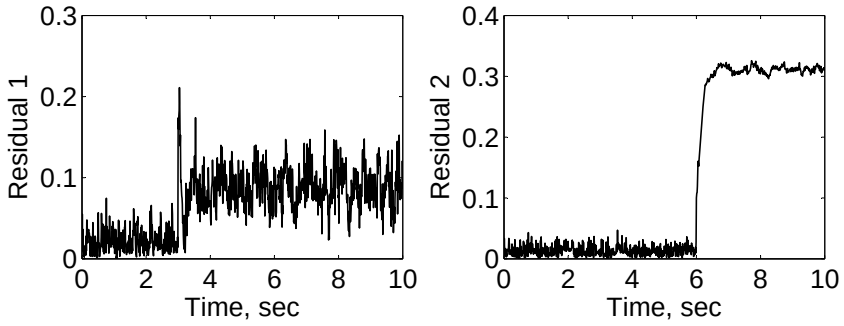

Figure 2.7. Residuals of residual based approach: residual r_1 sensitive to velocity sensor fault (left); residual r_2 sensitive to current sensor fault (right).

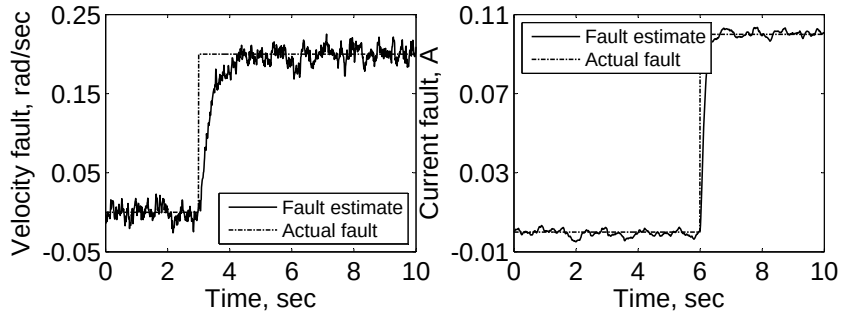

Figure 2.8. The results of fault estimation based approach: velocity sensor fault estimation (left); the current sensor fault estimation (right).

sensor fault at 3rd second, the residual 1 suddenly increases but then quickly reduces and even disappears in the effect of noise. This is due to self-correction feature in state observer which forces the estimated output close to the measurement output as much as possible. As a result, certain kind of faults may be missed by the residual based approach, especially when the fault amplitude is small.

Case 2: Secondly, the robustness issue of the aforementioned approaches is tested, since robustness is a critical metric to evaluate model based fault diagnosis approaches and there exist many uncertainties in motor driving system, such as resistance R, reluctance L, among many others. To this end, suppose there exists 5% parameter uncertainty in resistance R. Simulation results for the same system as that of case 1 are shown in Figs. 2.9 and 2.10.

Robustness Issue: One can see from Figs. 2.9 and 2.10 that the residual based approach is more sensitive to parameter uncertainties and will result in false fault diagnosis information. Since one can see from Fig. 2.9 (a) that the residual r_1 substantially deviates from zero under normal case. In addition, although one can detect the presence of current sensor fault from Fig. 2.9 (b), the threshold has to be re-determined carefully. From Fig. 2.10, one can see that fault estimation based

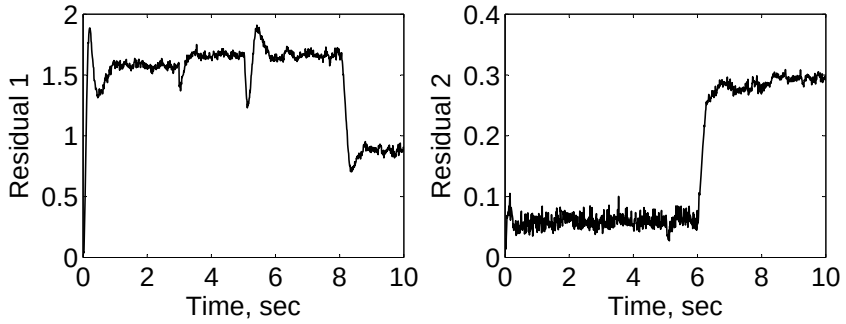

(a) (b)

Figure 2.9. Residual based approach under resistance uncertainties.

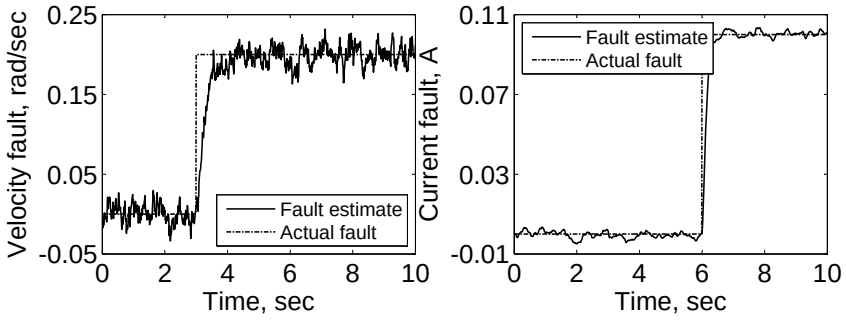

(a) (b)

Figure 2.10. Fault estimation based approach under resistance uncertainties.

diagnosis approach is more robust to parameter uncertainties and can still obtain a relatively accurate estimation of faults and consequently better fault diagnosis performance.

Complex Diagnosis Logic: Another possible drawback of residual based approach is its complex diagnosis logic, since in residual based approach there need to be a bank of observers to isolate a set of faults. And this issue is severe especially when there exist large number of faults. Supposing there are k components to be monitored, there needs to be $C_k^1 + \cdots + C_k^{k-1}$ observers to isolate all combinations of possible faults, where C_k^i is defined as $C_k^i = \frac{k!}{i!(k-i)!}$, $k! = 1 \times 2 \times \cdots \times k$. However, in the context of fault estimation based approach only one observer is needed for the purpose of all fault estimation as long as the extended system is observable and one can isolate the fault based on the estimated faults.

Observability Condition: Another possible drawback of residual based approach is poor observability in sensor fault isolation, although this condition is satisfied in the simulation example of [65], which firstly proposed the concept of fault isolation based on a bank of observers. The reason is that the observability condition may not be satisfied any more in the stage of fault isolation since (A, C_i)

may not satisfy the observability condition although the original (A, C) is observable. Again, take the aforementioned motor system as an example, by checking the observability condition one can easily obtain that it is not possible to estimate the whole states of the motor system without position measurement information.

Since fault estimation based fault diagnosis algorithms possess some advantages over the conventional residual based one under certain circumstances. Attention is paid to fault estimation based fault diagnosis in this thesis. In the following few Chapters, several disturbance estimation algorithms are proposed for the purpose of fault estimation under different design requirements and specifications.

Chapter 3

UNIFIED LINEAR FILTER

3.1 Introduction

In this Chapter, a Unified Linear Filter (ULF) is introduced for stochastic linear systems, which can accommodate the Kalman Filter and Unknown Input Observer as its special cases. Then it is applied to the problem of simultaneous input and state filter. The structure of this Chapter and how it expands the knowledge boundaries are illustrated in Fig. 3.1.

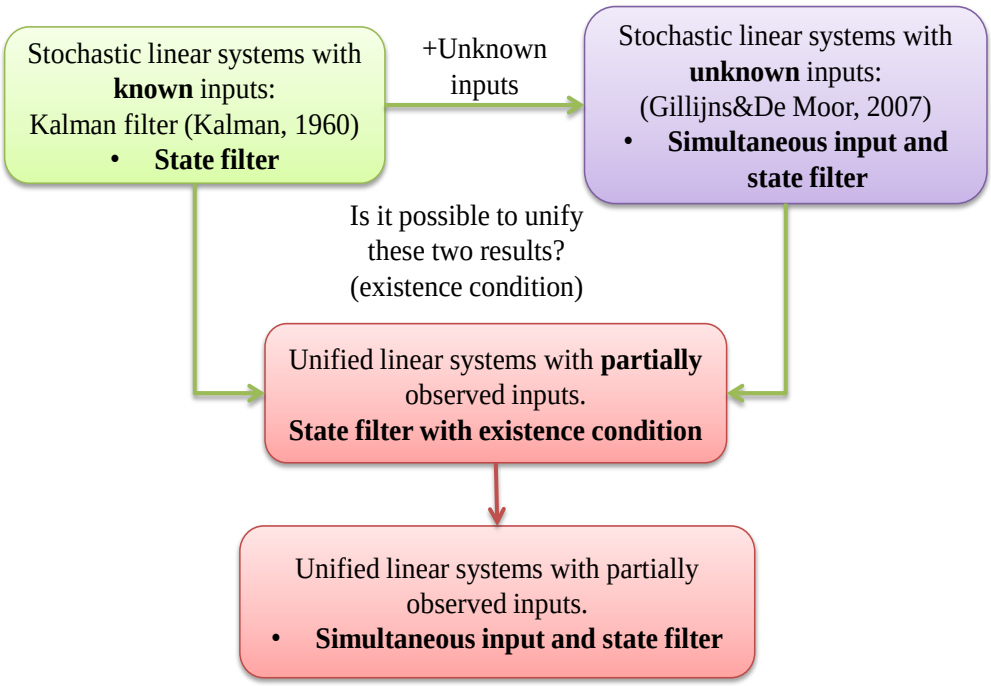

Figure 3.1. Illustration of this Chapter's structure and its relationship with the existing results.

3.1.1 Properties of ULF

State estimation for discrete-time linear stochastic systems with unknown inputs (also termed unknown input filtering (UIF) problem) has received considerable attention since the original work of [67] first appeared. Various filters were developed under different assumptions for the systems with unknown inputs (see, e.g., [2,67–72] among many others). Most of these researches used the technique of minimum variance unbiased estimation (MVUE), hence leading to an unbiased minimum-variance filter (UMVF). In addition, various properties for these developed filters have been investigated, including the existence condition [69], asymptotic stability [72] and global optimality of the UMVF [71].

In some applications such as population estimation, traffic management [3], and chemical engineering [73], however, the information on the input variables is not completely unknown; rather, it is available at an aggregate level. Recently, [3] has developed a Kalman filter (KF) for linear systems with partially observed inputs, where the inputs are observed not at the level of interest but rather the input information is available at an aggregate level. It has been shown that the developed filter provides a unified approach to state estimation for linear systems with Gaussian noise (consequently termed Unified Linear Filter (ULF)). In particular, it includes two important extreme scenarios as its special cases: (a) the filter where all the inputs are completely available (i.e. the classical KF [74]); and (b) the filter where all inputs are unknown (i.e. the filter investigated in [67] and many others for the UIF problem). Potentially the proposed filter can be applied to a variety of practical problems in many different areas such as population estimation and traffic control [3].

So far there is not any study discussing the properties of this newly proposed unified filter including existence and asymptotic stability issues. So the first part of the Chapter discusses the properties of the ULF developed in [3]. For linear stochastic time-varying systems with partially observed inputs, the existence condition for a general linear filter is established. Then it is shown that the developed filter is optimal in the sense of minimum error covariance matrix. Finally, the asymptotic stability of the filter for the corresponding time-invariant systems is considered based on the established existence condition and optimality result.

The results in this Chapter can provide a unified approach to accommodating existence and asymptotic stability conditions in a variety of filtering scenarios: it includes the results on existence and asymptotic stability for some important filters as its special cases, e.g., the filters developed for the problems where the inputs are completely available and where all the inputs are unknown. Note that the

former is the classical Kalman filtering problem and the corresponding existence and asymptotic stability conditions are well established in the literature. For the latter case with unknown inputs, there has been a continuing research interest in existence and asymptotic stability conditions for various discrete-time systems (e.g., [67, 69, 71, 72]) and continuous-time systems (e.g., [75–77]).

3.1.2 Extension: SISE

However, the aforementioned filter developed in [3] only considered the problem of sole state estimation; the problem of simultaneous input and state estimation (SISE) with partial information on the inputs has not been investigated. In the second part of this Chapter, based on the resulted existence condition, the problem of SISE is further considered for the case where the unknown inputs are partially observed.

To obtain simultaneous estimates of the state variables and unknown inputs, Bayesian inference (see, e.g. [3, 78]) is drawn on both state and input on the basis of [3]. According to the Bayesian theory, the obtained estimates are optimal in the sense of minimum mean square estimation under the assumption of Gaussian noise terms [3]. Then, the estimates of the original unknown inputs can be worked out by pooling together all the available information on the unknown inputs.

Compared with the filter in [3] where only state estimate is of interest, the proposed method obtains simultaneous input and state estimates, and hence the estimated inputs can be used in fault detection and other applications. Compared to the results in [2, 59], the results in the Chapter take into account the additional information on the unknown inputs, and hence it results in a better estimate of the state and input vectors. In addition, it is shown that the Bayesian approach to SISE provides an alternative derivation for the filter in [2]. The relationships of the proposed filter with some existing estimation methods are further investigated. In particular, it is shown in this Chapter that: (a) when the inputs are completely available, the proposed filter reduces to the classical Kalman filter [74]; (b) when no information on the unknown inputs is available, it reduces to the results of [2] where both state and input estimation are concerned; and (c) if only state estimation is of interest, it is equivalent to the filter for partially available inputs developed in [3].

3.2 Problem statement

Consider a discrete-time linear stochastic system

$$\begin{cases} x_{k+1} = A_k x_k + G_k d_k + \omega_k \\ y_k = C_k x_k + \upsilon_k \end{cases} \tag{3.2.1}$$

where $x_k \in R^n$ is the state vector, $d_k \in R^m$ is the input vector, and $y_k \in R^p$ is the measurement vector at each time step k with $p \geq m$ and $n \geq m$. The process noise $\omega_k \in R^n$ and the measurement noise $\upsilon_k \in R^p$ are assumed to be mutually uncorrelated with zero-mean and a known covariance matrix, $Q_k = E[\omega_k \omega_k^T] \geq 0$ and $R_k = E[\upsilon_k \upsilon_k^T] > 0$, respectively. A_k, G_k and C_k are known matrices. Without loss of generality, following [2] and [67], it is assumed that G_k has a full column-rank. The initial state x_0 is independent of ω_k and υ_k with a mean $\hat{x}_0$ and covariance matrix $P_0 > 0$.

The scenario is considered where the input vector d_k is not fully observed at the level of interest but rather it is available only at an aggregate level. Specifically, let D_k be a $q_k \times m$ known matrix with $0 \leq q_k \leq m$ and F_{0k} an orthogonal complement of D_k^T such that $D_k F_{0k} = O_{q_k \times (m-q_k)}$ and $F_{0k}^T F_{0k} = I_{m-q_k}$, where O and I represent the zero matrix and identity matrix of appropriate dimensions. It is supposed that the input data is available only on some linear combinations:

$$r_k = D_k d_k, \tag{3.2.2}$$

where r_k is available at each time step k. D_k is assumed to have a full row-rank; otherwise the redundant rows can be removed.

As pointed out in [3], the matrix D_k characterizes the availability of input information at each time step k. It includes two extreme scenarios that are usually considered: (a) $q_k = m$ and D_k is an identity matrix, i.e. the complete input information is available; this is case that the classical KF can be applied; (b) $q_k = 0$, i.e. no information on the input variables is available; this is the problem investigated in [2, 67, 69]. Define $\Omega_k = [G_k, G_k^{\perp}]$ and

$$\Pi_k = \begin{pmatrix} D_{k-1} \\ C_k G_{k-1} \end{pmatrix}. \tag{3.2.3}$$

The objectives is twofold: firstly the properties of ULF (for state estimation) proposed in [3] for system (3.2.1) and (3.2.2) will be exploited; secondly, a SISE filter is proposed for system (3.2.1) and (3.2.2).

3.3 Existence condition of ULF

The existence condition of ULF is first considered. To establish the existence condition of a general linear filter for system (3.2.1) with (3.2.2), an invertible linear transformation is first introduced.

3.3.1 Transformation

Consider the following invertible matrix:

$$M_k = \begin{bmatrix} D_k & O_{q_k\times(n-m)} \\ O_{(n-m)\times m} & I_{n-m} \\ F_{0k}^T & O_{(m-q_k)\times(n-m)} \end{bmatrix} \Omega_k^{-1}.$$

It is straightforward to verify that $M_k G_k d_k$ can be expressed as:

$$\begin{aligned} M_k G_k d_k &= [D_k^T, O_{m\times(n-m)}, F_{0k}]^T d_k \\ &= [(D_k d_k)^T, (O_{(n-m)\times m} d_k)^T, (F_{0k}^T d_k)^T]^T \\ &= [r_k^T, O_{1\times(n-m)}, (F_{0k}^T d_k)^T]^T \\ &= \tilde{r}_k + \tilde{G}_k \delta_k, \end{aligned} \tag{3.3.1}$$

where $\tilde{r}_k = [r_k^T, O_{1\times(n-m)}, O_{1\times(m-q_k)}]^T$, $\delta_k = F_{0k}^T d_k$ and $\tilde{G}_k = [O_{(m-q_k)\times q_k}, O_{(m-q_k)\times(n-m)}, I_{m-q_k}]^T$. One notes that $\tilde{r}_k$ is completely available due to (3.2.2).

Left-multiplying both sides of (3.3.1) by M_k^{-1}, $G_k d_k$ can be decoupled into two parts:

$$G_k d_k = M_k^{-1}\tilde{r}_k + M_k^{-1}\tilde{G}_k\delta_k. \tag{3.3.2}$$

From (3.3.2), the dynamics of x_{k+1} can be rewritten as:

$$x_{k+1} = A_k x_k + M_k^{-1}\tilde{r}_k + M_k^{-1}\tilde{G}_k\delta_k + \omega_k = A_k x_k + u_k + F_k\delta_k + \omega_k,$$

where $u_k = M_k^{-1}\tilde{r}_k$ is a known term, and F_k is given by

$$F_k = M_k^{-1}\tilde{G}_k = [G_k, G_k^{\perp}] \begin{bmatrix} F_{0k} \\ O \end{bmatrix} = G_k F_{0k}. \tag{3.3.3}$$

Consequently, linear system (3.2.1) with the partially observed inputs $r_k = D_k d_k$

can be equivalently represented by the following system:

$$\begin{cases} x_{k+1} = A_k x_k + u_k + F_k \delta_k + \omega_k \\ y_k = C_k x_k + \upsilon_k \end{cases} \tag{3.3.4}$$

The above manipulation shows that a linear stochastic system with partially observed inputs (3.2.2) can be transformed into a linear system with both known inputs and unknown inputs.

3.3.2 Existence condition

In this subsection, the existence condition is established for a general, asymptotically stable and unbiased linear filter for system (3.3.4) and hence for its equivalent system, (3.2.1) and (3.2.2).

Motivated by the linear filter structure in the literature (e.g. [68]), a general linear filter for discrete-time linear system (3.3.4) is considered with the form

$$\hat{x}_{k+1} = E_k \hat{x}_k + J_k u_k + K_{k+1} y_{k+1}, \tag{3.3.5}$$

where the gain matrices E_k, J_k and K_{k+1} are to be designed. Based on (3.3.4) and (3.3.5), one can obtain the error dynamics $e_{k+1} = x_{k+1} - \hat{x}_{k+1}$:

$$\begin{aligned} e_{k+1} &= (A_k x_k + u_k + F_k \delta_k + \omega_k) - (E_k \hat{x}_k + J_k u_k + K_{k+1} y_{k+1}) \\ &= E_k e_k - (J_k - I + K_{k+1} C_{k+1}) u_k + (A_k - K_{k+1} C_{k+1} A_k - E_k) x_k \\ &\quad - (K_{k+1} C_{k+1} F_k - F_k) \delta_k + (I - K_{k+1} C_{k+1}) \omega_k - K_{k+1} \upsilon_{k+1}. \end{aligned}$$

To ensure the filter is unbiased, it is required that the filtering error is independent of u_k, x_k and δ_k. In addition, it is expected that the error approaches to zero as time k increases. Hence the existence condition for filter (3.3.5) is given by:

(i) E_k is stable (i.e., any eigenvalue of E_k satisfies $|\lambda(E_k)| < 1$);

(ii) $E_k = A_k - K_{k+1} C_{k+1} A_k$;

(iii) $K_{k+1} C_{k+1} F_k = F_k$;

(iv) $J_k = I - K_{k+1} C_{k+1}$.

For system (3.2.1) and (3.2.2), however, the existence condition for system (3.3.4) should be expressed in terms of matrices A_k, G_k, C_k and D_k. To this end, a lemma is first given.

Lemma 1. *For system (3.2.1) and (3.2.2), one has*

$$rank(\begin{bmatrix} zI_n - A_k & -G_k \\ C_{k+1} & O \\ O & D_k \end{bmatrix}) = rank(\begin{bmatrix} zI_n - A_k & -F_k \\ C_{k+1} & O \end{bmatrix}) + rank(D_k D_k^T).$$

See the Appendix A.2 for proof. A condition for the existence of a general linear filter for a dynamic system with partially observed inputs is provided.

Theorem 1. *Suppose that both matrices D_k^T and G_k have a full column-rank. Then a sufficient condition for the existence of a general linear filter (3.3.5) for system (3.2.1) and (3.2.2) is given by:*

$$rank(\Pi_{k+1}) = m \tag{3.3.6}$$

and for all $z \in \mathcal{C}$ ($\mathcal{C}$ is the field of complex numbers) such that $|z| \geq 1$:

$$rank(\begin{bmatrix} zI_n - A_k & -G_k \\ C_{k+1} & O \\ O & D_k \end{bmatrix}) = n + m. \tag{3.3.7}$$

Proof: It is noted that one can select matrices $E_k = A_k - K_{k+1}C_{k+1}A_k$ and $J_k = I - K_{k+1}C_{k+1}$ to ensure that condition parts (ii) and (iv) are satisfied. Hence, the focus is on condition parts (i) and (iii). It is first shown that (3.3.6) guarantees there exists a matrix K_{k+1} such that condition part (iii) holds. It is noted

$$\begin{bmatrix} D_k \\ C_{k+1}G_k \end{bmatrix} \begin{bmatrix} F_{0k} & D_k^T \end{bmatrix} = \begin{bmatrix} O_{q_k \times (m-q_k)} & D_k D_k^T \\ C_{k+1}G_k F_{0k} & C_{k+1}G_k D_k^T \end{bmatrix}. \tag{3.3.8}$$

Since $[F_{0k}, D_k^T]$ is invertible and Π_{k+1} has a full column-rank, one can obtain that $C_{k+1}G_kF_{0k} = C_{k+1}F_k$ (see, Eq. (3.3.3)) is also of full column-rank, i.e.

$$rank(C_{k+1}F_k) = m - q_k. \tag{3.3.9}$$

Eq. (3.3.9) guarantees there exists a matrix K_{k+1} such that condition part (iii) holds.

Next, since $C_{k+1}F_k$ has a full column-rank, there exists an invertible matrix

$N_k \in R^{p\times p}$ such that

$$N_k C_{k+1} F_k = \begin{bmatrix} O_{(p-m+q_k)\times(m-q_k)} \\ I_{m-q_k} \end{bmatrix}.$$

The general solution K_{k+1} of $K_{k+1}C_{k+1}F_k = F_k$ is given by $K_{k+1} = [\Gamma_k, F_k]N_k$, where Γ_k can be any matrix of suitable dimensions and is to be designed for the gain matrix K_{k+1}.

Now define S_{1k} and S_{2k} such that

$$\begin{bmatrix} S_{1k} \\ S_{2k} \end{bmatrix} = N_k C_{k+1} A_k, \tag{3.3.10}$$

Then from condition part (ii), one can obtain

$$\begin{aligned} E_k &= A_k - K_{k+1}C_{k+1}A_k \\ &= A_k - [\Gamma_k, F_k]N_k C_{k+1}A_k = A_k - [\Gamma_k, F_k]\begin{bmatrix} S_{1k} \\ S_{2k} \end{bmatrix} \\ &= A_k - F_k S_{2k} - \Gamma_k S_{1k}. \end{aligned} \tag{3.3.11}$$

According to [79] (see, pp. 342), the existence condition part (i) holds if and only if the following equivalent conditions holds:
(a) $A_k - F_k S_{2k} - \Gamma_k S_{1k}$ is stable for a matrix Γ_k;
(b) $S_{1k}\eta = 0$ and $(A_k - F_k S_{2k})\eta = \lambda\eta$ for some constant λ and vector η implies $|\lambda| < 1$ or $\eta = 0$.

The condition (b) can be expressed in the following equivalent form for all $z \in \mathcal{C}$ and $|z| \geq 1$:

$$rank(\begin{bmatrix} zI_n - A_k + F_k S_{2k} \\ S_{1k} \end{bmatrix}) = n. \tag{3.3.12}$$

The following identity, in conjunction with Lemma 1, shows that (3.3.12) is satisfied:

$$
\begin{aligned}
&rank(\begin{bmatrix} zI_n - A_k & -F_k \\ C_{k+1} & O \end{bmatrix}) = rank(\begin{bmatrix} I_n & O \\ -C_{k+1} & zI \end{bmatrix}\begin{bmatrix} zI_n - A_k & -F_k \\ C_{k+1} & O \end{bmatrix})\\
&= rank(\begin{bmatrix} zI_n - A_k & -F_k \\ C_{k+1}A_k & C_{k+1}F_k \end{bmatrix}) = rank(\begin{bmatrix} I_n & O \\ O & N_k \end{bmatrix}\begin{bmatrix} zI_n - A_k & -F_k \\ C_{k+1}A_k & C_{k+1}F_k \end{bmatrix})\\
&= rank(\begin{bmatrix} zI_n - A_k & -F_k \\ S_{1k} & O \\ S_{2k} & I_{m-q_k} \end{bmatrix}) = rank(\begin{bmatrix} zI_n - A_k + F_kS_{2k} & -F_k \\ S_{1k} & O \\ O & I_{m-q_k} \end{bmatrix})\\
&= rank(\begin{bmatrix} zI_n - A_k + F_kS_{2k} & O \\ S_{1k} & O \\ O & I_{m-q_k} \end{bmatrix}) = rank(\begin{bmatrix} zI_n - A_k + F_kS_{2k} \\ S_{1k} \end{bmatrix}) + m - q_k.
\end{aligned}
$$

Hence, Eqs. (3.3.6) and (3.3.7) guarantee there exists a gain K_{k+1} such that: (a) $K_{k+1}C_{k+1}F_k = F_k$; and (b) $E_k = A_k - K_{k+1}C_{k+1}A_k$ is stable.

Remarks:

(i) Eq. (3.3.6) is the estimability condition for the filter developed in [3] for system (3.2.1) with partially observed inputs (3.2.2). From the proof of Theorem 1, it also guarantees the unbiasedness of a general linear filter. In addition, Theorem 1 shows that to ensure the estimation error of a general linear filter is stable as time k increases, a detectability condition (3.3.7) needs to be met.

(ii) When condition (i)-(iv) is satisfied, the general linear filter (3.3.5) is given by

$$\hat{x}_{k+1} = (A_k - K_{k+1}C_{k+1}A_k)\hat{x}_k + (I - K_{k+1}C_{k+1})u_k + K_{k+1}y_{k+1}. \tag{3.3.13}$$

(iii) The error dynamics of the above filter (3.3.13) that satisfy condition (i)-(iv) become

$$e_{k+1} = (A_k - K_{k+1}C_{k+1}A_k)e_k + [I - K_{k+1}C_{k+1}, -K_{k+1}][\omega_k, \upsilon_{k+1}]^T. \tag{3.3.14}$$

3.3.3 Relationships with the existing filters

As mentioned earlier, system (3.2.1) with partially observed inputs (3.2.2) includes two important scenarios as its special cases: (a) the complete input information is available; and (b) no information on the input variables is available. In this subsection, the developed existence condition in the previous subsection for partially observed inputs is compared to the condition derived for the classical KF with complete information on the inputs, and to that of the filter with unknown inputs.

Theorem 2. *The proposed existence condition for filter (3.3.5) in Theorem 1 reduces to: (a): the existence condition of the classical KF when the complete information on the inputs is available, i.e., D_k is invertible; and (b) the existence condition of the filter with unknown inputs, i.e. D_k is an empty matrix.*

Proof: First, the case that matrix D_k is invertible is considered. It is clear that (3.3.6) is satisfied due to the non-singularity of D_k. In addition,

$$rank(\begin{bmatrix} zI_n - A_k & -G_k \\ C_{k+1} & O \\ O & D_k \end{bmatrix}) = rank(\begin{bmatrix} zI_n - A_k & O \\ C_{k+1} & O \\ O & D_k \end{bmatrix})$$
$$= rank(\begin{bmatrix} zI_n - A_k \\ C_{k+1} \end{bmatrix}) + rank(D_k D_k^T).$$

Since $rank(D_k D_k^T) = m$, the existence condition (3.3.7) reduces to

$$rank(\begin{bmatrix} zI_n - A_k \\ C_{k+1} \end{bmatrix}) = n, \forall z \in \mathcal{C}, |z| \geq 1$$

which is the detectability condition of the classical KF (see, e.g. [74, 79]).

Next, the scenario where no information on the inputs d_k is available is considered. Since matrix D_k reduces to a zero-by-zero empty matrix in this case, Eq. (3.3.6) becomes

$$rank\,(C_{k+1}G_k) = m. \tag{3.3.15}$$

In addition, Eq. (3.3.7) reduces to

$$rank(\begin{bmatrix} zI_n - A_k & G_k \\ C_{k+1} & O \end{bmatrix}) = n + m, \forall z \in \mathcal{C}, |z| \geq 1. \tag{3.3.16}$$

Eqs. (3.3.15)-(3.3.16) are identical to the results for the filter with unknown inputs [69]. This completes the proof.

Theorem 2 shows that the obtained existence condition is a more generic condition. In addition, comparing the existence condition (3.3.6) and (3.3.7) of the general linear filter (3.3.5) for systems with partially available inputs to the existence condition (3.3.15)-(3.3.16), it can be seen that partial information on the unknown inputs has relaxed the existence condition of a general linear filter. In other words, with the information on the unknown inputs at an aggregate level (3.2.2), it is more likely that the general linear filter (3.3.5) exists.

3.4 The filter with partially observed inputs

Now attention is paid on the filter proposed in [3] for linear stochastic systems when the inputs are partially observed. Note that this filter was derived under the Bayesian framework with the assumption that ω_k and υ_k follow a Gaussian distribution, and δ_k has a noninformative prior distribution. The results of the filter is summarized as below. Define

$$\tilde{D}_k = \begin{pmatrix} D_k & O_{q_k\times(n-m)} \\ O_{(n-m)\times m} & I_{n-m} \end{pmatrix}.$$

Let $\tilde{M}_k = \tilde{D}_k\Omega_k^{-1}$. It is shown in [3] that for system (3.2.1) with the input data available at an aggregate level (3.2.2), if matrix Π_k has a full column-rank, then the posterior distribution for x_k at any time step k is a Gaussian distribution with posterior mean $\hat{x}_{k|k}$ and posterior covariance matrix $P_{k|k}$ given by:

$$\begin{aligned}\hat{x}_{k|k} = A_{k-1}\hat{x}_{k-1|k-1} + P_{k|k}\tilde{M}_{k-1}^T(\tilde{M}_{k-1}P_{k|k-1}M_{k-1}^T)^{-1} \\ \times \bar{r}_{k-1} + K_k(y_k - C_kA_{k-1}\hat{x}_{k-1|k-1}),\end{aligned} \tag{3.4.1}$$

and

$$\begin{aligned}P_{k|k} = P_{k|k-1} - P_{k|k-1}C_k^TH_k^{-1}C_kP_{k|k-1} + [F_{k-1} \\ - P_{k|k-1}C_k^TH_k^{-1}C_kF_{k-1}][F_{k-1}^TC_k^TH_k^{-1}C_kF_{k-1}]^{-1} \\ \times [F_{k-1} - P_{k|k-1}C_k^TH_k^{-1}C_kF_{k-1}]^T,\end{aligned} \tag{3.4.2}$$

with

$$\begin{aligned}K_k = P_{k|k-1}C_k^TH_k^{-1} + [F_{k-1} - P_{k|k-1}C_k^TH_k^{-1}C_kF_{k-1}] \\ \times [F_{k-1}^TC_k^TH_k^{-1}C_kF_{k-1}]^{-1}F_{k-1}^TC_k^TH_k^{-1},\end{aligned} \tag{3.4.3}$$

where $\bar{r}_k = [r_k^T, O^T]^T$, $P_{k|k-1} = A_{k-1}P_{k-1|k-1}A_{k-1}^T + Q_{k-1}$ and $H_k = C_kP_{k|k-1}C_k^T + R_k > 0$. Note that (3.3.6) guarantees (3.3.9) holds, and hence $F_{k-1}^TC_k^TH_k^{-1}C_kF_{k-1}$ is invertible in the above equations.

Under the Bayesian framework, $\hat{x}_{k|k}$ was shown to be a minimum mean square error (MMSE) estimate in [3]. However, no further properties of the filter were explored. The dynamics of the state estimation error $e_k = x_k - \hat{x}_{k|k}$ will be derived.

Lemma 2. *The estimation error $e_k = x_k - \hat{x}_{k|k}$ of the filter (3.4.1)-(3.4.3) follows the recursive equation*

$$e_k = (A_{k-1} - K_kC_kA_{k-1})e_{k-1} + [I - K_kC_k, -K_k][\omega_{k-1}, \upsilon_k]^T, \tag{3.4.4}$$

where K_k is given by (3.4.2)-(3.4.3).

Proof: Let $W_{k-1} = P_{k|k}\tilde{M}_{k-1}^T(\tilde{M}_{k-1}P_{k|k-1}\tilde{M}_{k-1}^T)^{-1}$. The error dynamics of the filter (3.4.1)-(3.4.3) are given by

$$\begin{aligned} e_k &= A_{k-1}x_{k-1} + G_{k-1}d_{k-1} + \omega_{k-1} - A_{k-1}\hat{x}_{k-1|k-1} \\ &\quad - W_{k-1}\bar{r}_{k-1} - K_k(y_k - C_kA_{k-1}\hat{x}_{k-1|k-1}) \\ &= (A_{k-1} - K_kC_kA_{k-1})e_{k-1} + (G_{k-1} - K_kC_kG_{k-1})d_{k-1} \\ &\quad - W_{k-1}\bar{r}_{k-1} + (I - K_kC_k)w_{k-1} - K_kv_k. \end{aligned}$$

Noting that $\bar{r}_{k-1} = \tilde{M}_{k-1}G_{k-1}d_{k-1}$, one can obtain

$$\begin{aligned} &(G_{k-1} - K_kC_kG_{k-1})d_{k-1} - W_{k-1}\bar{r}_{k-1} \\ &= [I - K_kC_k - W_{k-1}\tilde{M}_{k-1}]G_{k-1}d_{k-1}. \end{aligned} \tag{3.4.5}$$

Inserting (3.4.2) and (3.4.3) into (3.4.5), one can obtain (3.4.4) by noting that $I - K_kC_k - W_{k-1}\tilde{M}_{k-1} = O$. This completes the proof.

Lemma 2 shows that, for the gain K_k given in Eqs. (3.4.2)-(3.4.3), if $A_{k-1} - K_kC_kA_{k-1}$ is stable, the error of the developed filter in [3] will be stable as time k increases. In addition, the estimation error (3.4.4) shares the same structure as that of (3.3.14), upon which one can conclude that the filter (3.4.1)-(3.4.3) falls into the filter family with the generic linear structure (3.3.5).

Now the error covariance matrix $P_{k|k}$ is considered.

Theorem 3. *Let $\tilde{P}_{k|k}$ denote the error covariance matrix of any filter $\hat{x}_k(Y_k)$ based on the sequence of measurements $Y_k = \{y_0, y_1, \cdots, y_k\}$. Then for linear system (3.2.1) with partially observed inputs (3.2.2), one has $\tilde{P}_{k|k} \geq P_{k|k}$, where $P_{k|k}$ is given by (3.4.2).*

Proof: By definition, the conditional covariance matrix of the estimate $\hat{x}_k(Y_k)$ for given Y_k is

$$\tilde{P}_{k|k} = E\{[x_k - \hat{x}_k(Y_k)][x_k - \hat{x}_k(Y_k)]^T|Y_k\}.$$

It is easy to verify the following identity:

$$\begin{aligned} \tilde{P}_{k|k} &= E\{[x_k - \hat{x}_{k|k} + \hat{x}_{k|k} - \hat{x}_k(Y_k)][x_k - \hat{x}_{k|k} + \hat{x}_{k|k} - \hat{x}_k(Y_k)]^T|Y_k\} \\ &= P_{k|k} + E\{[\hat{x}_{k|k} - \hat{x}(Y_k)][\hat{x}_{k|k} - \hat{x}_k(Y_k)]^T|Y_k\} \\ &\quad + E\{[x_k - \hat{x}_{k|k}][\hat{x}_{k|k} - \hat{x}_k(Y_k)]^T|Y_k\} + E\{[\hat{x}_{k|k} - \hat{x}_k(Y_k)][x_k - \hat{x}_{k|k}]^T|Y_k\}. \end{aligned}$$

Li [3] shows that the estimated state vector $\hat{x}_{k|k}$ in (3.4.1) is the posterior mean conditional on the sequence of measurements $Y_k = \{y_0, y_1, \cdots, y_k\}$. Hence, one has $E\{x_k|Y_k\} = \hat{x}_{k|k}$ and the last two terms on the right-hand side of the above equation

vanish, i.e.

$$\tilde{P}_{k|k} = P_{k|k} + E\{[\hat{x}_{k|k} - \hat{x}(Y_k)][\hat{x}_{k|k} - \hat{x}_k(Y_k)]^T | Y_k\}.$$

It is thus concluded that $\tilde{P}_{k|k}$ attains the minimum if and only if the second term of the right-hand side is equal to zero, i.e. $\hat{x}_k(Y_k) = \hat{x}_{k|k}$. This completes the proof.

Theorem 3 shows that the filter given by Eqs. (3.4.1)-(3.4.3) is optimal in the sense of both MMSE and minimum covariance matrix. This result is not only important in its own right but also useful in the subsequent asymptotic stability analysis.

3.5 Asymptotic stability

In this section, the asymptotic stability of the filter developed in [3] for time-invariant system (3.2.1) and (3.2.2) is discussed. Hence the subscript k of matrices A_k, G_k, C_k, D_k, Q_k and R_k is suppressed.

Noting from Lemma 2 that the covariance matrix in (3.4.2) can be re-written as

$$\begin{aligned} P_{k|k} = {} & (A - K_k CA) P_{k-1|k-1} (A - K_k CA)^T \\ & + (I - K_k C) Q (I - K_k C)^T + K_k R K_k^T. \end{aligned} \tag{3.5.1}$$

Under the condition given in Theorem 1 and in conjunction with Theorem 3 that the covariance matrix of the filter given by (3.4.1)-(3.4.3) is optimal, it can be shown that the covariance matrix $P_{k|k}$ in (3.5.1) is bounded for all k and for an arbitrary bounded initial covariance $P_{0|0}$. On the basis of boundedness of $P_{k|k}$ and inspired by the approaches in [72, 79], one can further show the following result.

Theorem 4. *If the condition in Theorem 1 is satisfied and $(A, Q^{\frac{1}{2}})$ is stabilizable, then the covariance matrix $P_{k|k}$ of the filter filter (3.4.1)-(3.4.3) will converge to a unique fixed positive semi-definite matrix $\bar{P}$ for any given initial condition $P_{0|0}$. Moreover, with the associated limiting gain matrices $\bar{K}$, the time-invariant filter is also stable, i.e. all the eigenvalues of $A - \bar{K}CA$ satisfy $|\lambda(A - \bar{K}CA)| < 1$.*

The proof is given in Appendix A.2.

It is of interest to compare the asymptotic stability condition obtained with partially observed inputs to the asymptotic stability conditions when the complete information on the inputs is available and when the inputs are completely unknown. This is investigated in the following theorem. It shows that Theorem 4 provides a

unified approach to accommodating asymptotic stability conditions in a variety of filtering scenarios.

Theorem 5. *The asymptotic stability condition for the filter (3.4.1)-(3.4.3) in Theorem 4 reduces to: (a): the asymptotic stability condition of the classical Kalman filter when the complete information on the inputs is available, i.e. D is invertible; and (b) the asymptotic stability condition of the filter with unknown inputs, i.e. D is an empty matrix.*

Proof: First, one notes that when matrix D is invertible, the asymptotic stability condition reduces to: (a) (A, C) is detectable; and (b) $(A, Q^{\frac{1}{2}})$ is stabilizable. These are the asymptotic stability condition of the classical KF (see, e.g. [79]).

Next, when no information on the inputs is available, one knows from Theorem 2 that (3.3.7) in Theorem 1 reduces to (3.3.16). In addition, condition $(A, Q^{\frac{1}{2}})$ along with $R > 0$ (and hence $R^{\frac{1}{2}} > 0$) can guarantee that the matrix below has a full row-rank, i.e.,

$$\begin{aligned} &rank(\begin{bmatrix} A - e^{jw}I & G & Q^{\frac{1}{2}} & O \\ e^{jw}C & O & O & R^{\frac{1}{2}} \end{bmatrix}) \\ &= n + p, \forall w \in [0, 2\pi]. \end{aligned} \tag{3.5.2}$$

Eqs. (3.3.16) and (3.5.2) are identical to the asymptotic stability condition for the filter with unknown inputs [69]. This completes the proof.

3.6 Extension to SISE

The problem of SISE for system (3.2.1) and (3.2.2) is then considered. Bayesian inference is drawn to obtain recursive estimates of both state variables x_k and unknown inputs δ_k for system (3.3.4), upon which the estimate of the original input vector d_k is obtained. The relationships between the proposed method and the relevant existing filters are discussed. The diagram of the system and the proposed filter structure is shown in Fig. 3.2.

3.6.1 Filter design

It can be seen from Eq. (3.3.4) that y_k is a function of x_k, and x_k is related to the unknown inputs δ_{k-1}. Hence the unknown input estimate of δ_k is delayed by one time unit [2]. The objective of filter design is to obtain the estimate of x_k and δ_{k-1} based on the available measurement sequence $Y_k = \{y_1, y_2, \ldots, y_k\}$. For the new system (3.3.4), one can either solve the filtering problem based on the approach

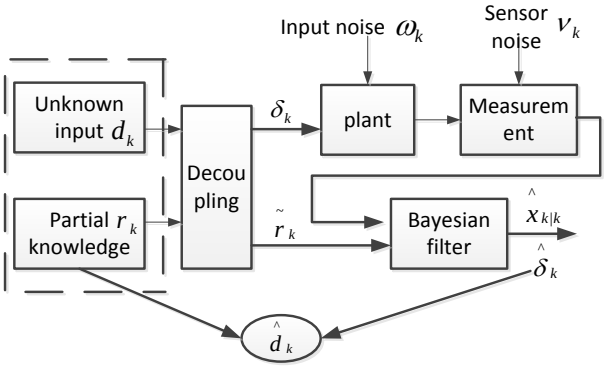

Figure 3.2. Diagram of the system and filter structure.

of minimum variance unbiased estimation (MVUE) (e.g. [2]) or Bayesian inference (e.g. [3, 59, 78]). The Bayesian method is used which can be seen as an alternative approach to that of [2].

In the context of Bayesian inference, the first step is to predict the dynamics of x_k and δ_{k-1} based on the available measurement sequence $Y_{k-1} = \{y_1, y_2, \ldots, y_{k-1}\}$. Since it is not assumed that the unknown input vector δ_k satisfies any transition dynamics, prediction is only performed to determine the dynamics of x_k, i.e. $p(x_k|Y_{k-1})$. The likelihood function can be determined based on the observation equation of system (3.3.4). The second step is to obtain the posterior distribution of the concerned variables after the measurement vector y_k is received based on Bayes' chain rule:

$$p(x_k, \delta_{k-1}|Y_k) \propto p(y_k|x_k)p(x_k, \delta_{k-1}|Y_{k-1}). \tag{3.6.1}$$

The main results on filtering design are summarised in Theorem 6.

Theorem 6. *For state space model (3.3.4), suppose the matrix C_kF_{k-1} has a full column-rank, then the prior and posterior distribution for x_k and δ_{k-1} at any time step k can be obtained sequentially as follows:*

(i) Posterior of x_{k-1} for given Y_{k-1}: $x_{k-1} \sim N(\hat{x}_{k-1|k-1}, P^x_{k-1|k-1})$.
(ii) Prediction for x_k:
$N(\hat{x}_{k|k-1}, P^x_{k|k-1})$, *with* $\hat{x}_{k|k-1} = A_{k-1}\hat{x}_{k-1|k-1} + M^{-1}_{k-1}\tilde{r}_{k-1}$,

$$P^x_{k|k-1} = A_{k-1}P^x_{k-1|k-1}A^T_{k-1} + Q_{k-1}. \tag{3.6.2}$$

(iii) Posterior of δ_{k-1} for given Y_k: $\delta_{k-1} \sim N(\hat{\delta}_{k-1}, P^\delta_{k|k})$.

where the posterior mean is given by

$$\hat{\delta}_{k-1} = P^{\delta}_{k|k}(C_k F_{k-1})^T \tilde{R}_k^{-1}(y_k - C_k \hat{x}_{k|k-1}), \tag{3.6.3}$$

and the posterior covariance matrix is given by

$$P^{\delta}_{k|k} = (F_{k-1}^T C_k^T \tilde{R}_k^{-1} C_k F_{k-1})^{-1}, \tag{3.6.4}$$

while posterior of x_k for given Y_k is: $x_k \sim N(\hat{x}_{k|k}, P^x_{k|k})$,
where the posterior mean is given by

$$\begin{aligned} \hat{x}_{k|k} = \hat{x}_{k|k-1} &+ P^x_{k|k-1} C_k^T \tilde{R}_k^{-1}(y_k - C_k \hat{x}_{k|k-1}) \\ &+ (F_k - P^x_{k|k-1} C_k^T \tilde{R}_k^{-1} C_k F_k)\hat{\delta}_{k-1}, \end{aligned} \tag{3.6.5}$$

and the posterior covariance matrix is given by

$$\begin{aligned} &P^x_{k|k} = P^x_{k|k-1} - P^x_{k|k-1} C_k^T \tilde{R}_k^{-1} C_k P^x_{k|k-1} \\ &+(F_{k-1} - P^x_{k|k-1} C_k^T \tilde{R}_k^{-1} C_k F_{k-1})(P^{\delta}_{k|k})^{-1}(F_{k-1} - P^x_{k|k-1} C_k^T \tilde{R}_k^{-1} C_k F_{k-1})^T, \end{aligned} \tag{3.6.6}$$

where $\tilde{R}_k = C_k P^x_{k|k-1} C_k^T + R_k$, $()^T$ in $(*)A()^T$ stands for the transpose of $*$.

Proof From Eq. (3.6.1), the posterior distribution $p(x_k, \delta_{k-1}|Y_k)$ is governed by:

$$\begin{aligned} &p(x_k, \delta_{k-1}|Y_k) \propto exp\{-(y_k - C_k x_k)^T R_k^{-1}(y_k - C_k x_k) \\ &-(x_k - \hat{x}_{k|k-1} - F_{k-1}\delta_{k-1})^T (P^x_{k|k-1})^{-1}(x_k - \hat{x}_{k|k-1} - F_{k-1}\delta_{k-1})\}. \end{aligned}$$

By completing the square on $[x_k^T, \delta_{k-1}^T]^T$, the exponent can be rewritten as $-([x_k^T, \delta_{k-1}^T] - [\hat{x}_{k|k}^T, \hat{\delta}_{k-1}^T])P^{-1}_{k|k}()^T$, where

$$\begin{bmatrix} \hat{x}_{k|k} \\ \hat{\delta}_{k-1} \end{bmatrix} = P_{k|k} \begin{bmatrix} C_k^T R_k^{-1} y_k + (P^x_{k|k-1})^{-1}\hat{x}_{k|k-1} \\ -F_{k-1}^T (P^x_{k|k-1})^{-1} x_{k|k-1} \end{bmatrix}$$

and

$$P_{k|k} = \begin{bmatrix} C_k^T R_k^{-1} C_k + (P^x_{k|k-1})^{-1} & -(P^x_{k|k-1})^{-1} F_{k-1} \\ -F_{k-1}^T (P^x_{k|k-1})^{-1} & F_{k-1}^T (P^x_{k|k-1})^{-1} F_{k-1} \end{bmatrix}^{-1}.$$

This indicates that the posterior distribution is a Gaussian distribution with mean $[\hat{x}_{k|k}^T, \hat{\delta}_{k-1}^T]^T$ and covariance matrix $P_{k|k}$. When $C_k F_{k-1}$ is of full row-rank, based on the inverse of partitioned matrix, one can obtain the recursive estimation of both x_k and δ_{k-1} as shown in Eqs. (3.6.2) to (3.6.6).

So far, the state estimate $\hat{x}_{k|k}$ and estimate $\hat{\delta}_{k-1}$ for the transformed system have been obtained. When $F_{0k-1}^T d_{k-1} = \hat{\delta}_{k-1}$ is obtained, based on Eq. (3.3.2) one

can further obtain the estimate of the original unknown inputs d_{k-1} as follows:

$$\hat{d}_k = (G_k^T G_k)^{-1} G_k^T (M_k^{-1} \tilde{r}_k + M_k^{-1} \tilde{G}_k \hat{\delta}_k) \ .$$

It can be verified that the obtained unknown input estimate satisfies the unknown input information Eq. (3.2.2), i.e.,

$$D_k \hat{d}_k = r_k. \tag{3.6.7}$$

The proof is given in the Appendix A.2.

Remark: The proposed SISE filter can be seen as a Full Order Disturbance OBserver (FODOB) since all the state information is required in derivation of the disturbance estimates. Besides, from the results of ULF in [3] and the proposed SISE filter, one can find that the existence of ULF can guarantee the existence of SISE, consequently the existence results on ULF established in the first part of this Chapter can guarantee the existence of SISE filter proposed in the second part of this Chapter.

3.6.2 Relationships with the existing results

In this subsection, the relationships between the proposed approach and the relevant results in the existing literature are investigated, which is summarized in the Theorem 7.

Theorem 7. *The set of recursive formulas (3.6.2) to (3.6.6) reduces to:*

1. *the classical Kalman filter when all entries of the input vector d_k are available;*
2. *the filter in [2] when no information on the unknown inputs d_k is available;*
3. *the filter in [3]when only state estimation is concerned.*

Proof: For the case where all the input variables are available at the level of interest, D_k becomes an $m \times m$ identity matrix, and F_{0k}^T becomes an zero-by-zero empty matrix. Consequently the last term on the right-hand-side of (3.6.5) and (3.6.6) vanishes, and (3.6.5) and (3.6.6) reduces to

$$P_{k|k}^x = P_{k|k-1}^x - P_{k|k-1}^x C_k^T H_k^{-1} C_k P_{k|k-1}^x.$$

Since $M_{k-1}^{-1}\hat{r}_{k-1} = G_{k-1}d_{k-1}$, Eq. (3.6.5) becomes

$$\begin{aligned}\hat{x}_{k|k} = {} & A_{k-1}\hat{x}_{k-1|k-1} + G_{k-1}d_{k-1} \\ & + P_{k|k-1}^{x}C_k^T H_k^{-1}(y_k - C_k(A_{k-1}\hat{x}_{k-1|k-1} + G_{k-1}d_{k-1})).\end{aligned}$$

Clearly, these recursive formulas are identical to the classical Kalman filter [74].

Next, consider the case where no input information is available. Clearly $\tilde{r}_k$ is an empty vector, F_k becomes G_k, and $\delta_k = d_k$. Hence, Eq. (3.6.6) reduces to

$$\begin{aligned}P_{k|k}^{x} = {} & P_{k|k-1}^{x} - P_{k|k-1}^{x}C_k^T\tilde{R}_k^{-1}C_kP_{k|k-1}^{x} \\ & + [G_k - P_{k|k-1}^{x}C_k^T H_k^{-1}C_kG_{k-1}]P_{k|k}^{\delta}[G_k - P_{k|k-1}^{x}C_k^T H_k^{-1}C_kG_{k-1}]^T\end{aligned}$$

and the unknown input covariance matrix (3.6.4) becomes

$$P_{k|k}^{\delta} = (G_{k-1}^T C_k^T \tilde{R}_k^{-1} C_k G_{k-1})^{-1}.$$

In addition, Eq. (3.6.5) becomes

$$\hat{x}_{k|k} = \hat{x}_{k|k-1} + P_{k|k-1}^{x}C_k^T\tilde{R}_k^{-1}(y_k - C_k\hat{x}_{k|k-1}) + (G_k - P_{k|k-1}^{x}C_k^T\tilde{R}_k^{-1}C_kG_k)\hat{\delta}_{k-1}$$

and the unknown input estimation Eq. (3.6.3) becomes

$$\hat{\delta}_{k-1} = P_{k|k}^{\delta}(C_kG_{k-1})^T\tilde{R}_k^{-1}(y_k - C_k\hat{x}_{k|k-1}).$$

These recursive formulas are identical to: (a) the results in [67] when only state filtering is of interest; and (b) the results in [2] for both unknown input and state estimation obtained using the approach of minimum variance unbiased estimation.

Finally, if only state estimation is concerned, the proposed method leads to the same results as those in [3]. To show this, it is noted that the state estimation error covariance matrix Eq. (3.6.6) is the same as the one in [3]. In addition, inserting Eqs. (3.6.3) and (3.6.4) into Eq. (3.6.5), Eq. (3.6.5) can be rewritten in the following form:

$$\hat{x}_{k|k} = \hat{x}_{k|k-1} + K_k(y_k - C_k\hat{x}_{k|k-1})$$

where the gain matrix K_k is defined as

$$K_k = P_{k|k-1}^{x}C_k^T\tilde{R}_k^{-1} + +[F_{k-1} - P_{k|k-1}^{x}C_k^T\tilde{R}_k^{-1}C_kF_{k-1}](P_{k|k}^{\delta})^{-1}F_{k-1}^T C_k^T\tilde{R}_k^{-1}.$$

It can be further shown that (see Appendix A.2 for details)

$$M_{k-1}^{-1}\tilde{r}_{k-1} - K_k C_k M_{k-1}^{-1}\tilde{r}_{k-1} = P_{k|k}\bar{M}_{k-1}^T(\bar{M}_{k-1}P_{k|k-1}\bar{M}_{k-1}^T)^{-1}\bar{r}_{k-1} \tag{3.6.8}$$

where the left hand side of Eq. (3.6.8) is the term associated with the prior information of the proposed filter, whereas the right hand side of Eq. (3.6.8) is the term associated with the prior information of the filter in [3]. This completes the proof.

3.7 Simulation study

In this section, a numerical example is given to illustrate the developed filter. First, it will be shown that, when only state estimation is of interest, the proposed filter can obtain the same result as that of [3]. Next it is further demonstrated that incorporating the partially available information on the unknown inputs can effectively improve on both state estimation and unknown input estimation in comparison with the one without using the unknown input knowledge [2].

The system for the simulation is chosen the same as that of [80] that has been widely used in many previous studies (see, e.g., [71]). However, to better assess the performance of the proposed filter under uncertainties, a system subject to larger random variation is considered: the covariance matrices Q_k and R_k of the system and measurement noises were taken 10 times as those of [71]. The detailed matrices are given as follows.

$$A_k = \begin{bmatrix} 0.5 & 2 & 0 & 0 & 0 \\ 0 & 0.2 & 1 & 0 & 1 \\ 0 & 0 & 0.3 & 0 & 1 \\ 0 & 0 & 0 & 0.7 & 1 \\ 0 & 0 & 0 & 0 & 0.1 \end{bmatrix}, G_k = \begin{bmatrix} 1 & 0 & 0 \\ 0 & 0 & 0 \\ 0 & 1 & 0 \\ 0 & 0 & 0 \\ 0 & 0 & 0.1 \end{bmatrix},$$

$$Q_k = 10^{-2} \times \begin{bmatrix} 1 & 0 & 0 & 0 & 0 \\ 0 & 1 & 0.5 & 0 & 0 \\ 0 & 0.5 & 1 & 0 & 0 \\ 0 & 0 & 0 & 1 & 0 \\ 0 & 0 & 0 & 0 & 1 \end{bmatrix}, R_k = 10^{-1} \times \begin{bmatrix} 1 & 0 & 0 & 0.5 & 0 \\ 0 & 1 & 0 & 0 & 0.3 \\ 0 & 0 & 1 & 0 & 0 \\ 0.5 & 0 & 0 & 1 & 0 \\ 0 & 0.3 & 0 & 0 & 1 \end{bmatrix},$$

and $C_k = I_5$ is a 5×5 identity matrix. Q_k and R_k are the input and sensor noise covariance matrices respectively.

To investigate the effect of partial information of unknown inputs on state filtering performance, it is further assumed that the unknown input variables are

observed at an aggregate level with

$$D_k = \begin{bmatrix} 1 & 0 & 1 \\ 0 & 1 & 1 \end{bmatrix}.$$

For the input vector $d_k = [d_{1k}, d_{2k}, d_{3k}]^T$, this means that the information on $d_{1k} + d_{3k}$ and $d_{2k} + d_{3k}$ is available at each time step although each individual input is unknown.

The recursive formulas are applied to estimate the state and unknown input vectors at each time step. To evaluate the quality of the state estimate and unknown input estimate obtained using the developed filter, one can calculate the trace of the error covariance matrix $P^x_{k|k}$ and the trace of the error covariance matrix $P^\delta_{k|k}$ at each time step, as displayed in Fig. 3.3 (a) and Fig. 3.3 (b) (real red line), respectively. For comparison, the state estimation algorithms using the filter in [3] (only state estimation is concerned) and [2] (assuming the inputs were completely unknown) are also considered. The traces of $P^x_{k|k}$ are superimposed in Fig. 3.3 (a) (dotted line for [3] and dashed line for [2]), and the trace of $P^\delta_{k|k}$ is superimposed in Fig. 3.3 (b) (dashed line for [2]).

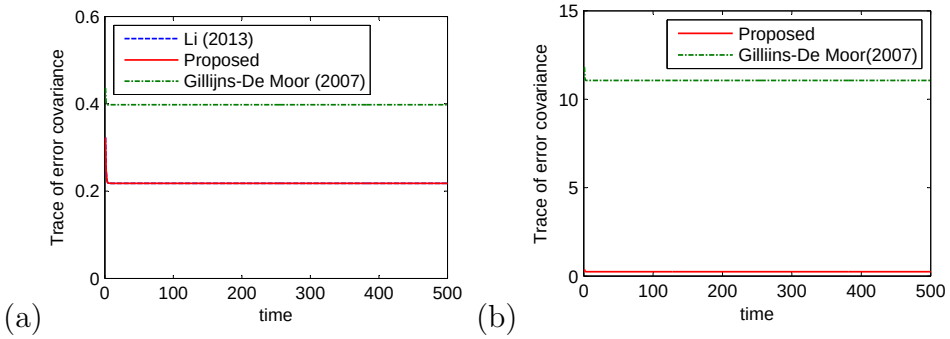

Figure 3.3. (a) Traces of the covariance matrix $P^x_{k|k}$ for three different filters; (b) Traces of the covariance matrix $P^\delta_{k|k}$ for the proposed approach and the filter in [2].

It can be seen from Fig. 3.3 (a) that the trace of state estimation error covariance using the proposed filter is the same as that of [3]. Both the method in [3] and the proposed method have a smaller trace of the covariance matrix than that of [2].

In addition, Fig. 3.3 (b) shows that the trace of the error covariance matrix of the unknown input estimate using the proposed filter is smaller in comparison with that of [2]. This is because more information on the unknown inputs was used by the filter developed. This demonstrates that when the unknown inputs are of practical interest, the proposed method will have a better performance than [2] if

there is additional information available on the unknown inputs for filtering.

The state estimates obtained using the three filters are also compared, i.e., the filter in [3] (Fig. 3.4), the proposed filter (Fig. 3.5) and the filter in [2] (Fig. 3.6). The upper graphs of Figs. 3.4-3.6 display the simulated true values of the fifth state variable (real line) and the estimated state using the filters (dotted line), while the lower graphs plot the corresponding state estimation error for each filter.

It can be seen from Figs. 3.4-3.6 that the three methods can provide a reasonably good estimate of the state vector. However, overall the state estimation errors using the proposed filter and the filter in [3] are smaller compared with that of [2] because the additional unknown input information was incorporated into the proposed filter and that of [3].

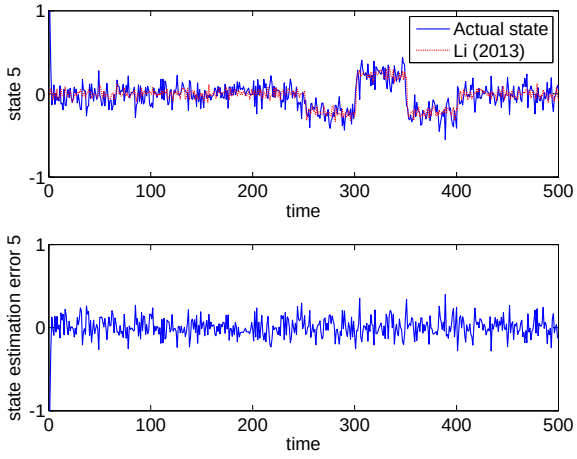

Figure 3.4. State estimation of the filter in [3] and its estimation error.

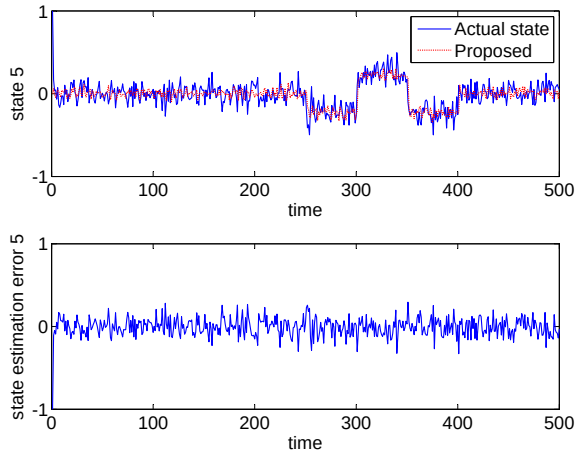

Figure 3.5. State estimation of the proposed filter and its estimation error.

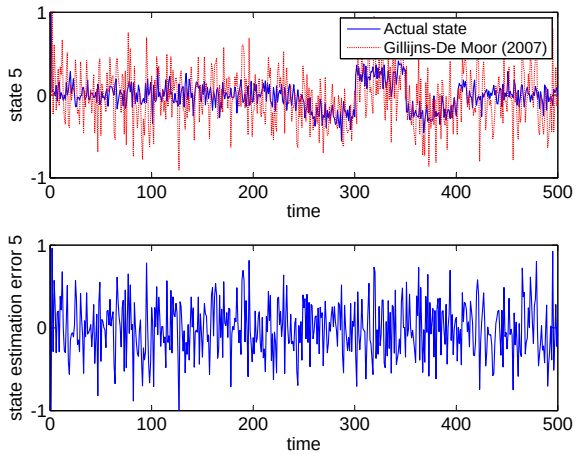

Figure 3.6. State estimation of the filter in [2] and its estimation error.

Finally, the proposed method is further compared with the results in [2] for the purpose of unknown inputs estimation. The comparison results are shown in Fig. 3.7 (the proposed method) and Fig. 3.8 (the method in [2]), where real unknown inputs are depicted by real lines, and the unknown input estimations are depicted by the dotted lines.

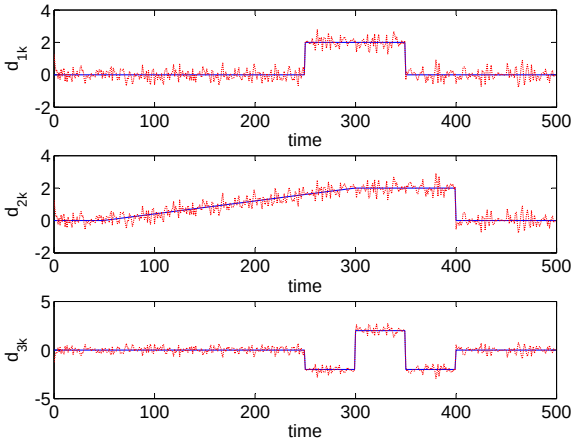

Figure 3.7. Unknown input estimation based on the proposed filter.

One can see from Figs. 3.7 and 3.8 that, by incorporating the information on the unknown inputs, the proposed method can obtain a much better performance for the unknown input estimation.

3.8 Summary

This Chapter first established existence and asymptotic stability conditions for the recently developed filter with partially observed inputs in [3]. The obtained existence

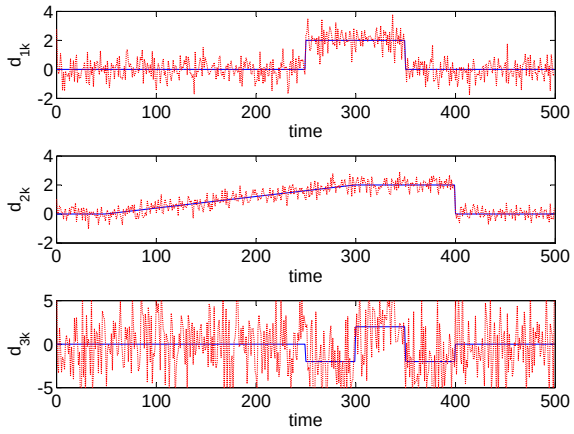

Figure 3.8. Unknown input estimation based on the filter in [2].

and asymptotic stability conditions provide a unified approach to accommodating a variety of filtering scenarios as its special cases, including the important Kalman filter and the unknown input filtering problems. On this basis, Bayesian inference is drawn to obtain simultaneous input and state estimation. The relationships of the proposed approach with the existing results are also discussed. Numerical example shows that, in comparison with the filter without using any input information, the proposed filter that makes use of the input information available at an aggregate level can substantially improve on the quality of both the state and input estimation.

Chapter 4

RODOB: WITH DISTURBANCE MODEL

4.1 Introduction

In Chapter 3, the problem of state filter in the presence of unknown inputs was considered. On this basis, the problem of simultaneous input and state filter was further considered, where no explicit assumption is made on the unknown inputs. In this Chapter the unknown input estimation problem is considered, where a slowly time-varying disturbance assumption is assumed. The contribution of this Chapter is illustrated in Fig. 4.1.

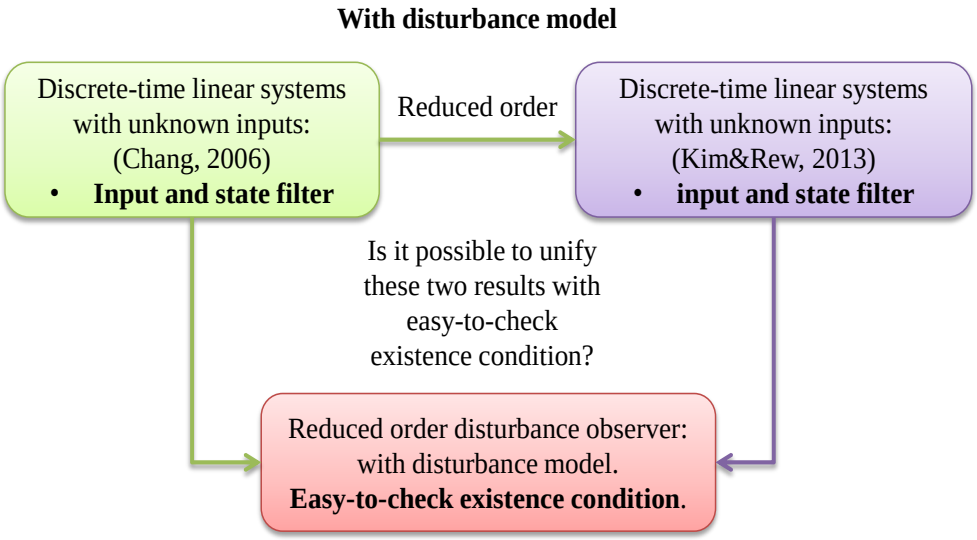

Figure 4.1. Illustration of the relationship between this Chapter with the existing results.

Different from the second part of Chapter 3, in this Chapter the focus is on *reduced order disturbance observer (RODOB) design*. Practically, there are three major reasons why a RODOB is needed. Firstly, in areas such as fault diagnosis, an

estimate of the entire states may not be necessary for the purpose of fault estimation [61]. Secondly, there are some practical scenarios where disturbance estimation is required even if the states are not fully estimable [81]. Finally, when a fast disturbance estimate is required, DOBs with a smaller order are more desirable [1].

The conventional DOBs assume that all the system states are estimable or even directly measurable, and consequently the disturbance estimation is dependent on the estimated system states. For example, the researchers in [1] proposed a DOB by treating the disturbances as additional states and estimating them using a deadbeat function observer [82] under the assumption that the augmented systems are completely observable and the disturbances can be approximated by known transition dynamics. A proportional integral observer was used in [58] for simultaneous estimation of system states and unknown disturbances under the slowly time-varying disturbances and state observability assumptions. On the other hand, to relax the assumption on disturbances and incorporate noise information for stochastic systems, the authors in [2] proposed a simultaneous state and disturbance observer on the basis of [69] using the minimum-variance-unbiased-estimation (MVUE) method. The assumption that the states are fully estimable inevitably restricts the applications of the FODOs. An important earlier work of RODOB can be traced back to [61] where the concept of state function observer based on the Lyapunov approach was investigated for continuous-time systems. Recently, a RODOB has been proposed in [57] by combining a state function estimator of minimal order and a full measurable state based DOB [4]. The existence condition in [4], however, involves a static output feedback problem, for which the general solvability is not known yet. It also depends on an assumption that the disturbances are slowly time-varying.

Consequently, the RODOB design is further improved by being formulated as a state functional observer problem. By carefully designing the state functional matrix L in the functional observer theory, a generic RODOB is resulted with an easily-checked existence condition. It is also shown that both the RODOB in [4] and the full order disturbance observer (FODOB) in [58] are special cases of the new RODOB.

4.2 Existing results

Motivated by the applications in disturbance rejection control and fault diagnosis, a discrete-time FODOB was proposed in [58]. To reduce the observer order and relax the existence condition, a RODOB was proposed in [57] to reconstruct disturbances/faults with a minimal observer order for continuous-time linear systems.

Recently, this work has been extended to the case of discrete-time linear systems in [4]. The discrete-time linear system under consideration (the matrix notations are directly borrowed from [4]) is

$$\begin{cases} x_{k+1} = \Phi x_k + \Gamma u_k + G d_k, \\ y_k = C x_k, \end{cases} \tag{4.2.1}$$

where $x_k \in \mathbb{R}^n$, $u_k \in \mathbb{R}^m$, $d_k \in \mathbb{R}^q$ and $y_k \in \mathbb{R}^l$ are the states, control inputs, disturbances and measurements at k^{th} step, respectively. G is supposed to have a full column-rank, i.e., $rank(G) = q$. The disturbances d_k are assumed to be unknown but slowly time-varying, i.e., the following assumption is assumed:

$$d_{k+1}^i = d_k^i + \Delta d_{k+1}^i, \tag{4.2.2}$$

with $d_k := [d_k^1, \cdots, d_k^q]^T$, $|\Delta d_{k+1}^i| = |d_{k+1}^i - d_k^i| \leq T\mu_i$ where T is the sampling time, μ_i is a small positive value. In practical application, if μ_i is not small enough, the disturbance estimate performance may not satisfy the specification.

Define $N_c := (I_n - C^+C)$ with C^+ being the Moore-Penrose pseudo-inverse of C and define H_e as

$$H_e := \begin{bmatrix} KN_c \\ K(\Phi - I_n)N_c \end{bmatrix} = \begin{bmatrix} H_1 \\ H_2 \end{bmatrix} V^T,$$

with K being a deigned gain matrix, $H_1 \in \mathbb{R}^{q\times h}$, $H_2 \in \mathbb{R}^{q\times h}$, $V^T \in \mathbb{R}^{h\times n}$ with $h = rank(H_e)$.

Defining $\eta_k := V^T x_k \in \mathbb{R}^h$, the RODOB constructed in [4] is given by

$$\begin{cases} \xi_{k+1} = R\xi_k + Sy_k + W_u u_k + W_d \hat{d}_k, \\ \hat{\eta}_k = \xi_k + Qy_k, \\ z_{k+1} = z_k + K\{(\Phi - I_n)C^+ y_k + \Gamma u_k\} + KG\hat{d}_k + H_2\hat{\eta}_k, \\ \hat{d}_k = KC^+ y_k - z_k + H_1\hat{\eta}_k, \end{cases} \tag{4.2.3}$$

where $z_k \in \mathbb{R}^q$ and $\xi_k \in \mathbb{R}^h$, $W_u = (V^T - QC)\Gamma$, $W_d = (V^T - QC)G$ for the matrices S, Q, R satisfying

$$(V^T - QC)\Phi - R(V^T - QC) - SC = 0. \tag{4.2.4}$$

Denoting the disturbance estimation error and the state function estimation error as $e_k = d_k - \hat{d}_k$ and $\epsilon_k = \eta_k - \hat{\eta}_k$ respectively, the composite error dynamic consisting

of both state function η_k and disturbance d_k estimation errors is given by [4]

$$\begin{bmatrix} e_{k+1} \\ \epsilon_{k+1} \end{bmatrix} = A_e \begin{bmatrix} e_k \\ \epsilon_k \end{bmatrix} + \begin{bmatrix} \Delta d_{k+1} \\ O_{h\times 1} \end{bmatrix},$$

where the composite error matrix A_e is defined as

$$A_e = \begin{bmatrix} I_q - KG + H_1(V^T - QC)G & H_1R - H_1 - H_2 \\ (V^T - QC)G & R \end{bmatrix}. \tag{4.2.5}$$

As pointed out by [4], the existence of a stable RODOB in (4.2.3) depends on whether there exists a gain K and other design parameters such that: (i). the Sylvester equation (4.2.4) holds; (ii). matrix A_e in (4.2.5) is asymptotically stable (i.e., the amplitudes of its eigenvalues are less than 1). Condition (i) is implied by the matrix rank equality

$$rank(\begin{bmatrix} Z_1 \\ V^T\Phi \end{bmatrix}) = rank(Z_1) \ , Z_1 := rank(\begin{bmatrix} C \\ C\Phi \\ V^T \end{bmatrix}). \tag{4.2.6}$$

However, condition (ii) is not easy to check directly. The existence problem is related to a static output feedback problem. As pointed out in [57] and [4], although numerical solutions are available, the general solvability of the static output feedback is not known.

To further develop this promising approach, this note improves the results in [4] by presenting a generic RODOB with an easily-checked existence condition.The disturbance observer design is transformed into a problem of state functional observer (SFO) design (see, [83, 84], etc.). This is achieved by first augmenting the disturbances with the state and then carefully designing the state functional matrix L. Consequently a generic RODOB is resulted with the necessary and sufficient existence condition. A promising feature of the new RODOB is that the corresponding existence condition is easy to check. On this basis, the relationship between the new RODOB with the RODOB in [4] and the FODOB in [58] is investigated in terms of the observer structure and existence condition.

4.3 RODOB design with SFO techniques

SFO firstly introduced in [23] received much attention in the field of control (see, [83, 84]) due to its properties such as lower observer order. Its existence condition

has been rigorously established in [83]. However, less attention has been paid on its applications in disturbance or fault estimation.

4.3.1 Observer design

Combining systems (4.2.1) and (4.2.2), and defining $\bar{x}_k = [x_k^T, d_k^T]^T$, an augmented system can be obtained as

$$\begin{cases} \bar{x}_{k+1} = \bar{A}\bar{x}_k + \bar{\Gamma}u_k + \Delta\bar{d}_k, \\ y_k = \bar{C}\bar{x}_k, \end{cases} \tag{4.3.1}$$

where the gain matrices and $\Delta\bar{d}_k$ are given as follows:

$$\bar{A} = \begin{bmatrix} \Phi & G \\ O_{n\times q} & I_q \end{bmatrix}, \bar{\Gamma} = \begin{bmatrix} \Gamma \\ O_{n\times q} \end{bmatrix},$$
$$\bar{C} = \begin{bmatrix} C & O_{l\times q} \end{bmatrix}, \Delta\bar{d}_k = \begin{bmatrix} O_{n\times 1} \\ \Delta d_k \end{bmatrix}.$$

Remark 1: For the case where the measurement outputs are also subjected to disturbances, i.e., $y_k = Cx_k + G_2 d_k$, this approach is also applicable by choosing $\bar{C} = \begin{bmatrix} C & G_2 \end{bmatrix}$.

To obtain the disturbance estimate, the state function matrix L in [83] is chosen with a special structure:

$$L = \begin{bmatrix} L_0 & O_{\bar{h}\times q} \\ O_{q\times n} & I_q \end{bmatrix}. \tag{4.3.2}$$

The design of $L_0 \in \mathbb{R}^{\bar{h}\times n}$ with full row-rank will be discussed in Section 4.3.3.

Define

$$v_k = L\bar{x}_k, \text{ with } d_k = [O_{q\times n},\ I_q]v_k, \tag{4.3.3}$$

which is the state function to be estimated.

The problem of disturbance observer design is now transformed into the problem of state functional observer design for system (4.3.1) with state function v_k in (4.3.3) to be estimated.

According to [83] and [84], the disturbance observer $\hat{d}_k$ along with the state functional observer $\hat{v}_k$ takes the following form

$$\begin{cases} w_{k+1} = Nw_k + Jy_k + Hu_k, \\ \hat{v}_k = Bw_k + Ey_k, \\ \hat{d}_k = [O_{q\times n}\ I_q]\hat{v}_k. \end{cases} \tag{4.3.4}$$

Define an intermediate error $\chi_k = \bar{P}\bar{x}_k - w_k$ with $\bar{P}$ being an intermediate matrix, its dynamics is given by

$$\chi_{k+1} = N\chi_k + (\bar{P}\bar{A} - N\bar{P} - J\bar{C})\bar{x}_k + (\bar{P}\bar{\Gamma} - H)u_k + \bar{P}\Delta\bar{d}_k. \tag{4.3.5}$$

The state function estimation error $e_k = v_k - \hat{v}_k$ can be written as

$$e_k = B\chi_k + (L - E\bar{C} - B\bar{P})\bar{x}_k, \tag{4.3.6}$$

from which one can obtain $e_k \to 0$ as $k \to \infty$ for any $\bar{x}_k$ if and only if the following two conditions hold:

(i) $\chi_k \to 0$ as $k \to \infty$;

(ii) $L - E\bar{C} - B\bar{P} = O$.

For any invertible B, the aforementioned condition (ii) is implied by choosing $\bar{P}$ as

$$\bar{P} = B^{-1}L - B^{-1}E\bar{C}. \tag{4.3.7}$$

Ignoring the term $\bar{P}\Delta\bar{d}_k$ as it does not affect the analysis, (4.3.5) implies that $\chi_k \to 0$ as $k \to \infty$ if and only if the following condition holds

(a) $\bar{P}\bar{A} - N\bar{P} - J\bar{C} = O$ (Sylvester equation);

(b) $\bar{P}\bar{\Gamma} - H = O$;

(c) N is asymptotically stable.

Choosing $\bar{P}$ according to (4.3.7) with any invertible B and H according to Condition (b), then the existence condition reduces to condition (c) N being asymptotically stable under the constraint Sylvester equation condition (a). The existence condition in the form of easily-checked matrix rank equalities has been rigorously established in [83] with $B = I$ and later in [84] with B being any invertible matrix, summarized in Theorem 8.

Theorem 8. *There exists a stable generic RODOB given by (4.3.4) for system (4.2.1) if and only if the following condition holds:*

i) the matrix rank equality holds:

$$rank\left(\begin{bmatrix} L_0\Phi \\ C\Phi \\ C \\ L_0 \end{bmatrix}\right) = rank\left(\begin{bmatrix} C\Phi \\ C \\ L_0 \end{bmatrix}\right), \tag{4.3.8}$$

ii) $\forall s \in C$ *with* $Re(s) \geq 1$,

$$rank(\begin{bmatrix} sL_0 - L_0\Phi & -L_0G \\ O_{q\times n} & sI_q - I_q \\ C\Phi & CG \\ C & O_{l\times q} \end{bmatrix}) = rank(\begin{bmatrix} C\Phi \\ C \\ L_0 \end{bmatrix}) + q. \tag{4.3.9}$$

Proof: The existence condition is established by substituting the chosen state function gain matrix (4.3.2) and the definition of the variables to be estimated as in (4.3.3) into the existence conditions in Lemmas 1 and 2 of [83] and Theorem 3 of [84]. After a number of manipulations, (4.3.8) and (4.3.9) are resulted.

4.3.2 Relationships with the existing results

In this section, the relationship of the RODOB designed with the SFO technique with the existing disturbance observers is investigated including the RODOB proposed in [4] and FODOB proposed in [58].

Relationship with RODOB [4]

Inserting $\hat{\eta}_k$ of (4.2.3) into $\hat{d}_k$ yields

$$\hat{d}_k = KC^+ y_k - z_k + H_1(\xi_k + Qy_k). \tag{4.3.10}$$

Combing $\hat{\eta}_k$ of (4.2.3) with (4.3.10), one can obtain

$$\underbrace{\begin{bmatrix} \hat{\eta}_k \\ \hat{d}_k \end{bmatrix}}_{\hat{v}_k} = \underbrace{\begin{bmatrix} I & O_{h\times q} \\ H_1 & -I \end{bmatrix}}_{B} \underbrace{\begin{bmatrix} \xi_k \\ z_k \end{bmatrix}}_{w_k} + \underbrace{\begin{bmatrix} Q \\ KC^+ + H_1Q \end{bmatrix}}_{E} y_k. \tag{4.3.11}$$

Substituting the dynamics of $\hat{\eta}_k$ and $\hat{d}_k$ in (4.3.11) into that of ξ_k and z_k in (4.2.3), a compatible form with SFO based RODOB (4.3.4) for ξ_k and z_k is given by

$$\begin{aligned} \underbrace{\begin{bmatrix} \xi_{k+1} \\ z_{k+1} \end{bmatrix}}_{w_{k+1}} &= \underbrace{\begin{bmatrix} R + W_dH_1 & -W_d \\ KGH_1 + H_2 & I - KG \end{bmatrix}}_{N} \underbrace{\begin{bmatrix} \xi_k \\ z_k \end{bmatrix}}_{w_k} \\ &+ \underbrace{\begin{bmatrix} S + W_d(KC^+ + H_1Q) \\ KG(KC^+ + H_1Q) + K(\Phi - I_n)C^+ + H_2Q \end{bmatrix}}_{J} y_k + \underbrace{\begin{bmatrix} W_u \\ K\Gamma \end{bmatrix}}_{H} u_k, \end{aligned} \tag{4.3.12}$$

which means the RODOB (4.2.3) proposed in [4] is a special case of the proposed RODOB (4.3.4) with $L_0 = V^T$ in (4.3.2) and B in a special form as in (4.3.11). All the other corresponding matrices are defined in (4.3.11) and (4.3.12).

It shall be noticed that the existence condition (4.3.8) in Theorem 8 is actually the same as condition (i) (4.2.6) of [4] with $L_0 = V^T$. However, condition (4.3.9) with $L_0 = V^T$ in Theorem 8 is a matrix rank equality, which is much easier to check than that of [4] (i.e., no general solvability for the existence of a static output feedback).

Relationship with FODOB [58]

An observer simultaneously estimating full states and disturbances was proposed in [58] for system (4.2.1), given by

$$\begin{cases} \hat{x}_{k+1} = \Phi\hat{x}_k + \Gamma u_k + L_1(y_k - C\hat{x}_k) + G\hat{d}_k, \\ \hat{d}_{k+1} = d_k + L_2(y_k - C\hat{x}_k). \end{cases} \tag{4.3.13}$$

One can put (4.3.13) into an equivalent form to have a compatible structure with the generic RODOB (4.3.4).

$$\begin{cases} \underbrace{\begin{bmatrix} \hat{x}_{k+1} \\ \hat{d}_{k+1} \end{bmatrix}}_{w_{k+1}} = \underbrace{\begin{bmatrix} \Phi - L_1C & G \\ -L_2C & I \end{bmatrix}}_{N} \underbrace{\begin{bmatrix} \hat{x}_k \\ \hat{d}_k \end{bmatrix}}_{w_k} + \underbrace{\begin{bmatrix} L_1 \\ L_2 \end{bmatrix}}_{J} y_k + \underbrace{\begin{bmatrix} \Gamma \\ O_{q\times m} \end{bmatrix}}_{H} u_k, \\ \hat{v}_k = \underbrace{I_{n+q}}_{B} w_k + \underbrace{O_{(n+q)\times l}}_{E} y_k, \ \hat{d}_k = [O_{q\times n}, I_q]\hat{v}_k. \end{cases}$$

which means the FODOB proposed in [58] is a special case of the proposed RODOB with $L_0 = I_n$ and so $L = I_{n+q}$.

In addition, with $L_0 = I_n$ the existence condition (4.3.8) in Theorem 1 always holds and the condition (4.3.9) reduces to $\forall s \in C$ with $Re(s) \geq 1$,

$$rank\begin{pmatrix} \begin{bmatrix} sI_n - \Phi & -G \\ O_{q\times n} & sI_q - I_q \\ C & O_{l\times q} \end{bmatrix} \end{pmatrix} = n + q,$$

which is equivalent to that of [58].

4.3.3 Design process of the generic RODOB

The design of the generic RODOB using the SFO technique starts from choosing L_0 to satisfy the existence conditions in Theorem 8. In practice, an observer with small

order may be more desirable. So the selection of L_0 could start with a low order and then increase the order until the conditions in Theorem 1 are satisfied. This could make sure a disturbance observer with a minimal order is designed. Then a similar design procedure as [83] (except $B = I$ in [83]) can be followed as summarized below for the sake of completeness:

Form the state functional matrix L according to (4.3.2) and choose an invertible matrix B. Then define matrices F and M as

$$F = B^{-1}L\bar{A}L^{+}B - B^{-1}L\bar{A}N_L\Sigma^{+}\begin{bmatrix}\bar{C}\bar{A}L^{+}B\\ \bar{C}L^{+}B\end{bmatrix},$$

$$M = [I - \Sigma\Sigma^{+}]\begin{bmatrix}\bar{C}\bar{A}L^{+}B\\ \bar{C}L^{+}B\end{bmatrix},$$

where $\Sigma = \begin{bmatrix}\bar{C}\bar{A}N_L\\ \bar{C}N_L\end{bmatrix}$, L^{+} is the Moore-Pensrose pseudo-inverse inverse of the matrix L, given by $L^{+} = L^{T}(L^{T}L)^{-1}$ due to L being of full-row rank, $N_L = (I - L^{+}L)$. Then the matrix N can be calculated by any pole placement procedure for the pair (F, M) as

$$N = F - ZM, \tag{4.3.14}$$

where Z is the matrix obtained from the pole placement of the pair (F, M). The observability of the pair (F, M) is guaranteed by the condition (4.3.9).

Then one can further obtain gain matrices J and E based on the following relationship

$$[B^{-1}E \quad J - NB^{-1}E] = B^{-1}L\bar{A}N_L\Sigma^{+} + Z\left[I - \Sigma\Sigma^{+}\right].$$

Finally the matrix H is obtained by

$$H = (B^{-1}L - B^{-1}E\bar{C})\bar{\Gamma}.$$

Remark 2: From (4.3.5) and (4.3.6), one can obtain $e_{k+1} = BNB^{-1}e_k + B\bar{P}\Delta\bar{d}_k$, which means the convergence rate of disturbance observer is determined by the eigenvalues of N. From (4.3.14), the relationship between convergence rate with gain matrices has been established in the proposed approach.

4.4 Simulation study

In this section, a numerical example in [4] and [58] with two different types of disturbances will be used to verify the effectiveness of the proposed disturbance observer in estimating slowly time-varying disturbances and also its limitation in estimating fast time-varying disturbances.

The system matrices in (4.2.1) are given by

$$\Phi = \begin{bmatrix} 0.9630 & 0.0181 & 0.0187 \\ 0.1808 & 0.8195 & -0.0514 \\ -0.1116 & 0.0344 & 0.9586 \end{bmatrix}, G = \begin{bmatrix} 0.0996 & 0.0213 \\ 0.0050 & 0.1277 \\ 0.1510 & 0.0406 \end{bmatrix},$$

$$C = \begin{bmatrix} 1 & 0 & -1 \\ -1 & 1 & 1 \end{bmatrix}, \Gamma = O.$$

L_0 is chosen as $L_0 = [0\ 0\ 1]$ such that the existence condition of RODOB is satisfied, which means the third state is required to be estimated to obtain disturbance estimate. The eigenvalues for matrix N in (4.3.4) are designed as $p_1 = 0.5; p_2 = 0.55; p_3 = 0.6$, based on which the rest matrices can be calculated. The initial states for system dynamics and observer dynamics are selected as $x_0 = [0; 1; 0]$ and $\omega_0 = [0; 0; 0]$ respectively. The slowly time-varying disturbances and fast time-varying disturbances are considered respectively as follows.

Case 1: slowly time-varying disturbances First consider slowly time-varying disturbance estimation. The disturbances under consideration are given by

$$d_1(k) = 0.3 * sin(0.05k) + 2;\ d_2(k) = 0.2 * cos(0.05k) + 2.$$

The simulation results for d_1, d_2 and x_3 estimates are shown in Figs. 4.2 and 4.3,

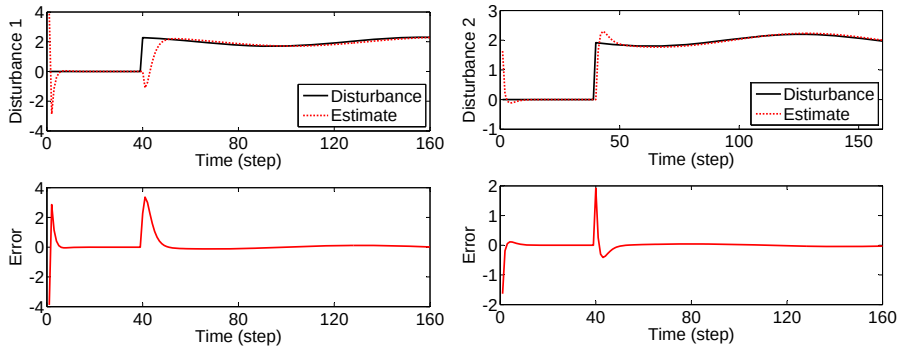

Figure 4.2. Slowly time-varying disturbance estimation: left figure (d_1); right figure (d_2).

One can see from Figs. 4.2 and 4.3, that the proposed reduced order disturbance observer can effectively estimate slow-varying disturbance with very small estimation

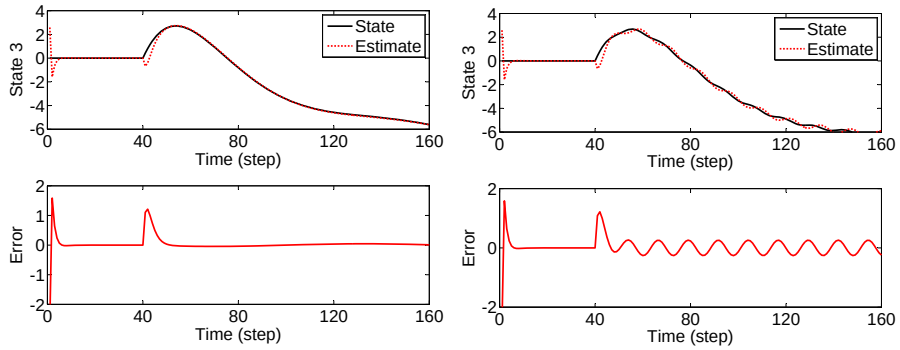

Figure 4.3. State x_3 estimate under slowly time-varying disturbances (left) and fast time-varying disturbance (right).

errors.

Case 2: fast time-varying disturbances The fast time-varying disturbance estimation is then considered. The disturbances under consideration are given by

$$d_1(k) = 0.3 * sin(0.5k) + 2;\ d_2(k) = 0.2 * cos(0.5k) + 2.$$

The simulation results for d_1, d_2 and x_3 estimates are shown in Figs. 4.4 and 4.3 (the right hand figure)

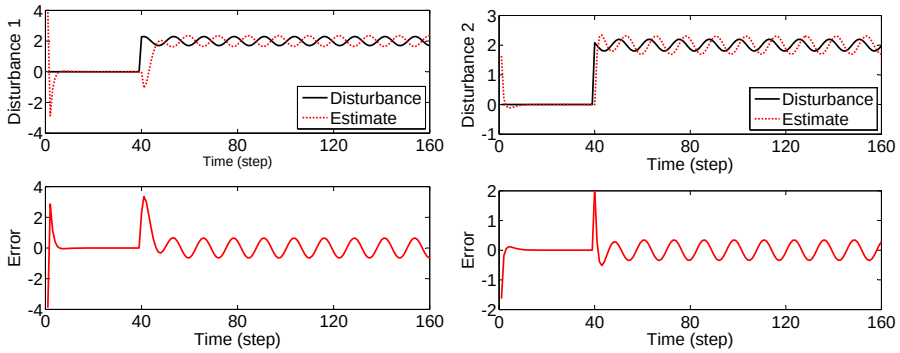

Figure 4.4. fast time-varying disturbance estimation: d_1 (left); d_2 (right).

One can see from Figs. 4.4 and 4.3 that the proposed RODOB may result in large estimation error for disturbance with fast time-varying dynamic. *And this motivates the research in Chapter 5, i.e., RODOB design with no disturbance model.*

4.5 Summary

In this Chapter, the state functional observer technique is applied to reduced-order disturbance observer design by augmenting the disturbances as additional states and carefully selecting the state function matrix L. As a result, the existence condition of a fixed order disturbance observer is represented in the forms of two easily-checked matrix rank equalities. It is also shown that both the RODOB in [4] and FODOB in [58] are special cases of the generic RODOB discussed in this Chapter.

Chapter 5

RODOB: WITHOUT DISTURBANCE MODEL

5.1 Introduction

In Chapter 4, RODOB algorithm was designed for discrete-time linear systems where the disturbances are assumed to be slowly time-varying. In the simulation study (see, Section 4.4), one can observe that the RODOB with slowly time-varying disturbance assumption may result in poor disturbance estimation performance for systems with fast time-varying disturbances such as periodic disturbances among many others. In this Chapter, another RODOB is designed, which can remove the slowly time-varying disturbance assumption and consequently can obtain a better disturbance estimation performance for fast time-varying disturbance. The motivations and the relationship with the existing results are illustrated in Fig. 5.1.

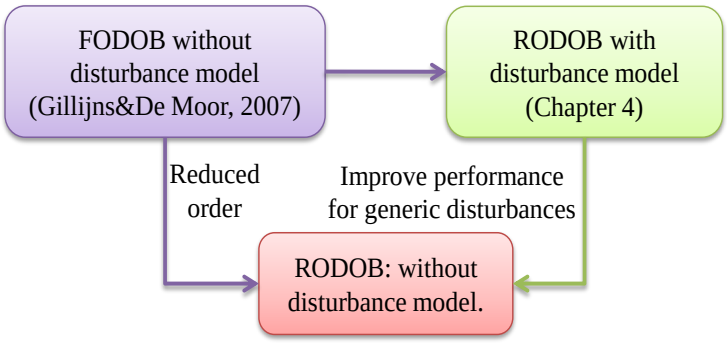

Figure 5.1. Illustration of the motivations and the relationship with the existing results.

The RODOB design for discrete-time linear stochastic systems is investigated without imposing any assumption on the disturbance dynamics. Compared with the existing FODOs, a simpler criterion for the existence of RODOB is developed and the full state estimability condition is removed. Compared with the existing

RODOB (e.g., the RODOB in Chapter 4), the RODOB in the Chapter does not make any assumption on disturbance dynamics. Hence it extends the applicability of the existing results in [2, 3, 8, 69] to a much wider application area.

5.2 Problem statement

Consider a discrete-time linear stochastic system in the presence of disturbances [2, 3, 69] as follows:

$$\begin{cases} x_{k+1} = Ax_k + Gd_k + \omega_k \\ y_k = Cx_k + \upsilon_k \end{cases}, \tag{5.2.1}$$

where $x_k = [x_{k,1}, ..., x_{k,n}]^T \in \mathbb{R}^n$ is the state vector, $d_k = [d_{k,1}, ..., d_{k,m}]^T \in \mathbb{R}^m$ is a vector of the lumped unknown disturbances, and $y_k \in \mathbb{R}^p$ is the measurement vector at each time step k with $p \geq m$ and $n \geq m$. The process noise $\omega_k \in \mathbb{R}^n$ and measurement noise $\upsilon_k \in \mathbb{R}^p$ are assumed to be mutually independent, and each follows a Gaussian distribution with a zero-mean vector and known covariance matrix, $Q_k = E[\omega_k \omega_k^T] > 0$ and $R_k = E[\upsilon_k \upsilon_k^T] > 0$ respectively. In addition, A, G and C are known matrices, where G is supposed to have a full column-rank [69], [8].

In general, the objective of a DO is to estimate the disturbance vector d_k based on the measurement output y_k and model (5.2.1). This Chapter, however, focuses on the design of RODOB, aiming to: (a) remove the assumptions of the full state estimability and assumption on the disturbance dynamics; (b) increase the estimation speed with a lower observer order.

5.3 Reduced-order disturbance observer

In this section, an existence condition of a general RODOB for system (5.2.1) is first established when the full state vector is not estimable. This is undertaken based on the fact that one can still estimate the disturbances using the information of the estimable part of the state vector [4], [81]. To this end, a reduced-order state function observer is used for disturbance estimation. Then on the basis of the existence condition, a set of recursive formulae are derived for the RODOB.

5.3.1 Existence condition

Define $\mathscr{L} = \{l | Al = \lambda l \text{ and } Cl = 0, \text{ with } l \in \mathbb{R}^n \text{ and } \lambda \text{ is a scalar}\}$ to be a set of eigenvectors of A that are orthogonal to C^T. Suppose there are in total n_1 linearly independent vectors in $\mathscr{L}$. Now, let $l_1, l_2, \cdots, l_{n_1}$ denote any of n_1 linearly independent vectors in $\mathscr{L}$ and let $L^T = [l_1, l_2, \cdots, l_{n_1}]$ be an $n \times n_1$ matrix. In

addition, define T to be an $(n-n_1)\times n$ matrix such that T^T is an orthogonal compliment of matrix L^T satisfying $TL^T=O$.

Let $z_k=Tx_k$. Then the dynamics of z_k are

$$\begin{aligned} z_{k+1} &= Tx_{k+1}=TAx_k+TGd_k+T\omega_k \\ &= TAT^+z_k+TA(I-T^+T)x_k+TGd_k+T\omega_k \\ &= TAT^+z_k+TA(L^+L)x_k+TGd_k+T\omega_k. \end{aligned}$$

Noting that $L^+=L^T(LL^T)^{-1}$ and each column of matrix L^T is an eigenvector of A that is orthogonal to T, one has $TAL^+L=TAL^T(LL^T)^{-1}L=O$. Hence, one can obtain

$$z_{k+1}=TAT^+z_k+TGd_k+T\omega_k. \tag{5.3.1}$$

In addition, noting that $CL^T=O$, a similar argument can be applied to the measurement equation of (5.2.1), yielding

$$y_k=CAT^+z_{k-1}+CGd_{k-1}+C\omega_{k-1}+\upsilon_k. \tag{5.3.2}$$

For the scenario that x_k is not fully estimable. d_k will be estimated based on (5.3.1) and (5.3.2).

First, motivated by the linear filter structure in [2], a general DO structure for system (5.3.1) and (5.3.2) is designed as

$$\begin{cases} \hat{z}_{k+1}=E_k\hat{z}_k+K_{k+1}y_{k+1} \\ \hat{d}_k=J_{k+1}(y_{k+1}-N\hat{z}_k) \end{cases}, \tag{5.3.3}$$

where the matrices E_k, K_{k+1}, J_{k+1} and N are to be designed (and as it will be shown later, the matrix N is time-invariant).

Based on (5.3.1)-(5.3.3), one can obtain the dynamics of the state function estimation error, $e_{k+1}=z_{k+1}-\hat{z}_{k+1}$, as

$$\begin{aligned} e_{k+1} &= TAT^+z_k+TGd_k+T\omega_k-(E_k\hat{z}_k+K_{k+1}y_{k+1}) \\ &= E_ke_k+(TAT^+-K_{k+1}CAT^+-E_k)z_k+(TG \\ &\quad -K_{k+1}CG)d_k+(T-K_{k+1}C)\omega_k-K_{k+1}\upsilon_{k+1}. \end{aligned} \tag{5.3.4}$$

The disturbance estimation is governed by

$$\begin{aligned} \hat{d}_k &= J_{k+1}(CAT^+z_k+CGd_k+C\omega_k+\upsilon_k-N\hat{z}_k) \\ &= J_{k+1}Ne_k+J_{k+1}(CAT^+-N)z_k \\ &\quad +J_{k+1}CGd_k+J_{k+1}(C\omega_k+\upsilon_{k+1}). \end{aligned} \tag{5.3.5}$$

First focus on (5.3.5). To ensure an unbiased disturbance estimate, $\hat{d}_k$ must be independent of the term z_k, and matrix J_{k+1} has to satisfy $J_{k+1}CG = I$. In addition, for (5.3.4), it is noted that the effect of e_k on $\hat{d}_k$ should disappear as k increases, and hence it is required that the filtering error e_k in (5.3.4) is independent of z_k and d_k. Moreover, the error e_k should also approach to zero as time k increases, i.e., E_k is a stable matrix. Therefore the existence condition for RODOB (5.3.3) is summarized as follows:

(i) E_k is stable (i.e., all the eigenvalues of E_k satisfy $|\lambda(E_k)| < 1$);

(ii) $E_k = TAT^+ - K_{k+1}CAT^+$;

(iii) $K_{k+1}CG = TG$;

(iv) $N = CAT^+$;

(v) $J_{k+1}CG = I$.

For system (5.2.1) with disturbance observer (5.3.3), however, the existence condition should be expressed in terms of matrices A, G, C and T. A condition for the existence of a general linear DOB is provided (5.3.3).

Theorem 9. *Suppose G has a full column-rank. A sufficient condition for the existence of a general RODOB (5.3.3) for system (5.2.1) is that*

$$rank(CG) = m, \tag{5.3.6}$$

and the matrix

$$P = \begin{bmatrix} zI_{n_1} - TAT^+ & -TG \\ CAT^+ & CG \end{bmatrix} \tag{5.3.7}$$

has a full column-rank for all $z \in \mathbb{C}$ such that $|z| \geq 1$.

Proof: First, one can select E_k based on condition part (ii) as

$$E_k = TAT^+ - K_{k+1}CAT^+ \tag{5.3.8}$$

and $N = CAT^+$ based on condition part (iv). J_{k+1} can be further chosen such that $J_{k+1}CG = I$ since CG has a full column rank. In addition, one can obtain from [67] that condition (5.3.6) guarantees there exists a matrix K_{k+1} such that condition part (iii) holds. Hence, one only has to focus on condition part (i) with the constraint on

K_{k+1} given by condition part (iii). Since CG has a full column-rank, there exists an invertible matrix $M \in R^{p\times p}$ [8] such that

$$MCG = \begin{bmatrix} O_{(p-m)\times m} \\ I_m \end{bmatrix}.$$

From (iii), the general solution K_{k+1} can be expressed as:

$$K_{k+1} = [\Gamma_k, TG]M, \tag{5.3.9}$$

where Γ_k can be any matrix with suitable dimension and is to be designed for the gain matrix K_{k+1}. Define S_1 and S_2 as

$$\begin{bmatrix} S_1 \\ S_2 \end{bmatrix} = MCAT^+.$$

Inserting (5.3.9) into (5.3.8) gives

$$\begin{aligned} E_k &= TAT^+ - K_{k+1}CAT^+ = TAT^+ - [\Gamma_k, TG]MCAT^+ \\ &= TAT^+ - [\Gamma_k, TG]\begin{bmatrix} S_1 \\ S_2 \end{bmatrix} = TAT^+ - TGS_2 - \Gamma_k S_1. \end{aligned}$$

According to [79] (pp. 342), existence condition part (i) holds if and only if either one of the equivalent conditions holds:
(a) $TAT^+ - TGS_2 - \Gamma_k S_1$ is stable for a matrix Γ_k;
(b) $S_1\eta = 0$ and $(TAT^+ - TGS_2)\eta = \lambda\eta$ for some constant λ and vector η implies $|\lambda| < 1$ or $\eta = 0$.

Condition (b) can equivalently be expressed as:

$$\begin{aligned} &rank(\begin{bmatrix} zI_{n_1} - TAT^+ + TGS_2 \\ S_1 \end{bmatrix}) = n_1, \\ &\forall z \in \mathbb{C}, |z| \geq 1. \end{aligned} \tag{5.3.10}$$

The following identity shows that (5.3.10) is satisfied if condition (5.3.7) holds:

$$
\begin{aligned}
&rank(\begin{bmatrix} zI_{n_1} - TAT^+ & -TG \\ CAT^+ & CG \end{bmatrix}) \\
&= rank(\begin{bmatrix} I_{n_1} & O_{n_1\times p} \\ O_{m\times n_1} & M \end{bmatrix} \begin{bmatrix} zI_{n_1} - TAT^+ & -TG \\ CAT^+ & CG \end{bmatrix}) \\
&= rank(\begin{bmatrix} zI_{n_1} - TAT^+ & -TG \\ MCAT^+ & MCG \end{bmatrix}) = rank(\begin{bmatrix} zI_{n_1} - TAT^+ & -TG \\ S_1 & O_{(p-m)\times m} \\ S_2 & I_m \end{bmatrix}) \\
&= rank(\begin{bmatrix} zI_{n_1} - TAT^+ + TGS_2 & O_{n_1\times m} \\ S_1 & O_{(p-m)\times m} \\ O_{n_1\times m} & I_m \end{bmatrix}) \\
&= rank(\begin{bmatrix} zI_{n_1} - TAT^+ + TGS_2 \\ S_1 \end{bmatrix}) + m.
\end{aligned}
$$

Therefore, Eqs. (5.3.6) and (5.3.7) guarantee there exists a gain matrix K_{k+1} such that: (a) $K_{k+1}CG = TG$; and (b) $E_k = TAT^+ - K_{k+1}CAT^+$ is stable. □

5.3.2 Condition relaxation

It is of particular interest to compare the proposed RODOB with the conventional FODOs. Apart from the fact that the proposed RODOB is a lower-order filter, The existence condition of RODOB can be more easily satisfied than that of FODOs, as shown in Theorem 10.

Theorem 10. *If the existence condition of FODOs (see, [69], [8]) holds for a system given by (5.2.1), then the existence condition (5.3.7) of RODOs is also satisfied.*

Proof: First, it is noted that the following identity holds for any non-singular matrix P_T:

$$
\begin{aligned}
&\begin{bmatrix} P_T & O \\ O & I_p \end{bmatrix} \begin{bmatrix} I_n & O \\ -C & zI \end{bmatrix} \begin{bmatrix} zI_n - A & -G \\ C & O \end{bmatrix} \begin{bmatrix} P_T^{-1} & O \\ O & I_p \end{bmatrix} \\
&\qquad = \begin{bmatrix} zI_n - P_TAP_T^{-1} & -P_TG \\ CAP_T^{-1} & CG \end{bmatrix}.
\end{aligned} \tag{5.3.11}
$$

Let P_F denote the matrix on the right-hand-side of (5.3.11). Then (5.3.11) indicates that $rank(\begin{bmatrix} zI_n - A & -G \\ C & O \end{bmatrix}) = rank(P_F)$. The full rank condition of left hand matrix for $|z| \geq 1$ is the part of the existence condition for FODO [8, 69].

Now choose $P_T = [T^T, L^T]^T$ and let $P_T^+ = [T^+ \ L^+]$ denote the Moore-Penrose

Pseudo inverse of matrix P_T. Substituting P_T and P_T^+ into P_F gives

$$\begin{aligned} P_F &= \begin{bmatrix} zI_{n-n_1} - TAT^+ & -TAL^+ & -TG \\ -LAT^+ & zI_{n_1} - LAL^+ & -LG \\ CAT^+ & CAL^+ & CG \end{bmatrix} \\ &= \begin{bmatrix} zI_{n-n_1} - TAT^+ & O & -TG \\ -LAT^+ & zI_{n_1} - LAL^+ & -LG \\ CAT^+ & O & CG \end{bmatrix}. \end{aligned} \tag{5.3.12}$$

From (5.3.7) and (5.3.12), it can be seen that matrix P in (5.3.7) is a sub-matrix of P_F. This indicates that matrix P is of full column-rank if P_F has a full column-rank.

5.3.3 Disturbance observer design

In this subsection, the two gain matrices of the RODOB in (5.3.3) will be investigated using the MVUE method. Under the existence condition given in Section 5.3.1, one can obtain the dynamics of $e_{k+1}^x = Tx_{k+1} - \hat{z}_{k+1}$ from (5.3.4) and (5.3.5):

$$e_{k+1}^x = E_k e_k^x + (T - K_{k+1}C)\omega_k - K_{k+1}\upsilon_{k+1}. \tag{5.3.13}$$

In addition, the dynamics $e_k^d = d_k - \hat{d}_k$ are governed by

$$e_k^d = -J_{k+1}Ne_k^x - J_{k+1}(C\omega_k + \upsilon_{k+1}). \tag{5.3.14}$$

State function observer

The estimation error covariance matrix $P_{k|k}^x = E(e_k^x e_k^{xT})$ can be calculated from (5.3.13):

$$\begin{aligned} P_{k+1|k+1}^x &= E_k P_{k|k}^x E_k^T + (T - K_{k+1}C)Q_k(T - K_{k+1}C)^T + K_{k+1}R_{k+1}K_{k+1}^T \\ &= (TAT^+ - K_{k+1}CAT^+)P_{k|k}^x(TAT^+ - K_{k+1}CAT^+)^T \\ &\quad + TQ_kT^T - TQ_kC^TK_{k+1}^T - K_{k+1}CQ_kT^T \\ &\quad + K_{k+1}CQ_kC^TK_{k+1}^T + K_{k+1}R_{k+1}K_{k+1}^T. \end{aligned} \tag{5.3.15}$$

Let $\bar{A} = TAT^+$, $\bar{C} = CAT^+$, $\Phi = \bar{C}P_{k|k}^x\bar{C}^T + CQ_kC^T + R_{k+1}$, $\Psi = CQ_kT^T + \bar{C}P_{k|k}^x\bar{A}^T$ and $P^* = \bar{A}P_{k|k}^x\bar{A}^T + TQ_kT^T$. Eq. (5.3.15) can be simplified to be:

$$P_{k+1|k+1}^x = K_{k+1}\Phi K_{k+1}^T - K_{k+1}\Psi - \Psi^T K_{k+1}^T + P^*. \tag{5.3.16}$$

In addition, the unbiasedness condition of state estimation imposes a constraint on the gain matrix K_{k+1} (see [85]), i.e.

$$K_{k+1}CG = TG. \tag{5.3.17}$$

One can solve the MVUE problem by finding K_{k+1} which minimizes the trace of (5.3.16), subject to the constraint (5.3.17). The Lagrangian for the problem of constraint optimization is

$$Tr[K_{k+1}\Phi K_{k+1}^T - 2\Psi^T K_{k+1}^T + P^*] - 2Tr[(K_{k+1}CG - TG)\Lambda_{k+1}^T], \tag{5.3.18}$$

where Λ_{k+1} is the Lagrange multiplier. Setting the derivative of (5.3.18) with respect to K_{k+1} equal to zero yields:

$$2\Phi K_{k+1}^T - 2\Psi - 2CG\Lambda_{k+1}^T = 0. \tag{5.3.19}$$

Combining (5.3.17) and (5.3.19), one can obtain the following equation:

$$\begin{bmatrix} \Phi & -CG \\ G^TC^T & O \end{bmatrix} \begin{bmatrix} K_{k+1}^T \\ \Lambda_{k+1}^T \end{bmatrix} = \begin{bmatrix} \Psi \\ G^TT^T \end{bmatrix}. \tag{5.3.20}$$

Then using the approach in [67] and [85] (see, pp. 68), one can obtain K_{k+1} as follows:

$$K_{k+1} = \Psi^T\Phi^{-1} + (TG - \Psi^T\Phi^{-1}CG)(G^TC^T\Phi^{-1}CG)^{-1}G^TC^T\Phi^{-1}. \tag{5.3.21}$$

Inserting K_{k+1} in (5.3.21) into (5.3.16), one can obtain:

$$\begin{aligned} P_{k+1|k+1}^x = P^* - \Psi^T\Phi^{-1}\Psi + (TG - \Psi^T\Phi^{-1}CG) \\ \times (G^TC^T\Phi^{-1}CG)^{-1}(TG - \Psi^T\Phi^{-1}CG)^T. \end{aligned} \tag{5.3.22}$$

Disturbance observer

One can work out J_{k+1} in (5.3.3) in a similar manner. First, from (5.3.14) one can obtain the disturbance estimation error covariance matrix $P_{k|k}^d = E(e_k^d e_k^{dT})$:

$$P_{k|k}^d = J_{k+1}NP_{k|k}^x N^T J_{k+1}^T + J_{k+1}(CQ_kC^T + R_{k+1})J_{k+1}^T. \tag{5.3.23}$$

Noting $N = CAT^+$ and by the definition of Φ, Eq. (5.3.23) can be re-arranged as

$$P_{k|k}^d = J_{k+1}\Phi J_{k+1}^T. \tag{5.3.24}$$

In addition, the unbiased estimation of d_k also imposes a constraint on gain matrix J_{k+1}, i.e. $J_{k+1}CG = I$. One can obtain the optimal J_{k+1} below via minimizing the trace of (5.3.24), subject to this constraint:

$$J_{k+1} = (G^T C^T \Phi^{-1} CG)^{-1} G^T C^T \Phi^{-1}. \tag{5.3.25}$$

Inserting (5.3.25) into (5.3.24), one can obtain an explicit expression of the disturbance estimation error covariance matrix:

$$P^d_{k|k} = (G^T C^T \Phi^{-1} CG)^{-1}. \tag{5.3.26}$$

The obtained RODOB is summarized in Theorem 11.

Theorem 11. *Under the existence condition given in Theorem 9, there exists a minimum-variance unbiased estimator of the disturbances d_k given by*

$$\begin{cases} \hat{z}_{k+1} = TAT^+ \hat{z}_k + K_{k+1}(y_{k+1} - CAT^+ \hat{x}_k) \\ \hat{d}_k = J_{k+1}(y_{k+1} - CAT^+ \hat{z}_k) \end{cases},$$

where the gain matrices K_{k+1} and J_{k+1} are given by (5.3.21) and (5.3.25) respectively, and the corresponding state function estimation error covariance matrix and disturbance estimation error covariance matrix are given by (5.3.22) and (5.3.26) respectively.

5.3.4 Relationships with the existing results

The relationships between these FODOs and the proposed RODOB are summarized in Theorem 12.

Theorem 12. *When the states are fully estimable in the presence of disturbances, the proposed RODOB is equivalent to the FODO in [67] for sole state estimation, and to the one in [2] for the estimation of both states and disturbances.*

Proof: When the states are fully estimable, T can be chosen as the identity matrix and hence the RODOB reduces to:

$$\begin{cases} \hat{x}_{k+1} = A\hat{x}_k + K_{k+1}(y_{k+1} - CA\hat{x}_k) \\ \hat{d}_k = J_{k+1}(y_{k+1} - CA\hat{x}_k) \end{cases}, \tag{5.3.27}$$

where $J_{k+1} = (P^d_{k|k})^{-1} G^T C^T H^{-1}_{k+1}$, and

$$K_{k+1} = P_{k+1|k} C^T H^{-1}_{k+1} + (G - P_{k+1|k} C^T H^{-1}_{k+1} CG) \times (G^T C^T H^{-1}_{k+1} CG)^{-1} CG H^{-1}_{k+1}$$

with $P_{k+1|k} = A P_{k|k} A^T + Q_k$, $H_{k+1} = C P_{k+1|k} C^T + R_{k+1}$.

In addition, Eq. (5.3.22) reduces to

$$P^x_{k+1|k+1} = P^x_{k+1|k} - P^x_{k+1|k} C^T H^{-1}_{k+1} C P^x_{k+1|k} + B(G^T C^T \tilde{R}^{-1}_k CG)^{-1} B^T,$$

with $B = G - P^x_{k+1|k} C^T H^{-1}_{k+1} CG$ and Eq. (5.3.26) reduces to $P^d_{k|k} = (G^T C^T H^{-1}_k CG)^{-1}$. These recursive formulae are identical to the results in [67] for sole state estimation, and the same as the results in [2] for the estimation of states and disturbances. □

Next, the proposed RODOB is briefly compared with the recently developed RODOB for deterministic discrete-time systems in [4]. It is first pointed out that the existence condition in [4] requires the existence of a gain matrix such that the corresponding composite matrix is asymptotically stable. This gain matrix also involves a static output feedback problem, for which the general solvability is not known yet (see [4] for details). In contrast, the existence condition of the proposed RODOB without disturbance model is easy to check and it collapses to that of the conventional FODOs for fully estimable states. In addition, unlike the RODOB in [4] that assumes the disturbances are slowly time-varying, no particular assumption on the disturbance dynamics is imposed in the proposed method, hence extending its applicability.

5.4 Case studies

5.4.1 Simulation study 1: performance comparison

First of all a simple numerical example is used to compare the proposed algorithm with the RODO in [4]. Consider systems (5.2.1) with $A = \begin{bmatrix} 1.1 & 0.5 & 0 \\ 0 & 0.9 & 0 \\ 0 & 0.5 & 2 \end{bmatrix}$, $G = \begin{bmatrix} 1 \\ 0 \\ 1 \end{bmatrix}$, $C = \begin{bmatrix} 1 & 0 & 0 \\ 0 & 1 & 0 \end{bmatrix}$, $Q_k = 0.02 \times I_3$, and $R_k = 0.01 \times I_2$. The disturbance profile in simulation study as shown in the upper plot of Fig. 5.2 was used to represent a generic disturbance which included a slowly time-varying disturbance (i.e., step-type disturbance) and a fast time-varying disturbance (i.e., sinusoidal

disturbance). The step amplitudes at 0 and 70^{th} step were taken as 7 and -7 respectively, whereas the sinusoidal function between 30^{th} step and 70^{th} step was chosen as $4\sin(40\pi t/180) + 2$ with t being each step index. The disturbance profile was designed to verify the effectiveness of different disturbance observer algorithms and therefore was assumed to be completely unknown to the observer design.

It can be easily verified that this system does not satisfy the existence condition of the FODO in [2] and [83], and hence no FODO exists.

In the proposed RODO, we chose $T = \begin{bmatrix} 1 & 0 & 0 \\ 0 & 1 & 0 \end{bmatrix}$ which satisfies the existence condition in Theorem 9. The initial states of the system and observer are taken as $x_0 = [1, 2, 1]^T$ and $z_0 = [0, 0]^T$ respectively. The RODO in [4] for discrete-time system with slowly time-varying disturbance assumption is also applied for the purpose of comparison, where the matrix K therein is chosen as $K = [0.9, 0, 0]$. The comparison results are shown in Fig. 5.2, where upper figure depicts the disturbance estimates and the lower figure displays the disturbance estimation errors.

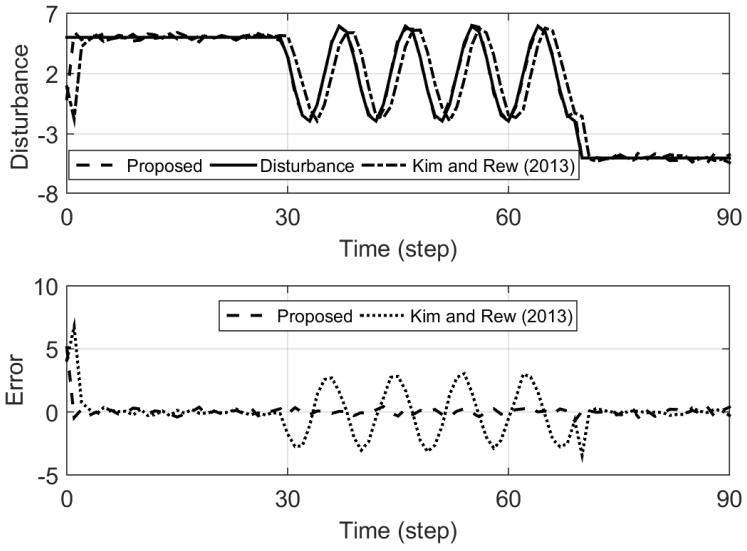

Figure 5.2. Disturbance estimation based on the proposed RODO and the algorithm in [4]: real line (actual disturbance), dashed line (the proposed RODO) and dotted line (the result in [4]).

We can see from Fig. 5.2 that in the presence of unknown disturbance consisting of step-type and sinusoidal-type, the proposed RODO can obtain unbiased estimation. For the algorithm in [4], on the other hand, it can be seen that it works well and obtains unbiased estimate for constant disturbance. However, the disturbance estimation error is quite large in the presence of sinusoidal-type disturbance; this is due to the fact that the RODO proposed in [4] requires that the disturbance is slowly

time-varying and will result in disturbance estimation error for fast time-varying disturbances. This example demonstrates the advantages of the proposed RODO in generic disturbance estimation that includes both slowly and fast time-varying disturbances over the traditional algorithms.

In some applications in practice, the covariance matrices of input noises and measurement noises may not be exactly known. It is therefore of practical interest to investigate the performance of the proposed algorithm in such scenarios. For this end, we tested the robustness of the proposed RODO by choosing different covariance matrices for data generation. Specifically, we first considered the effect of input noises. In this scenario, the measurement covariance matrix was fixed as $R_k = 0.01 \times I_2$ but a different input noise covariance matrix was used, i.e. $Q_k = 0.04 \times I_3$ and $Q_k = 0.06 \times I_3$ respectively. Next, we considered the effect of measurement noises. In this scenario, the input covariance matrix was fixed as $Q_k = 0.02 \times I_3$ but a different measurement noise covariance matrix was used, i.e. $R_k = 0.03 \times I_2$ and $R_k = 0.05 \times I_2$ respectively.

During the estimation stage, however, we supposed that the true covariance matrices used to simulate the system states and measurements were not perfectly known; rather, it was the covariance matrices $Q_k = 0.02 \times I_3$, and $R_k = 0.01 \times I_2$ that were used to estimate the states and the unknown disturbances. The mean squared error (MSE) was used as the criterion in the performance comparison between the proposed RODO with the one in [4].

Simulations were run for 50 times for each scenario and the average MSEs were calculated and summarized in Table 5.1.

Table 5.1. Average MSE comparison under different noises

Method/Noise × I	$Q_k = 0.04$	$Q_k = 0.06$	$R_k = 0.03$	$R_k = 0.05$
Proposed	0.3475	0.3637	0.3668	0.4135
Kim and Rew (2013)	2.7946	2.8351	2.8301	2.8461

One can see from Table 5.1 that both methods were still valid in terms of convergences when the true covariance matrices were not perfectly known in the state and disturbance estimation. In addition, the performances for both methods became worse when the true covariance matrices deviated more substantially from the ones used in the estimation. Overall, the proposed RODO still outperformed the one in [4].

5.4.2 Simulation study 2: double-effect pilot plant evaporator

Next, we apply the proposed RODO to the disturbance estimation problem for a double-effect pilot plant evaporator represented by a fifth-order linear model investigated in [4, 61, 86]. The problem is briefly outlined as follows. The feed solution (flow F_0 and concentration C_0) is pumped into the first effect, where the first effect solution (hold-up W_1) is heated by saturated steam (temperature T_s) and the boil-off travels into the second effect steam jacket. The concentrated solution from the first effect (flow F_1 and concentration C_1) enters the second effect which operates under vacuum. The hold-up in the second effect is W_2. The concentrated product (flow F_2 and concentration C_2) is pumped to storage. Based on the physical properties, the evaporator can be modelled by a fifth-order linear state-space model with unobservable states, where the system variables and disturbance variables are $x = [W_1, C_1, T_1, W_2, C_2]$ (T_1 denotes the temperature of the first effect solution) and $d = [C_0, F_0]$ respectively. A schematic diagram of the pilot plant double effect evaporator system is available in [86].

In our case study, we chose the system matrix in continuous time domain used in [61], and then we discretized the continuous-time model with a sampling time of $30s$ (see, [86]). This resulted in the following discrete-time system

$$A = \begin{bmatrix} 1 & 0 & -0.0030 & 0 & 0 \\ 0 & 0.2923 & 0.0003 & 0 & 0 \\ 0 & 0 & 0 & 0 & 0 \\ 0 & 0 & -0.0031 & 1 & 0 \\ 0 & 0.7121 & 0.0019 & 0 & 0.2165 \end{bmatrix}, G = \begin{bmatrix} 0 & 30.6207 \\ 1.0702 & -2.4170 \\ 0 & -6.2671 \\ 0 & 0.6572 \\ 1.1068 & -3.0385 \end{bmatrix},$$

$$C = \begin{bmatrix} 1 & 0 & 0 & 0 & 0 \\ 0 & 1 & 0 & 0 & 0 \end{bmatrix}.$$

In the simulation, the parameters are given as follows: $Q_k = 0.1 \times I_5$, $R_k = 0.05 \times I_2$, and $d_{k,1} = -d_{k,2}$. The initial values of system (5.2.1) and observer (5.3.3) were taken as $x_0 = [1, 2, 5, 1, 1]^T$ and $z_0 = [0, 0, 0]^T$ respectively.

It can be easily verified that this system does not satisfy the existence condition of the FODOs in [2], [69], [8]. Hence the system state variables $x_{k,i}$ $(i = 1, ..., 5)$ are not fully estimable and no FODOs exist. Now the proposed RODOB is applied. $T = [I_3, O_{3\times 2}]$ is chosen, which satisfies the existence condition in Theorem 9. The simulation results for disturbance $d_{k,1}$ and state $x_{k,3}$ are shown in Fig. 5.3, where the left (or right) two graphs display the estimated disturbance (or state) and the corresponding estimation error where the simulated (estimated) values are plotted using a real (dotted) line.

One can see from Fig. 5.3 that the proposed RODOB can obtain a reasonably

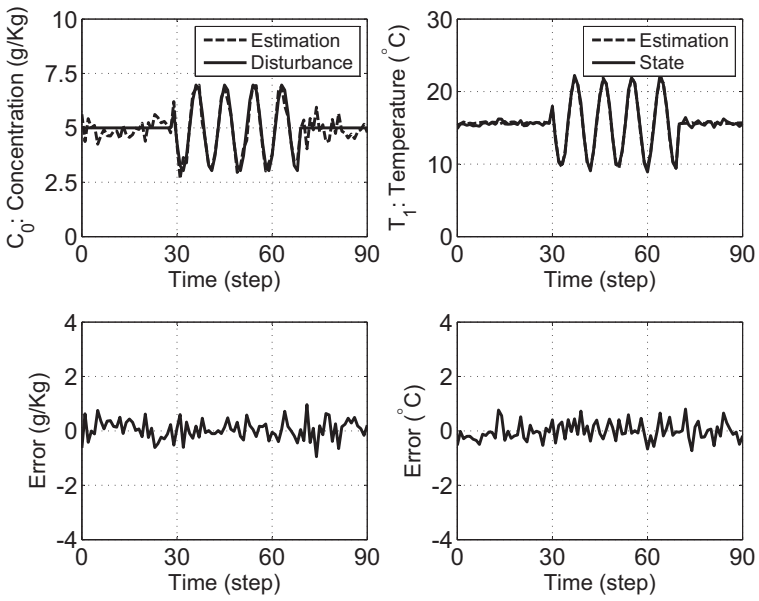

Figure 5.3. Disturbance estimation based on the proposed RODOB.

good (by taking the larger noises into account) unbiased disturbance estimate even if no FODOs exist.

5.5 Summary

This Chapter investigates reduced-order disturbance observer (RODOB) design for discrete-time linear stochastic systems when the states are not fully estimable. An existence condition of a general form of RODOB is established. It shows that under some mild condition, the disturbances can still be estimated even if the full state vector is not estimable. The existing FODOs in the literature are shown to be a special case of the proposed RODOB when the states are fully estimable. In comparison with the recently developed RODOB in [4], the proposed RODOB does not impose any particular assumption on the disturbance dynamics. Hence, this research extends the applicability of the disturbance observer techniques to a wider application area.

Chapter 6

TIME/FREQUENCY DOMAIN DOBS

6.1 Introduction

In the previous Chapters, disturbance observer (full order or reduced order) design for discrete-time systems (deterministic or stochastic) was considered, which can be applied for fault estimation in fault diagnosis design. In this Chapter, however, attention is moved to continuous-time domain, particularly emphasis is put on the relationship between time-domain DOB and frequency-domain DOB, and its application. The motivations and contribution of this Chapter is illustrated in Fig. 6.1.

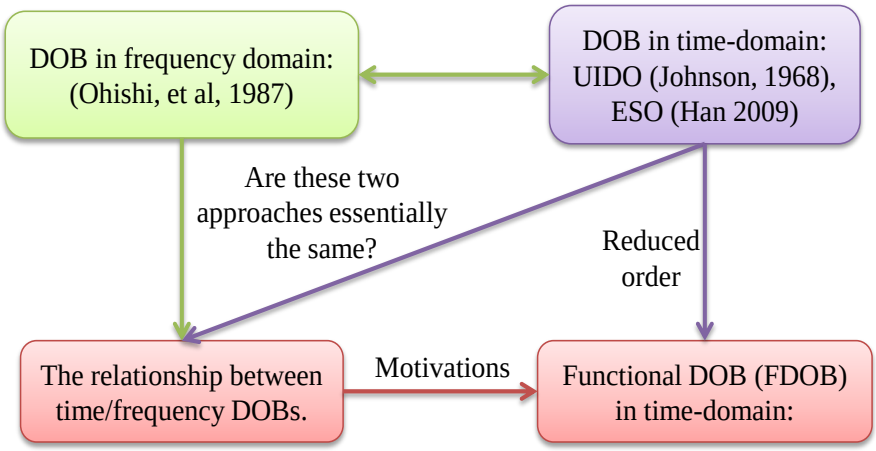

Figure 6.1. Illustration of the motivations and the relationship of the results in this Chapter with the existing ones.

There are two distinct approaches for linear system disturbance observer design including time-domain DOBs [8, 48, 49, 63, 87] and frequency-domain DOBs [1, 52, 88, 89]. The time-domain DOB firstly appeared in the late 1960s when [48] first developed the *Disturbance Accommodation Control* by proposing *Unknown In-*

put Disturbance Observer (UIDO). Recently, from different prospects, Han [49, 87] developed *Active Disturbance Rejection Control (ADRC)* through the technique of *Extended State Observer (ESO)*. The key idea behind the above state space approaches is to firstly augment the plant with the disturbances/uncertainties and then construct an observer estimating the augmented states including the disturbances. On the other hand, the frequency-domain DOBs were originally proposed by [1] (see also recent work [90] for detailed design guidance). The original idea is to obtain the disturbance estimate by filtering the difference between control input and the calculated input using the inverse model of nominal plant. This approach has recently been further developed to achieve robust stability in [91] and handle system with unknown relative degree in [89].

The aforementioned two types of DOBs were developed from different prospects with different design principles and tools. So far, little literature is available to investigate the relationship between them except the work in [52]. [52] pioneered the study of the relationship between frequency domain and time domain DOBs by analysing their structure and transfer functions. It is concluded in [52] that the frequency domain DOB is a generalization of the time domain DOB. This is because that there is less freedom in time domain DOB of choosing the order and the relative degree of the transfer function from control to disturbance estimate, and the time domain DOB generates an observer with a higher order compared with frequency domain DOB. However, as pointed out in [92], the frequency domain DOB structure in [52] mainly focused on minimum phase system due to the involvement of the inverse of the normal plant. It shall be highlighted that both the system model and disturbance model are supposed to be in an observable canonical forms in the time domain DOB design discussed in [52]. Therefore it may not be easy to see how the disturbance model is incorporated in the corresponding transfer functions of the time domain DOB. Consequently, as pointed out in [52], it becomes hard to select the equivalent low pass filter in corresponding frequency domain DOB to handle generic disturbances for non-minimum phase systems.

This Chapter first presents more generic analysis of the relationship between time-domain and frequency-domain DOB design methods, which extends the work of [52] from a frequency domain DOB structure mainly for minimum phase systems to a more general DOB structure. Furthermore, the system model and disturbance model of the time domain DOB discussed in this Chapter are in a generic form. As a result, it is explicitly pointed out how the system model and disturbance model are incorporated in the equivalent transfer functions realisation of the DOB designed in the state space approach. It is also discovered that the traditional frequency domain

DOB employing a low pass filter with unity gain is only able to effectively handle a specific class of disturbance that satisfies the matching condition.

As pointed out in [52], compared with the frequency domain DOB, the existing time domain DOB generates an observer of a high order. This Chapter then further addresses this issue by proposing a new type of time domain DOB (termed as Functional Observer based DOB (FDOB)). This new state space DOB design method reduces the observer order by combining the idea of augmenting the system states with disturbance states and the functional observer design method proposed in [4,83,84]. Detailed discussion on FDOB is given including the observer structure, transfer function implementation of the time domain DOB, geometric interpretation, and its existence condition. Compared with frequency domain DOB, the proposed FDOB can directly handle more classes of disturbances (matched or mismatched disturbances, harmonic disturbance, etc.), while compared with the traditional time domain DOB, the proposed FDOB can generate an observer with a lower order.

6.2 Preliminaries

In this section, preliminary results on the frequency-domain DOBs in [1] and time domain DOBs in [48, 52, 63] are briefly reviewed.

6.2.1 Frequency-domain DOBs

The frequency-domain DOBs were originally proposed in [1]. Suppose that the transfer function of the considered system is $G(s)$. The basic idea in [1] is to obtain disturbance estimate by filtering (through a low pass filter $Q(s)$) the difference between control input and the calculated input using the inverse model of nominal plant $G_n(s)$. The basic diagram in [52] with some modification from [53] is given in Fig. 6.2, where $Q(s)$ is designed as a low-pass filter with unity gain and the relative

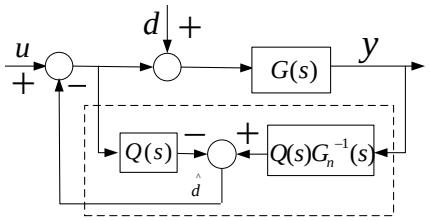

Figure 6.2. The diagram of classic Q-filter based DOB in [1]

degree of $Q(s)$ is no less than that of the nominal plant $G_n(s)$ such that $Q(s)G_n^{-1}(s)$ is implementable (see, [1, 52] among many others).

However, as pointed out in [92], the original structure in [1] can not effectively handle the non-minimum phase systems since the direct inverse of the nominal plant $G_n(s)$ brings unstable poles in $Q(s)G_n^{-1}(s)$. To this end, an improved and more generic version of DOB in frequency domain is given in [53], which can be equivalently represented in Fig. 6.3, where M(s) and N(s) take the following form

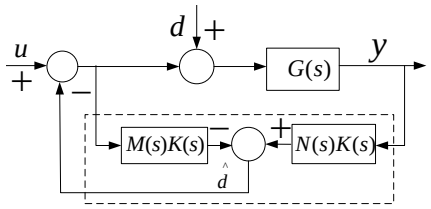

Figure 6.3. The diagram of a generic DOB structure.

ng

$$M(s) = \frac{M_n(s)}{L_1(s)},\ N(s) = \frac{N_n(s)}{L_1(s)}, \tag{6.2.1}$$

where the nominal plant $G_n(s) = M_n(s)/N_n(s)$, $L_1(s)$ is a stable polynomial, $K(s) = K_n(s)/L_2(s)$ is designed as a low pass filter such that $M(s)K(s)$ is a low-pass filter with unity gain.

6.2.2 Time-domain DOBs

The time domain DOB was originally proposed in [48, 63] to remove the effect of unmeasurable disturbances on control system performance. Its basic philosophy is that the disturbance estimate can be obtained by simultaneously estimating the augmented states consisting of state dynamics and the disturbance dynamics. The mathematical interpretation is given as follows. Without loss of generality, consider a single-input-single-output (SISO) linear system (it should be noted that this approach can directly handle multiple-input-multiple-output (MIMO) systems) subjected to unknown disturbances, given by

$$\begin{cases} \dot{x} = Ax + Bu + Dd, \\ y = Cx, \end{cases} \tag{6.2.2}$$

where $x \in R^n$, $u \in R$, $d \in R$ and $y \in R$ are the system states, control input, disturbance and measurement, respectively. A, B, C, D are the corresponding system matrices, which can be considered as a state space realization of the nominal plant $G_n(s)$ in Fig. 6.2. If there does not exist a $\bar{D}$ of appropriate dimension such that $D = B\bar{D}$, then d becomes a mismatched disturbance [66, 93].

The disturbance is supposed to be generated by the following linear exogenous system [63]

$$\dot{\omega} = S\omega, \quad d = H\omega, \tag{6.2.3}$$

where $\omega \in R^q$ and the pair (S, L) is known and observable.

To facilitate the discussion, a definition is given here to category the different disturbance models.

Definition: If the matrix S in (6.2.3) satisfies $det(S) = 0$, the disturbance is defined as Type I disturbance; otherwise, the disturbance is defined as Type II disturbance for $det(S) \neq 0$.

Remark 1: It should be noted that the widely investigated *high order disturbance* is a special case of Type I disturbance, e.g., constant disturbance when $S = 0$ and $H = 1$, which is the case investigated by DAC in [48] and Extended State Observer (ESO) in [49] and r-th polynomial disturbance when $S = \begin{bmatrix} O_{(r-1)\times 1} & I_{r-1} \\ 0 & O_{1\times(r-1)} \end{bmatrix}$ and $H = \begin{bmatrix} 1 & O_{1\times(r-1)} \end{bmatrix}$, which is the case investigated by high order disturbance observer in [94], generalized ESO in [95], Generalized Proportional Integral (GPI) observer in [96], etc. While harmonic disturbance represented by $S = \begin{bmatrix} 0 & \lambda \\ -\lambda & 0 \end{bmatrix}$ with $\lambda \neq 0$ and $H = \begin{bmatrix} 1 & 0 \end{bmatrix}$ (e.g. [62]) is a special case of Type II disturbance.

Combing the system dynamics (6.2.2) and disturbance dynamics (6.2.3), a composite system can be obtained:

$$\begin{cases} \dot{\bar{x}} = \bar{A}\bar{x} + \bar{B}u, \\ y = \bar{C}\bar{x}, \end{cases} \tag{6.2.4}$$

where $\bar{x} = [x^T, \omega^T]^T$, the system matrices are given by

$$\bar{A} = \begin{bmatrix} A & DH \\ O_{q\times n} & S \end{bmatrix}, \bar{B} = \begin{bmatrix} B \\ O_{q\times 1} \end{bmatrix}, \bar{C} = \begin{bmatrix} C & O_{1\times q} \end{bmatrix}.$$

Under the detectability condition of the matrix pair $(\bar{A}, \bar{C})$, an observer estimating the augmented states $\bar{x}$ of (6.2.4) and consequently the disturbance can be designed as

$$\begin{cases} \dot{\hat{\bar{x}}} = \bar{A}\hat{\bar{x}} + \bar{B}u + K(y - \bar{C}\hat{\bar{x}}), \\ \hat{\omega} = \tilde{C}\hat{\bar{x}}, \ \hat{d} = H\hat{\omega}, \end{cases} \tag{6.2.5}$$

where K is the observer gain matrix to be designed (e.g. pole assignment of the matrix pair $(\bar{A}, \bar{C})$) and $\tilde{C} = [O_n, I]$. Similar technique has also been used for stochastic systems in Chapter 5.

6.3 Relationship between DOBs in time/frequency domain

In this section, frequency-domain analysis is performed on the time domain DOB (6.2.5) to derive a set of transfer functions such that comparison can be made between the time and frequency domain DOB design methods. It should be noted that the frequency-domain analysis of time domain DOB has been investigated in [52] with both the system model and disturbance model (6.2.2) and (6.2.3) in observable canonical forms. A generic system model and a generic disturbance model are considered in this Chapter which explicitly shows how the system model and disturbance model are incorporated in the transfer functions.

From (6.2.5), one can obtain the transfer functions from control input $u(s)$ and measurement $y(s)$ to disturbance estimate $\hat{d}(s)$ using Laplace transformation, given by

$$\hat{d}(s) = -G_{u\hat{d}}(s)u(s) + G_{y\hat{d}}(s)y(s), \tag{6.3.1}$$

where

$$G_{u\hat{d}}(s) = -H\tilde{C}[sI - (\bar{A} - K\bar{C})]^{-1}\bar{B}, \tag{6.3.2}$$

$$G_{y\hat{d}}(s) = H\tilde{C}[sI - (\bar{A} - K\bar{C})]^{-1}K. \tag{6.3.3}$$

The transfer function realisation of the time domain DOB (6.2.5) is represented in Fig. 6.4

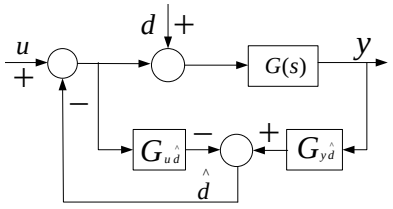

Figure 6.4. Frequency-domain interpretation of time-domain DOBs.

To explicitly find out the relationship between the transfer functions $G_{u\hat{d}}(s)$, $G_{y\hat{d}}(s)$ and the system/disturbance models (6.2.2), (6.2.3), rigorously theoretical analysis is performed on (6.3.2) and (6.3.3), and the results are summarized in Theorem 13.

Theorem 13. *For linear system (6.2.2) with disturbance model (6.2.3), if the time domain DOB is designed by (6.2.5), then the transfer function realisation (6.3.1) is given by*

$$G_{u\hat{d}}(s) = \frac{Hadj(sI - S)K_2M_n(s)}{det(sI - (\bar{A} - K\bar{C}))}, \tag{6.3.4}$$

$$G_{y\hat{d}}(s) = \frac{Hadj(sI - S)K_2N_n(s)}{det(sI - (\bar{A} - K\bar{C}))}, \tag{6.3.5}$$

where $M_n(s)$ and $N_n(s)$ are the numerator and denominator of the nominal plant $G_n(s)$.

The proof is given in Appendix A.3.

Remark 2: Different from the results of [52], it can be explicitly seen from Eqs. (6.3.4) and (6.3.5) that how the system model (i.e., the system matrices (A, B, D, C)) and disturbance model (i.e., the pair (S, H)) of the DOB (6.2.5) are incorporated into the transfer functions.

6.3.1 Similarities of time/frequency-domain DOBs

The relationship between frequency domain DOB and frequency domain DOB given in Fig. 6.2 was first investigated in [52]. However, as pointed out in [92], the classic frequency-domain DOB structure in [52] can not effectively handle non-minimum phase system. To this end, much generic relationship is established in the comparison analysis. Specifically, generic system dynamics (6.2.2) with generic disturbance dynamics (6.2.3) are directly handled, and the frequency domain DOB in Fig. 6.3 proposed in [53] can effectively handle non-minimum phase system. The result in [52] is shown to be a special case of the results in this work.

Equivalence between time domain and frequency domain DOBs

The comparison results between the time domain DOB (6.2.5) and the frequency domain DOB with generic structure given in Fig. 6.3 are summarized in the following points.

i. The denominator of (6.3.4) (i.e., a stable polynomial of degree n+q) can be factored into $det(sI-(\bar{A}-K\bar{C})) = L_1(s)L_2(s)$. Consequently, Eqs. (6.3.4) and (6.3.5) can be reformulated into the same format of $M(s)K(s)$ and $N(s)K(s)$ in Fig. 6.3 by treating $K_n(s) := Hadj(sI - S)K_2$;

ii. Comparing the structures of frequency domain DOB in Fig. 6.3 and time domain DOB in Fig. 6.4, one can obtain that they share a same structure in transfer function form by treating $M(s)K(s)$ as $G_{u\hat{d}}$ and $N(s)K(s)$ as $G_{y\hat{d}}$.

iii. For Type I disturbance (see, Definition 1, i.e., $det(S) = 0$) under disturbance satisfying matching condition (i.e., D=B), one can prove that

$$G_{u\hat{d}}(0) = 1, \tag{6.3.6}$$

which means $G_{u\hat{d}}$ is a low-pass filter with unity gain. The proof is given in Appendix A.3.

iv. One can also obtain the following identity

$$\frac{1}{1-G_{u\hat{d}}} = \frac{det(sI-(\bar{A}-K\bar{C}))}{det(sI-A+K_1C)det(sI-S)}. \tag{6.3.7}$$

The proof is given in Appendix A.3. One can see from (6.3.7) that $1/1-G_{u\hat{d}}$ includes the disturbance model information $1/det(sI-S)$. The need of $1/1-G_{u\hat{d}}$ including the disturbance model has been identified in [52] but it is hard to choose $Q(s)$ to implement it.

Relationship with the results in [52]

The results in this work significantly extend the celebrated work in [52]. First, the aforementioned Points i and ii reduce to the results in [52] when the system dynamics (6.2.2) and disturbance dynamics (6.2.3) take the special observable canonical structure, and the frequency domain DOB in Fig. 6.3 reduces to the traditional one in Fig. 6.2. This can be obtained by selecting

$$L_1(s) = M_n(s),\ K(s) = Q(s).$$

In Point iii, it is rigorously proved that $G_{u\hat{d}} = 1$ holds only for Type I disturbance satisfying matching condition. Specifically, the high order disturbance $1/s^n$ discussed in [52] is a special case of matched Type I disturbance. Based on the results, the traditional frequency domain DOBs using low pass filter $Q(s)$ with unity gain in Fig. 6.2 can only handle matched Type I disturbance and fail to handle mismatched disturbance or Type II disturbance such as harmonic disturbance, etc.

It has been pointed out in [52] that it is not trivial to select $G_{u\hat{d}}$ to handle generic disturbance model for non-minimum phase system, but the Theorem 1 and Point iv explicitly point out how the $G_{u\hat{d}}$ contains the unstable zeros of the plant M_n and $1/(1-G_{u\hat{d}})$ includes the disturbance model information $1/det(sI-S)$. This result can help us propose a frequency domain DOB which can handle generic disturbances for non-minimum phase systems, which is discussed in Section 6.5.

6.3.2 Motivations: gaps of time/frequency-domain DOBs

Although the frequency domain DOB is equivalent to the frequency domain in terms of structure, there still exist some gaps summarized in the following points.

Observer order and minimum relative degree

Firstly, the observer order of time domain DOB is larger than that of frequency-domain DOB for plants with stable zeros (see, P 546 of [52]). This can be explained as follows. One can first obtain from the denominator of (6.3.4) and (6.3.5) that the order of time domain DOB is $n+q$. Suppose the relative degree of normal plant $G_n(s)$ is n_r. One can obtain from [52] (see, p. 541) that the minimum degree of the denominator of equivalent $G_{u\hat{d}}$ is $q+n_r-1$ and consequently the minimum order of the frequency domain DOB is determined by the equivalent $G_{y\hat{d}}$, i.e., $q+n_r-1+n-n_r=n+q-1$, which is smaller than the order of time domain DOB.

Secondly, the minimum relative degree of $G_{u\hat{d}}$ of time domain DOB is larger than that of frequency domain DOB. As pointed out in [52] the relative degree of equivalent $G_{u\hat{d}}$ is larger than or equal to the relative degree of the nominal plant, so the minimum relative degree of $G_{u\hat{d}}$ in frequency domain DOB as given in Fig. 6.3 can be chosen to equal to that of $G_n(s)$, i.e., n_r. However, this observation does not hold in the time-domain DOB results. One can obtain from (6.3.4) that

$$\begin{aligned} &deg(Hadj(sI-S)K_2) \leq q-1; \\ &deg(M_n(s)) = n-n_r; \\ &deg(det(sI-(\bar{A}-K\bar{C}))) = n+q, \end{aligned} \tag{6.3.8}$$

where q and n are the dimension of system matrix S and A of disturbance model (6.2.3) and system model (6.2.2) respectively. The minimum relative degree of $G_{u\hat{d}}(s)$ happens when $deg(Hadj(sI-S)K_2)=q-1$, and equals to

$$n+q-(q-1+n-n_r)=n_r+1, \tag{6.3.9}$$

which is larger than that of frequency domain DOB by 1.

Disturbance types

In addition, from the proof of (6.3.6) (see Appendix A.3), one can see that $G_{u\hat{d}}(0)=1$ holds only when the following two conditions hold simultaneously

$$D=B,\ det(S)=0, \tag{6.3.10}$$

which means the frequency domain DOB using a low-pass filter $Q(s)$ with unity DC gain in Fig. 6.2 can only effectively handle matched Type I disturbances rather than generic disturbance or mismatched disturbances.

To avoid the aforementioned drawbacks of the current DOB design methods (i.e., higher observer order in existing time domain DOB and hard to handle generic and mismatched disturbances in existing frequency domain DOB), a new type of time domain DOB (termed as functional observer based DOB (FDOB)) is proposed to reduce the observer order by combing the idea of augmenting the system states with disturbance states and the functional observer design method proposed in [4,83,84]. The frequency-domain DOBs can also be designed to handle more types of disturbances (mismatched disturbance and Type II disturbance) using FDOB techniques and its frequency domain counterpart through transfer function realization.

6.4 Functional observer based DOB

The basic philosophy of functional observer based DOB is that since part of the states are directly available by the measurement $y = \bar{C}\bar{x}$, there is no need estimating that part of the states and sometimes even part of the unmeasurable states do not need to be estimated for the purpose of disturbance estimation. So only estimating $L\bar{x}$ rather than $\bar{x}$ is needed, where L is designed in the special structure

$$L = \begin{bmatrix} L_0 & O \\ O & I_q \end{bmatrix}, \tag{6.4.1}$$

where the gain matrix L_0 in L lies in the orthogonal complement space of measurement matrix C and so $\begin{bmatrix} L \\ \bar{C} \end{bmatrix}$ has a full row-rank. When $L\bar{x}$ is obtained, one can obtain the disturbance estimate $\hat{d} = \tilde{C}L\bar{x}$ with $\tilde{C} = [O, I_q]$. In the following part, the FDOB is introduced in terms of observer structure, transfer function realization, geometric interpretation, existence condition and design procedure respectively.

6.4.1 Observer structure

To develop a FDOB, the idea of augmenting the system state with disturbance state and the functional observer design method proposed in [83,84] are combined together. After choosing L in the special form as in (6.4.1), the FDOB for linear system (6.2.4) has the form,

$$\begin{cases} \dot{z} = Fz + Gy + Tu, \\ \hat{\xi} = z + Jy, \\ \hat{\omega} = \tilde{C}\hat{\xi},\ \hat{d} = H\hat{\omega}. \end{cases} \tag{6.4.2}$$

where the gain matrices are designed such that the following matrix identities hold:

$$\begin{cases} W\bar{A} = FW + G\bar{C}, \text{ (Sylvester equation)} \\ W = L - J\bar{C}, \\ T = W\bar{B}, \\ F \text{ is stable.} \end{cases} \tag{6.4.3}$$

Under condition (6.4.3), one can prove that the estimation error $e = L\bar{x} - \hat{\xi}$ converges to zero and consequently $\hat{\xi}$ is the estimate of the state function $L\bar{x}$ (e.g., [83]).

6.4.2 Geometric interpretation

Inspired by the approach in [97], a geometric interpretation of the FDOB is given. This geometric interpretation is not only important in understanding the observer structure but also plays a key role in frequency-domain analysis for the purpose of transfer function implementation.

Define an intermediate variable $z_i = L\bar{x}$, from which one can obtain

$$\bar{x} = L^+ z_i + (I - L^+ L)x_d, \tag{6.4.4}$$

where x_d is an arbitrary vector and may contain unobservable states if the original $\bar{x}$ system is not fully observable. This is also a division of the state space into a space of dimension corresponding to the functional $z_i = L\bar{x}$ and its complement in terms of projection operators, L^+L and $I - L^+L$. Then one can obtain the following model regarding the variable z_i,

$$\begin{cases} \dot{z}_i = L\bar{A}L^+ z_i + L\hat{A}x_d + L\bar{B}u, \\ y = \bar{C}L^+ z_i + \hat{C}x_d, \end{cases} \tag{6.4.5}$$

where $\hat{A} = \bar{A}(I - L^+L)$ and $\hat{C} = C(I - L^+L)$.

In addition, one can obtain from (6.4.2) that

$$\dot{\hat{\xi}} = \dot{z} + J\dot{y},$$

which means in the observer (6.4.2), the information of $\dot{y}$ has actually been used in derivation of $\hat{\xi}$. In addition, one can obtain from (6.2.4) and (6.4.4) that

$$\dot{y} = \bar{C}\dot{\bar{x}} = \bar{C}\bar{A}\bar{x} + \bar{C}\bar{B}u = \bar{C}\bar{A}L^+ z_i + \bar{C}\hat{A}x_d + \bar{C}\bar{B}u. \tag{6.4.6}$$

Putting (6.4.5) and (6.4.6) together, one can obtain

$$\begin{cases} \dot{z}_i = L\bar{A}L^+ z_i + L\hat{A}x_d + L\bar{B}u, \\ \begin{bmatrix} \dot{y} \\ y \end{bmatrix} = \begin{bmatrix} \bar{C}\bar{A}L^+ \\ \bar{C}L^+ \end{bmatrix} z_i + \begin{bmatrix} \bar{C}\hat{A} \\ \hat{C} \end{bmatrix} x_d + \begin{bmatrix} \bar{C}\bar{B} \\ O \end{bmatrix} u. \end{cases} \tag{6.4.7}$$

Define $\Psi = \begin{bmatrix} \bar{C}\bar{A}L^+ \\ \bar{C}L^+ \end{bmatrix}$, $\Sigma = \begin{bmatrix} \bar{C}\hat{A} \\ \hat{C} \end{bmatrix}$, $y^* = \begin{bmatrix} \dot{y} \\ y \end{bmatrix}$ and $U^* = \begin{bmatrix} \bar{C}\bar{B} \\ O \end{bmatrix}$, (6.4.7) can be put into a compact form:

$$\begin{cases} \dot{z}_i = L\bar{A}L^+ z_i + L\hat{A}x_d + L\bar{B}u, \\ y^* = \Psi z_i + \Sigma x_d + U^* u. \end{cases} \tag{6.4.8}$$

For system (6.4.8), a Luenberger-type state observer can be designed as

$$\begin{aligned} \dot{\hat{z}}_i &= L\bar{A}L^+ \hat{z}_i + L\bar{B}u + [J,K](y^* - \Psi\hat{z}_i - U^*u) \\ &= (L\bar{A}L^+ - [J,K]\Psi)\hat{z}_i + [J,K]y^* + Tu, \end{aligned} \tag{6.4.9}$$

where gain matrix K is defined as $K := G - FJ$, and the identity $T = W\bar{B} = (L - J\bar{C})$ of (6.4.3) has been used in derivation of the second equality of (6.4.9).

Define $e_i = z_i - \hat{z}_i$, then its dynamic is given by

$$\begin{aligned} \dot{e}_i &= L\bar{A}L^+ \hat{z}_i + L\bar{B}u + [J,K](y^* - \Psi\hat{z}_i - U^*u) \\ &= (L\bar{A}L^+ - [J,K]\Psi)e_i + \underbrace{(L\hat{A} - [J,K]\Psi)x_d}_{unknown} \\ &= Fe_i, \end{aligned} \tag{6.4.10}$$

if the following matrix equalities hold simultaneously,

$$F = L\bar{A}L^+ - [J,K]\Psi, \quad L\hat{A} - [J,K]\Psi = O.$$

The observer structure in (6.4.9) gives another explanation of the original observer (6.4.2). One can obtain from (6.4.2) that

$$\begin{aligned} \dot{\hat{\xi}} &= \dot{z} + J\dot{y} = Fz + Gy + Tu + J\dot{y} \\ &= F(\hat{\xi} - Jy) + J\dot{y} + Tu \\ &= F\hat{\xi} + [J, \underbrace{G - FJ}_{K}] \begin{bmatrix} \dot{y} \\ y \end{bmatrix} + Tu, \end{aligned}$$

which is the same as (6.4.9).

one can see from (6.4.9) that different from the traditional Luenberger observer,

the gain matrix $[J, K]$ with $K = G - FJ$ should satisfy the following two criteria simultaneously, i.e.,

$$L\hat{A} - [J, K]\Psi = O, \tag{6.4.11}$$

$$F = (L\bar{A}L^{+} - [J, K]\Psi) \text{ is Hurwitz matrix.} \tag{6.4.12}$$

Remark 3: Through the geometric interpretation, one knows from z_i dynamic (6.4.5) and FDOB (6.4.9) that the observer error (6.4.10) converges to zero regardless of x_d in (6.4.5). That means the FDOB can still work due to the decoupling principle even if the original systems are not completely observable and x_d contains the unobservable states,

6.4.3 Transfer function realisation

In this subsection, frequency-domain analysis is performed on the FDOB (6.4.2) such that the relationship between the proposed FDOB and frequency domain DOB can be investigated, upon which the FDOB in time domain can be implemented in frequency domain using the derived transfer functions. One can obtain the transfer functions $G_{u\hat{d}}(s)$ and $G_{y\hat{d}}(s)$ based on Laplace transformation of (6.4.2), given by

$$\hat{d}(s) = -G_{u\hat{d}}(s)u(s) + G_{y\hat{d}}(s)y(s),$$

where

$$G_{u\hat{d}}(s) = -H\tilde{C}[sI - F]^{-1}T, \tag{6.4.13}$$

$$G_{y\hat{d}}(s) = H\tilde{C}[(sI - F)^{-1}G + J]. \tag{6.4.14}$$

To explicitly find out the relationship between the transfer functions $G_{u\hat{d}}(s)$, $G_{y\hat{d}}(s)$ and the system/disturbance model (6.2.2), (6.2.3), theoretical analysis is performed on (6.4.13) and (6.4.14) and the results are summarized in Theorem 14.

Theorem 14. *For linear system (6.2.2) with disturbance model (6.2.3), if the DOB is designed using FDOB (6.4.2), then the transfer functions from input $u(s)$ and measurement $y(s)$ to disturbance estimate $\hat{d}(s)$ are given by*

$$G_{u\hat{d}}(s) = \frac{Hadj(sI - S)J_2M_n(s)}{det(sI - F)}, \tag{6.4.15}$$

$$G_{y\hat{d}}(s) = \frac{Hadj(sI - S)J_2N_n(s)}{det(sI - F)}. \tag{6.4.16}$$

The proof is given in Appendix A.3. Similar to Theorem 13, the disturbance model (i.e., the pair (S, H)) is also explicitly reflected in the transfer functions

(6.4.15) and (6.4.16).

The comparison analysis of the newly proposed FDOB with the frequency domain DOB in Fig. 6.3 are performed in the following ways.

i. Firstly, similar to the case of the time domain DOB, the denominator of (6.4.15) (i.e., a stable polynomial) can also be factored into $det(sI - F) = L_1(s)L_2(s)$, then (6.4.15) and (6.4.16) can be put into the same format as $M(s)K(s)$ and $N(s)K(s)$ in Fig. 6.3 by treating $K_n(s) := Hadj(sI - S)K_2$.

ii. Secondly, the frequency-domain structure of the FDOB is the same as that of the time domain DOB in Fig. 6.4 and consequently the same as that of the frequency-domain DOB in Fig. 6.3.

iii. Thirdly, one can also prove that

$$G_{u\hat{d}}(0) = 1, \tag{6.4.17}$$

under the conditions $D = B$ and $det(S) = 0$, the proof is given in Appendix A.3.

iv. Fourthly, one can also obtain the following identity

$$\frac{1}{1 - G_{u\hat{d}}} = \frac{det(sI - F)}{det(sI - A_4 + J_1A_4)det(sI - S)}. \tag{6.4.18}$$

The proof is similar to that of (6.3.7) and so omitted here. One can see from (6.4.18) that $1/1 - G_{u\hat{d}}$ includes the generic disturbance model information $1/det(sI - S)$, which is consistent with the conclusion of [52] for the purpose of generic disturbance estimation through frequency domain DOB.

Remark 4: Compared the $G_{u\hat{d}}$ of the time domain DOB in (6.3.4) with that of FDOB in (6.4.15), one can see that the numerators of them are the same, however, the denominator has been changed from $det(sI - (\bar{A} - K\bar{C}))$ to $det(sI - F)$. On the one hand, the dimension of F equals to the row rank of $L = \begin{bmatrix} L_0 & O \\ O & I \end{bmatrix}$ and L_0 has a full row-rank and so the relative degree of $G_{u\hat{d}}$ of the FDOB in (6.4.15) is less than that of the time domain DOB in (6.3.4). More importantly, one can also see that the observer order of FDOB, i.e., the row number of L is smaller than that of the traditional time domain DOB, i.e., the order of $\bar{A}$. Consequently, the proposed FDOB can substantially reduce the DOB order, especially when multiple measurements are available. However, to reduce the observer order of FDOB, one can not choose an L with an arbitrarily small row number, the L should be selected

such that the existence condition of the FDOB is satisfied, which is summarized in the following section.

6.4.4 Existence condition

As the disturbance observer design problem has been transformed into the functional observer design, the existing results in [83] can be applied as summarized as follows.

First, the solvability of (6.4.11) is guaranteed by

$$rank(\begin{bmatrix} L\bar{A} \\ \bar{C}\bar{A} \\ \bar{C} \\ L \end{bmatrix}) = rank(\begin{bmatrix} \bar{C}\bar{A} \\ \bar{C} \\ L \end{bmatrix}), \tag{6.4.19}$$

and the solution $[J, K]$ in the constraint equation $L\hat{A} - [J, K]\Psi = O$ is given by

$$[J, K] = L\hat{A}\Sigma^{+} + Z(I - \Sigma\Sigma^{+}), \tag{6.4.20}$$

with Z being any compatible matrix.

Using (6.4.20), one can obtain that the matrix F in can be represented in the following form

$$F = U - ZV, \tag{6.4.21}$$

with

$$U = L\bar{A}L^{+} - L\hat{A}\Sigma^{+}\Psi, \tag{6.4.22}$$

$$V = (I - \Sigma\Sigma^{+})\Psi. \tag{6.4.23}$$

From [83], one can obtain the condition , i.e., F being Hurwitz (or the pair (U,V) is detectable) is equivalent to

$$rank(\begin{bmatrix} sL - L\bar{A} \\ \bar{C}\bar{A} \\ \bar{C} \end{bmatrix}) = rank(\begin{bmatrix} \bar{C}\bar{A} \\ \bar{C} \\ L \end{bmatrix}), \forall s \in C, Re(s) \geq 0. \tag{6.4.24}$$

To summarize, the existence conditions for the FDOB are (6.4.19) and (6.4.24).

6.4.5 Design procedure

The design procedure of FDOB is based on the functional observer design procedure in [83]. For the sake of completeness for the FDOB, the design procedure is also

given. With the aforementioned geometric interpretation and existence condition results, the design procedure of the FDOB is summarized as follows:

i. Matrices U and V are firstly obtained from (6.4.22) and (6.4.23);

ii. Z and F can be obtained from (6.4.21) based on pole assignment of U and V;

iii. The matrices J and K can be obtained from (6.4.20) and G can thus be obtained from $K = G - FJ$;

iv. Matrix T can be obtained from $T = (L - J\bar{C})\bar{B}$.

6.5 Applications of the results

One can see from the proof of (6.3.6) and (6.4.17) (see Appendix A.3) that, $G_{u\hat{d}}(0) = 1$ holds only when condition (6.3.10), i.e., $D = B$ and $det(S) = 0$ hold simultaneously. This two conditions may restrict the application scope of the existing frequency domain DOBs. Firstly, the existing frequency domain DOBs can only handle Type I disturbance under disturbance satisfying matching condition [98]. In classic frequency domain DOBs, the transfer function $G_{u\hat{d}}$ is designed as a low-pass filter with unity gain. However, for generic disturbances (harmonic disturbance, etc.), the filter $G_{u\hat{d}}$ actually relies on the disturbance model information, i.e., the pair (S, H) and may not always generate a unity gain. Secondly, the classic frequency-domain DOBs can only handle matched disturbance. For mismatched disturbance estimate [99], one can see from both Theorem 13 and Theorem 14) that the disturbance distribution matrix D should also be taken into account (see, the denominators of the transfer functions).

However, based on the frequency-domain analysis results (see, Theorem 13 and Theorem 14) of the time-domain filters (the traditional time domain filter and the newly proposed FDOB), one can actually extend the application scope of the frequency-domain DOBs based on their frequency domain counterparts. The method is summarized in the following steps:

Step 1: One can design the DOBs in time-domain, since the time-domain DOBs can directly handle matched, mismatched and generic disturbances.

Step 2: One can calculate two transfer functions $G_{u\hat{d}}$ and $G_{y\hat{d}}$ based on the results of Theorem 13 and 14.

Step 3: Implement the DOBs using the diagram in Fig. 6.4 based on the obtained two transfer functions.

6.6 Examples

In this section, two examples are given to illustrate the main findings. In the first example, a non-minimum phase system with three different kinds of disturbances are considered including matched step disturbance, mismatched step disturbance and matched harmonic disturbance with unknown amplitude and phase. This example is to illustrate the results in Sections 6.4 and 6.5. Then the proposed FDOB is applied to the disturbance estimation and rejection problem for a practical rotary mechanical system of non-minimum phase.

6.6.1 Numerical example

Consider a unstable non-minimum phase system with transfer function given by

$$G(s) = \frac{5(s-9)}{s(s-25)}. \tag{6.6.1}$$

The state space model of it in the presence of matched disturbance d is given by

$$\begin{cases} \begin{bmatrix} \dot{x}_1 \\ \dot{x}_2 \end{bmatrix} = \underbrace{\begin{bmatrix} 0 & 1 \\ 0 & 25 \end{bmatrix}}_{A} \underbrace{\begin{bmatrix} x_1 \\ x_2 \end{bmatrix}}_{x} + \underbrace{\begin{bmatrix} 5 \\ 80 \end{bmatrix}}_{B} u + \underbrace{\begin{bmatrix} 5 \\ 80 \end{bmatrix}}_{D} d, \\ y = \underbrace{\begin{bmatrix} 1 & 0 \end{bmatrix}}_{C} x. \end{cases}$$

Without loss of generality, suppose a state feedback controller $u = \begin{bmatrix} 20.67 & -2.37 \end{bmatrix} x$ has been pre-designed. The initial state for simulation study is chosen as $x_0 = [0,\ 5]^T$.

Matched disturbance

Fist consider the matched unknown step disturbance estimation based on the proposed FDOB, i.e., $S = 0, H = 1$ in disturbance model (6.2.3). The L_0 in functional matrix (6.4.1) as $L_0 = \begin{bmatrix} 0 & 1 \end{bmatrix}$, based on which one can check that the conditions (6.4.19) and (6.4.24) are satisfied. Then following the design procedure in Section 6.4.5, one can calculate U, V as

$$U = \begin{bmatrix} 25 & 80 \\ 0 & 0 \end{bmatrix}, V = \begin{bmatrix} 1 & 5 \\ 0 & 0 \end{bmatrix}.$$

By choosing the poles of F as $p_1 = -30, p_2 = -40$, one can calculate the corresponding Z, F and then the rest of the matrices J, G, T. The initial states of the FDOB

(6.4.2) are chosen as a zero vector. Simulation result of the disturbance estimate is shown in Fig. 6.5.

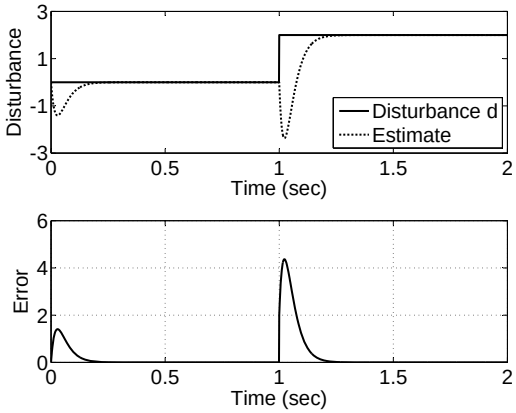

Figure 6.5. Matched step disturbance: upper plots (disturbance estimate), lower plot (estimation error).

One can see from Fig. 6.5 that the proposed FDOB can exponentially asymptotically estimate the step disturbance, where the initial disturbance estimation error is due to the mismatch between the initial states of original system and observer system.

Besides, one can calculate the transfer functions from the disturbance estimate to the control input and output, given by

$$G_{u\hat{d}}(s) = \frac{-400(s-9)}{3(s+30)(s+40)},$$

$$G_{y\hat{d}}(s) = \frac{-80(s-25)}{3(s+30)(s+40)}.$$

One can verify that $G_{u\hat{d}}(s)/G_{y\hat{d}}(s) = G(s)$ and $G_{u\hat{d}}(0) = 1$. Besides, the relative degree of $G_{u\hat{d}}(s)$ is 1, which is equal to that of the original system (6.6.1). And, the observer order of FDOB equals to the dimension of original plant. That means there exists a disturbance observer in state-space, where the relative degree of $G_{u\hat{d}}$ and the order of the observer are equal to those of the frequency domain DOB.

Mismatched disturbance

Then consider the case of mismatched unknown step disturbance estimation. The disturbance distribution matrix is selected as $D = \begin{bmatrix} 0 & 80 \end{bmatrix}^T$ and the matrices S, H, L_0 are selected the same as that of Section 6.6.1. One can calculate the U, V as

$$U = \begin{bmatrix} 25 & 80 \\ 0 & 0 \end{bmatrix}, V = \begin{bmatrix} 1 & 0 \\ 0 & 0 \end{bmatrix}.$$

The rest of the design procedure and parameter selection is the same as that in Section 6.6.1 and the simulation result of the disturbance estimate is shown in Fig. 6.6

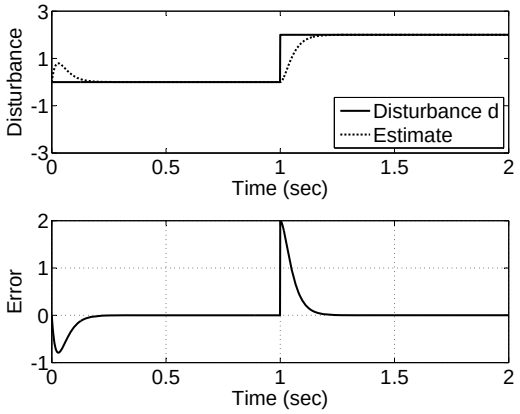

Figure 6.6. Mismatched step disturbance estimate: upper plots (disturbance estimate), lower plot (estimation error).

One can see from Fig. 6.6 that the proposed FDOB can exponentially asymptotically estimate the mismatched step disturbance. Besides, one can also calculate the transfer functions, given by

$$G_{u\hat{d}}(s) = \frac{75(s-9)}{(s+30)(s+40)},$$

$$G_{y\hat{d}}(s) = \frac{15s(s-25)}{(s+30)(s+40)}.$$

One can verify that $G_{u\hat{d}}(s)/G_{y\hat{d}}(s) = G(s)$. However $G_{u\hat{d}}(0) = -675/1200 \neq 1$, which verifies the observation in Section 6.5. For the case of mismatched disturbance estimate, the traditional frequency-domain DOBs can not be applies and so one can implement the FDOB in frequency-domain using the procedure given in Section 6.5.

Harmonic disturbance

In this part, the matched harmonic disturbance is considered. The harmonic disturbance with unknown amplitude and phase is supposed to act on the system at 1 sec,

$$d = 2sin(10t),$$

which can be put into the state space model (6.2.3) with $S = \begin{bmatrix} 0 & 10 \\ -10 & 0 \end{bmatrix}$, and $H = \begin{bmatrix} 1 & 0 \end{bmatrix}$. The initial value is selected as $\omega_0 = \begin{bmatrix} 2 & 0 \end{bmatrix}$ for simulation but is unknown for observer design.

The matrix L_0 is chosen as $L_0 = \begin{bmatrix} 0 & 1 \end{bmatrix}$, one can check the existing condition for FDOB is satisfied, then one can calculate U, V as

$$U = \begin{bmatrix} 25 & 80 & 0 \\ 0 & 0 & 10 \\ 0 & -10 & 0 \end{bmatrix}, V = \begin{bmatrix} 1 & 5 & 0 \\ 0 & 0 & 0 \end{bmatrix}.$$

Choosing the poles of F as $p_1 = -30, p_2 = -40, p_3 = -50$ and the rest of the design procedure is the same as that of Section 6.6.1 and the simulation result of the disturbance estimate is shown in Fig. 6.7

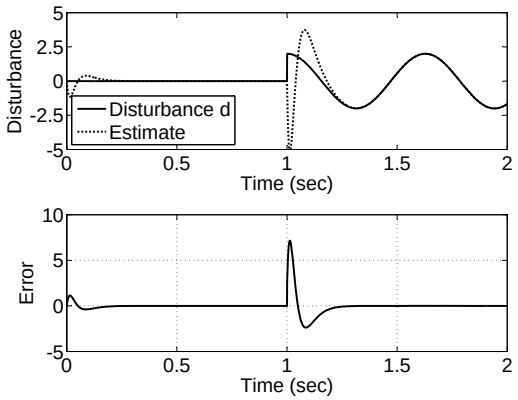

Figure 6.7. Mismatched step disturbance estimate: upper plots (disturbance estimate), lower plot (estimation error).

One can see from Fig. 6.7 that the proposed FDOB can exponentially asymptotically estimate the harmonic disturbance with unknown amplitude and initial phase. The transfer functions $G_{u\hat{d}}(s)$ and $G_{y\hat{d}}(s)$ can also be calculated. One can verify that $G_{u\hat{d}}(s)/G_{y\hat{d}}(s) = G(s)$. However $G_{u\hat{d}}(0) = -0.0232 \neq 1$, which verifies the observation in Section 6.5. For the case of Type II disturbance, the traditional frequency-domain DOBs can not be applied and so one can implement the FDOB in frequency-domain using the procedure given in Section 6.5, if the frequency domain DOB is preferred in applications.

6.6.2 Practical example

In this section, the proposed FDOB is applied to the disturbance estimation and rejection problem of a rotary mechanical system of non-minimum phase from [100].

The system can be represented using a transfer function

$$G(s) = \frac{1.202(4-s)}{s(s+9)(s^2+12s+56.25)}.$$

A normal controller has been pre-designed in state space such that the closed-loop poles are $-3,\ -2{+}1.5i,\ -2{-}1.5i,\ -4$. A step reference position with amplitude 5 is supposed to act on the system at 2 sec. At 10 sec, a harmonic disturbance with unknown amplitude, phase and bias is supposed to act on the system , which can be given by

$$d = 5 + 5sin(10t).$$

One can also put it into the state space model (6.2.3) with $S = \begin{bmatrix} 0 & 10 & 0 \\ -10 & 0 & 0 \\ 0 & 0 & 0 \end{bmatrix}$, and $H = \begin{bmatrix} 1 & 0 & 1 \end{bmatrix}$. The initial value is selected as $\omega_0 = \begin{bmatrix} 5 & 0 & 5 \end{bmatrix}$ for simulation but is unknown for observer design.

Then the proposed FDOB is used to estimate the disturbance, where the poles of matrix F is selected as $-5, -10, -15, -20, -25, -30$. When the disturbance is estimated, its effect can be rejected by direct feedforward the disturbance estimate based on the principle of disturbance observer based control (DOBC) (see, [50,51]). The initial values of the plant and FDOB is selected to be zeros. The disturbance estimation performance is shown in Fig. 6.8, where the upper plots give the disturbance estimate and the lower plot shows the disturbance estimation error. The position control results with and without disturbance compensation are given in Fig. 6.9 where the upper plots depict the position control and the lower plots depict the control error.

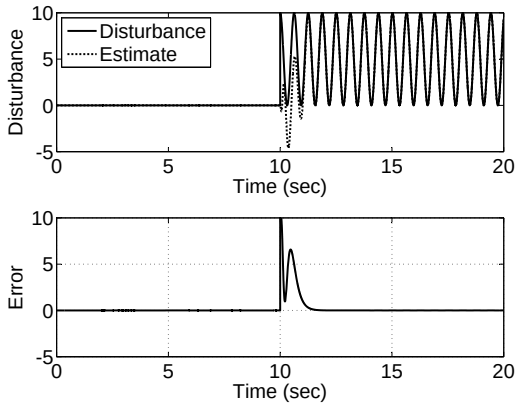

Figure 6.8. Biased harmonic disturbance estimate using FDOB: upper plots (disturbance estimate), lower plot (estimation error).

One can see from Fig. 6.8 that the proposed FDOB can asymptotically estimate the harmonic disturbance with unknown amplitude, phase and bias. One can see from Fig. 6.9 that the controller with direct feedforward the disturbance estimate

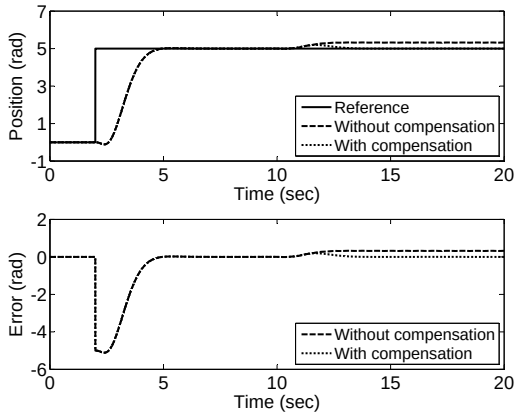

Figure 6.9. Position control performance with and without disturbance compensation: upper plots (position control), lower plots (control errors).

of the FDOB can effectively remove the effect of unknown disturbances, while the nominal controller results in control error in the presence of disturbances.

6.7 Summary

This Chapter provides a generic analysis of the relationship between time-domain and frequency-domain DOBs, which extends the work of [52] from minimum phase frequency-domain DOB structure to more general form DOB structure. The traditional frequency-domain DOB structure using a low pass filter with unity gain can only effectively handle a specific class of disturbances satisfying the so-called matching condition, while the existing time-domain DOB always generates a higher order observer. A functional observer based time-domain DOB (FDOB) is proposed to improve the existing time-domain DOB together with its existence condition, design guideline and transfer function implementation. Compared with frequency-domain DOBs, the proposed FDOB can handle more types of disturbances, while compared with the existing time-domain DOBs the proposed FDOB generates a lower-order observer. Numerical examples including a rotary mechanical system of non-minimum phase are given to verify the proposed algorithms. The proposed FDOB has the potential in the fields of both disturbance rejection control and fault diagnosis.

Chapter 7

SYSTEM VERIFICATION AND THRESHOLD SELECTION

7.1 Introduction

In the previous Chapters, the focus was mainly on observer design to generate fault estimate for the purpose of fault diagnosis. In this Chapter and the following one, attention is turned to the fault diagnosis system verification and robust threshold selection. The motivations of this research are illustrated in Fig. 7.1.

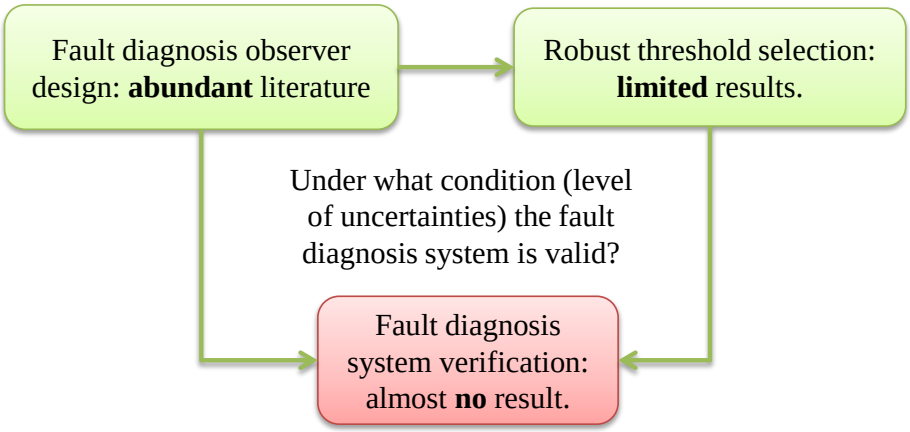

Figure 7.1. The status of fault diagnosis: observer design, threshold selection and system verification.

With the ever-increasing requirements on system safety and reliability in conjunction with the rapidly growing computation power, model-based fault diagnosis approaches are attracting more and more attentions in both academia and industry (see, [6, 101–103] and recent survey papers [13, 104] among many others). Observer based fault diagnosis, as one type of model-based diagnosis approaches, performs fault diagnosis by consistency-checking between the observed behaviour and predicted behaviour using observer techniques based on the mathematical model of

concerned plant [13]. There are generally two steps involved including observer design to produce a fault indicating signal (FIS) [105] and a threshold generation to evaluate the FIS such that a Boolean decision can be made–normal or faulty [6]. For example, in residual based diagnosis approach [13], a fault is alarmed when a residual (serves as the FIS, which is defined as the function of output estimation error) is larger than a given threshold (being zero in the ideal fault-free case). While in fault estimation based diagnosis approach [6], a fault is indicated when the fault estimates (serves as the FIS) deviate from a pre-defined threshold (also being zero in the ideal fault-free case).

The most important and challenging issue in model based fault diagnosis approaches is the robustness [13, 106]. Since in real applications, there are always some mismatches between the real plant and the mathematical model used for fault diagnosis observer design [8,50,93], such as system parameter uncertainties, external disturbances, sensor noises, etc. As a result, it brings many challenges to the problem of fault diagnosis algorithm verification, i.e., verifying whether a fault diagnosis algorithm is still valid in the presence of all kinds of system uncertainties, since any algorithms should go through verification and validation before being applied in real engineering to see whether certain performance criteria/specifications are satisfied. Besides, the FIS under normal cases are also inevitably corrupted by all kinds of system uncertainties, i.e., being non-zero even under normal cases [6,107,108], which brings challenges to the problem of robust threshold selection, since if the threshold is selected too small the false alarm rate will be high and if the threshold is selected too large the missing detection rate will be high.

To this end, many algorithms have been proposed to handle the robustness issue. According to at what stage the uncertainties are considered, they can be categorised into the active approach and the passive approach [109]. The active approaches reduce or even decouple the effect of the uncertainties on FIS in the stage of observer design based on unknown input observer [8, 110], robust filter (e.g., H_∞ observer) [104, 111, 112]. While the passive approaches solve the robustness issue at the stage of threshold selection (or residual evaluation, decision-making, etc.) by taking the uncertainties into account [35, 36, 109].

Although fault diagnosis observer design, algorithm verification and threshold selection are equally important for a successful fault diagnosis system in real application, less attention has been paid to algorithm verification and threshold selection in the existing literature. The commonly used approach for algorithm verification is stochastic simulation. Stochastic simulation based approach [37] obtains the envelope of states or outputs based on a finite (possibly large) number of different

linear models selected from a continuum of models corresponding to each possible value of the system parameters. However, as pointed out in [113], the number of required simulations grows exponentially with the number of state, input, and parametric variables due to a necessary gridding of the multidimensional set bounding all variables. Besides, although large numbers of different models are performed on fairly fine grids for uncertain parameters or Monte Carlo parameter sampling, it is still possible to miss the model corresponding to the most critical parameter combination.

The threshold should be selected such that the fault diagnosis system is robust to all possible model uncertainties, unknown inputs and faults of no interest (see pp. 8 of [114]). The existing robust threshold selection methods can be categorised into three groups including uncertainties amplification based [114] (see, pp. 289), [42, 115, 116], optimality based [35, 38], set-membership based approaches [35–37]. In amplification based approach, a traditional observer is firstly designed, then in the stage of FIS evaluation the system uncertainties are modelled (or approximated) as unknown input vector with limited bound or bounded by a known function and their effect on FIS is amplified based on norm inequality [114], triangular inequality [42], integral inequality [115, 116]. This method may result in conservative or even useless threshold, especially when multiple parameter uncertainties exist (see, pp. 251 of [114]). While, in the latter two approaches, the traditional fault diagnosis observer for FIS generation is replaced by new observers which can potentially capture the possible upper and lower bounds of system states, and consequently a fault is alarmed when the measured states deviate from the calculated state interval. Specifically, optimization based approach [35, 38] obtains the upper bound and lower bound of state envelop in each time step by solving a constrained optimization problem where the constraints may include the parameter uncertainties interval, initial state interval, input and output uncertainties interval, etc. However, due to the complexity of the non-linear optimisation in each time step, this method can not guarantee a globe optimum and is subjected to high computation problem especially for multiple parameter uncertainties and over a large time interval, which constrains its application [38, 39]. Set-membership based approaches [40, 43, 45] calculate the possible state or output interval by taking the system uncertainties into account. This method is promising and has been used for fault detection of an electrical drive in [45]. However, it has been pointed out in [46] that the existence issue of observer gains for interval observer is not yet clearly established even for linear system, since the observer gains should not only guarantee the error system matrix is Hurwitz, but also cooperative (all the off-diagonal term

are non-negative). Besides in the presence of system parameter uncertainties, two bounded functions are needed to cover the effect of parameter uncertainties, which is not an easy task due to the time-varying and unknown property of states. It should also be highlighted that the later two interval observer approaches provide new fault diagnosis solution by proposing new fault diagnosis observer, however, they do not actually evaluate the FIS for existing fault diagnosis observer since the system state interval rather than fault diagnosis observer state interval are calculated and consequently the problem of algorithm verification and threshold selection is not handled by them.

Rather than providing a new fault diagnosis observer, a solution to the problem of algorithm verification and threshold selection is proposed by evaluating the FIS of the existing fault diagnosis observer using the technique of reachable set computation. Its basic philosophy is to calculate the effect of all types of system uncertainties on the FIS. Specifically, the effect of parameter uncertainties on the FIS under the normal case is first analysed such that a normal reachable set can be obtained. Then, the same effect of system uncertainties on the FIS under a selected set of faults is further analysed such that a set of faulty reachable set is obtained. Based on the aforementioned two reachable sets, several objectives can be achieved. First, it can be qualitatively verified that whether a candidate fault diagnosis algorithm with a chosen threshold is still valid in the presence of system uncertainties. Second, an appropriate threshold can be quantitatively selected such that it is robust to all kinds of system uncertainties. Third, the level of fault that can be detected by a given algorithm can also be determined by checking the intersection of those two sets. Finally, the proposed approach is evaluated through the actuator and sensor fault diagnosis problem of a motor system using fault estimation based diagnosis approach.

7.2 Problem formulation and preliminaries

In this section, the problem will be first formulated including model based fault diagnosis, fault estimation based fault diagnosis approach and two challenging issues therein. Then the reachable set computation tool for linear system with system parameter uncertainties and uncertain inputs will be introduced, which plays a key role in fault diagnosis algorithm verification and robust threshold selection.

7.2.1 Problem formulation

Model based fault diagnosis system

Consider an uncertain linear system subjected to unknown load, actuator and sensor faults, given by

$$\begin{cases} \dot{x} = (A + \triangle A)x + B(u + f_a) + \Gamma\Gamma_d \\ y_m = C_m x + S f_s + N n \end{cases}, \tag{7.2.1}$$

where x, u, f_a, Γ_d are the system state, control input, actuator fault, unknown disturbance respectively, and A, B, D, Γ are the corresponding distribution matrices. y_m, f_s, n are the measurements, sensor faults, sensor noises and C_m, S, N are the corresponding distribution matrices respectively. $\triangle A$ is the system matrix perturbation to account for effect of system parameter uncertainties and each element of $\triangle A$ lies in a bounded interval.

To facilitate the design of integral control in state space modelling such that the steady state tracking error can be removed, the error integral (e.g., position error integral $\int(\theta - \theta_d)dt$ in the following case study) is also modelled into system (7.2.1), resulting in

$$\begin{cases} \dot{x} = (A + \triangle A)x + B(u + f_a) + Dy_d + \Gamma\Gamma_d \\ y_m = C_m x + S f_s + N n \end{cases}. \tag{7.2.2}$$

From system (7.2.2), the commonly used feedback control law $u = -K_c y_m + K_d y_d$ can be designed to achieve position tracking. It should be noted that although the same notations (e.g., x) have been used in (7.2.1) and (7.2.2), the variables in (7.2.2) accommodate the new state (i.e., the controlled output error integral).

The objective of model based fault diagnosis system is to detect the presence of fault f_a and f_s (i.e., fault detection) and determine what kind of fault has occurred when faults are detected (i.e., fault isolation) based on the system model (7.2.2). The fault diagnosis system should be designed to be robust to the system parameter uncertainties $\triangle A$, external disturbance Γ_d such that the false alarm rate is kept at a low level. To this end, without loss of generality the following fault estimation based fault diagnosis algorithm is introduced to detect and isolate the faults.

Fault estimation based diagnosis system

Fault estimation based diagnosis approaches perform fault diagnosis by directly estimating faults based on observer theory, such as Kalman filter type observers [107], disturbance observers [6], etc. So the diagnosis logic of fault estimation based approach is as follows: when faults are estimated by observers, one can directly tell whether a fault has occurred or not (i.e., fault detection) and where the faults come

from such as which actuator, sensor (i.e., fault isolation) by checking whether the fault estimate deviates from a pre-defined interval (i.e., threshold) centred at zero.

To obtain fault estimates for the linear system (7.2.2), the concept of state augmentation is used [66], which obtains the fault estimate by augmenting the faults as additional states. Since in real applications the external disturbance (for example, unknown load in a motor system) Γ_d has an enormous effect on the state estimation performance and consequently the FIS, its effect is reduced through estimating it by augmenting it as an additional state as well.

Let $\bar{x} = (x, f_a, f_s, \Gamma_d)$, then the system (7.2.2) can be equivalently represented by the following extended system equation:

$$\begin{cases} \dot{\bar{x}} = (\bar{A} + \triangle\bar{A})\bar{x} + \bar{B}u + \bar{D}y_d \\ y = \bar{C}\bar{x} + Nn \end{cases}, \tag{7.2.3}$$

where $\bar{A} = \begin{bmatrix} A & B & O & \Gamma \\ O & O & O & O \end{bmatrix}$, $\bar{B} = \begin{bmatrix} B \\ O \end{bmatrix}$, $\bar{D} = \begin{bmatrix} D \\ O \end{bmatrix}$ and $\bar{C} = \begin{bmatrix} C & O & S & O \end{bmatrix}$.

Then a state observer can be designed for extended system (7.2.3) under the observability of the pair $(\bar{A}, \bar{C})$:

$$\begin{cases} \dot{\hat{\bar{x}}} = \bar{A}\hat{\bar{x}} + \bar{B}u + \bar{D}y_d + \bar{K}_o(y - \hat{y}) \\ \hat{y} = \bar{C}\hat{\bar{x}} \end{cases}, \tag{7.2.4}$$

where the gain matrix $\bar{K}_o$ is the observer gain matrix to be designed (e.g., pole assignment of the pair $(\bar{A}, \bar{C})$). Combing (7.2.3) and (7.2.4), the error dynamic $e = \bar{x} - \hat{\bar{x}}$ can thus be obtained as follows:

$$\dot{e} = (\bar{A} - \bar{K}\bar{C})e + \triangle\bar{A}\bar{x} - \bar{K}_o Nn. \tag{7.2.5}$$

When the extended state $\bar{x}$ is obtained, one can approximately obtain the actuator fault f_a and sensor fault f_s, which will serve as the FIS. After the FIS are obtained, one should choose an appropriate threshold to evaluate the FIS such that a Boolean decision can be made–normal or faulty. The overall diagram for fault estimation based diagnosis approach is shown in Fig. 7.2,

Challenging issues

The fault diagnosis observer (7.2.4) is usually designed based on the normal model of real system (7.2.3). As a result, one can see from (7.2.5) that the state estimation error and consequently the fault estimates are inevitably corrupted by the

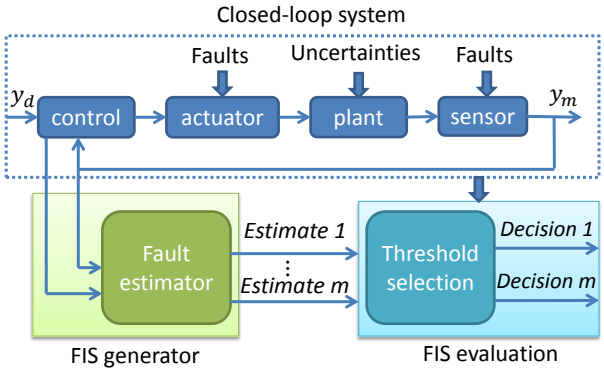

Figure 7.2. The diagram of fault estimation based FD approach including three elements: closed-loop system, FIS generator and FIS evaluation.

system uncertainties $\triangle \bar{A}\bar{x}$ and measurement noises. It should be noted that this phenomenon is inevitable in all kinds of model based fault diagnosis algorithms such as residual based [112], parameter estimation based [13] and parity space based approach [110], etc. and there is the reason why the robustness is seen as the most important and challenging issue of model based fault diagnosis algorithm [13]) in practice.

This phenomenon results in two challenging problems to the application of fault diagnosis algorithm in real engineering. *Firstly, how to verify whether a fault diagnosis algorithm with a given threshold is still valid in the presence of all kinds of system uncertainties, since verification is an essential and inevitable step if a fault diagnosis algorithm is to be applied in real engineering. Secondly, how to quantitatively choose the threshold evaluating the FIS such that the false alarm rate of a given fault diagnosis algorithm satisfies the given specifications.* A solution is proposed to the aforementioned two challenging problems. To achieve this goal, the following reachable set computing tool is introduced.

7.2.2 Reachable set computation

The reachable set computation plays a key role in fault diagnosis algorithm verification and robust threshold selection. Consequently, its principle will be briefly introduced in this section. The tool for reachable set computation of a linear system with uncertain initial states, system matrices and inputs is based on known techniques given in [113, 117, 118]. As discussed in [113] the reachable set computations are typically performed iteratively for short time intervals $\tau_k := [t_k, t_{k+1}]$ with $t_k := ki$ where $k \in N$ is the time step and $i \in R^+$ denotes the step-size. The reachable set iterative computation requires set-based addition and multiplication,

which are defined as follows.

Definition 1: (Set-based addition/multiplication) The rule for set-based addition and multiplication are defined as $\mathcal{X} \oplus \mathcal{Y} := \{x + y | x \in \mathcal{X}, y \in \mathcal{Y}\}$ and $\mathcal{X} \otimes \mathcal{Y} := \{xy | x \in \mathcal{X}, y \in \mathcal{Y}\}$ respectively.

Besides, there are multiple ways to represent a set including polytopes, zonotopes, ellipsoids, support function, etc [113]. The zonotopes are preferred to represent a reachable set of states since they can efficiently represent reachable sets in high-dimensional spaces while operations required for reachability analysis can efficiently be applied to them [113]. The definition of a zonotope is given as follows.

Definition 2: (Zonotope) Given a centre $c \in R^n$ and so-called generators $g^{(i)} \in R^n$, a zonotope is defined as

$$\mathcal{Z} := \{x \in R^n | x = c + \textstyle\sum_{i=1}^{p} \beta_i g^{(i)}, \beta_i \in [-1, 1]\},$$

which can be written in a short form as $\mathcal{Z} = (c, g^{(1)}, \cdots, g^{(p)})$. The order of a zonotope is defined as $\rho := \frac{p}{n}$, where p is the number of generators. The zonotope can also be seen as the set-based addition of line segments $[-1, 1]g^{(i)}$.

The multiplication of a zonotope with a matrix $M \in R^{o \times m}$ and the addition of two zonotopes $\mathcal{Z}_1 = (c, g^{(1)}, \cdots, g^{(p_1)})$ and $\mathcal{Z}_2 = (d, h^{(1)}, \cdots, h^{(p_2)})$ are also zonotopes, defined as

$$\begin{aligned} &\mathcal{Z}_1 \oplus \mathcal{Z}_2 = (c + d, g^{(1)}, \cdots, g^{(p_1)}, h^{(1)}, \cdots, h^{(p_2)}), \\ &M \otimes \mathcal{Z}_2 = (Mc, Mg^{(1)}, \cdots, Mg^{(p_1)}). \end{aligned}$$

Besides, other functions (such as the convex hull, Cartesian product, etc.) of two zonotopes are referred to [113].

Computation tool

Consider an uncertain linear system, which can be described by a differential inclusion,

$$\dot{x} = \mathcal{A}x + u_c \oplus u(t), \tag{7.2.6}$$

where the uncertain system matrix $\mathcal{A} \subset \mathcal{I}^{n \times n}$, initial state $x(0) \in X_0 \subset R^n$, $u_c \in R^n$ is the known input and $u(t) \in V \subset R^n$ is the uncertain input. The reachable set computation can over-approximately obtain the reachable set $R([0, r])$ of system (7.2.6) in a time interval $t \in [0, r]$ denoted as $R^d([0, r])$, where $R^d([0, r]) \supseteq R_e^d([0, r])$ with $R_e^d([0, r]) = \{x | x(t)$ is a solution of$(7.2.6), t = r, x(0) \in X_0\}$, which can be seen

as the exact reachable set [1].

The detailed algorithm and its implementation can be found in [113, 117, 118]. However, for the completeness, its basic algorithm structure for a time interval τ_k is given as follows. Suppose the reachable set of the affine dynamics $\dot{x} = Ax + u_c$ is $\mathcal{R}_a^d(t)$, the reachable set of the particular solution due to the uncertain input $u(t)$ is $\mathcal{R}_p^d(u(t), t)$, and the partial reachable set correcting the initial assumption that trajectories are straight lines between t_k and t_{k+1} is $\mathcal{R}_\epsilon^d$. According to [113,117,118], the reachable set for a time interval τ_k is computed as shown in Fig. 7.3[2]

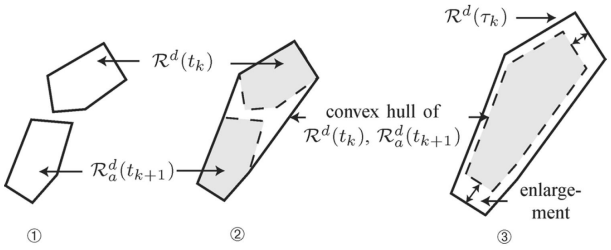

Figure 7.3. Steps for reachable set computation of uncertain linear systems.

i Starting from $\mathcal{R}^d(t_k)$, compute the reachable set $\mathcal{R}_a^d(t_{k+1})$

ii Obtain the convex hull of $\mathcal{R}^d(t_k)$ and $\mathcal{R}^d(t_{k+1})$ to approximate the reachable set for the time interval τ_k

iii Compute $\mathcal{R}^d(\tau_k)$ by considering uncertain inputs by adding $\mathcal{R}_p^d(u(t), \tau_k)$ and accounting for the curvature of trajectories by adding $\mathcal{R}_\epsilon^d$.

Numerical example

A numerical example in [118] is given to show the effectiveness of the reachable set computation algorithm. Suppose the uncertain matrix $\mathcal{A}$ in (7.2.6) is given by $\mathcal{A} = A_0 + [-0.1, 0.1] * \triangle A$, where the normal matrix and uncertain matrix are given by

$$A_0 = \begin{bmatrix} -1 & -4 & 0 & 0 & 0 \\ 4 & -1 & 1 & 0 & 0 \\ 0 & 0 & -3 & 1 & 0 \\ 0 & 0 & -1 & -3 & 0 \\ 0 & 0 & 0 & 0 & -2 \end{bmatrix}, \triangle A = \begin{bmatrix} 1 & 1 & 0 & 0 & 0 \\ 1 & 1 & 1 & 0 & 0 \\ 0 & 0 & 1 & 1 & 0 \\ 0 & 0 & 1 & 1 & 0 \\ 0 & 0 & 0 & 0 & 1 \end{bmatrix}.$$

[1] The computation of exact reachable set is an open problem [117] and consequently over-approximation is usually preferred.

[2] This illustrating figure is from [113].

The known control input u_c is a step input with amplitude 1 (the initial value is chosen as 0) at 3 sec and the amplitude is changed to 2 at 6 sec. Each element of the uncertain input $u(t)$ lies in the interval $[-0.05, 0.05]$. The step-size is chosen as 0.001 and the order of zonotope ρ is 600. The state reachable set of x_3 (red, green and yellow interval) and 200 stochastic trajectories (blue lines) are shown in Fig. 7.4

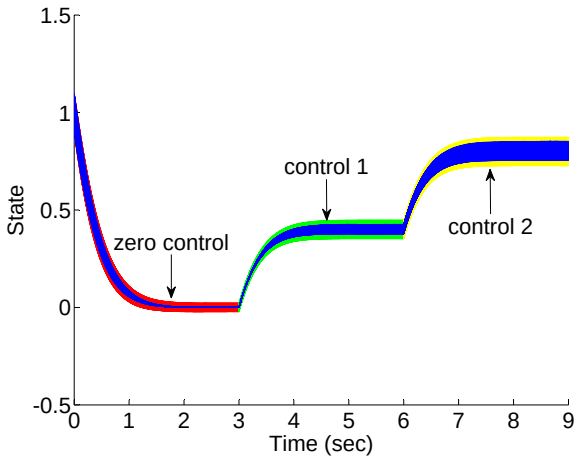

Figure 7.4. The state reachable set of x_3 and its stochastic trajectories under different control amplitudes: area in read: without control; area in green: control with amplitude 1; area in blue: control with amplitude 2.

One can see from Fig. 7.4 that: *(i) all the stochastic simulation trajectories of state x_3 lie in the calculated reachable set, which verifies the effectiveness of state reachable set computation tool; (ii) when the input amplitude is increased, the corresponding width of reachable sets will get larger. This is due to the fact that when the input amplitude is increased, the state amplitude and consequently the effect of system parameters on the states also get larger.*

7.3 Main results

In this section, the main results will be provided including the qualitative verification of a candidate fault diagnosis algorithm with a given threshold and the quantitatively robust threshold selection for a given fault diagnosis system. Besides, based on the robust threshold, the fault amplitude that can be detected by a given fault diagnosis algorithm can also be determined.

7.3.1 Fault diagnosis algorithm verification

Algorithm verification can answer the question that whether a given algorithm is still valid in realistic environment (i.e., in the presence of all kinds of system uncertainties, such as parameter uncertainties, external disturbances, sensor noises, etc.). It can be seen as a bridge between academia and industry, since any algorithm should go through verification and validation to see whether certain performance criteria are satisfied before being applied in industry. Although in the past few decades there are a lot of model based fault diagnosis algorithms proposed in academia, little attention has been paid to fault diagnosis algorithm verification and as a result the model based fault algorithms have not been extensively applied in industry. The commonly used algorithm verification tool in engineering is stochastic simulation, i.e., simulating the real system by choosing a large number of system models with different parameter combinations. However, as pointed out in [113], the number of required simulations grows exponentially with the number of state, input, and parametric variables and more importantly, it is still possible to miss the model corresponding to the most critical parameter combination. Consequently, efforts should be made to bridge this gap, i.e., proposing a systematic approach for fault diagnosis algorithm verification.

The philosophy of fault diagnosis algorithm verification is that, different intervals are used to capture the uncertainties in system parameters and sensor noises, such that an uncertain model (e.g., (7.2.2)) is obtained to represent the real system. Then for a candidate fault diagnosis system (e.g., (7.2.4)), the FIS reachable set under normal case is first obtained, i.e., with only system uncertainties and sensor noises; then the FIS reachable set under faulty case is further obtained, i.e., with all kinds of system uncertainties and a selected set of faults of interest. Then it can be qualitatively determined whether the candidate fault diagnosis system is still valid or not under uncertainties by comparing the normal FIS reachable set and faulty FIS reachable set. The rule is that if the normal FIS reachable set is close to zero, and the faulty FIS reachable set substantially deviates from the normal FIS reachable set then one can qualitatively conclude that the fault diagnosis system is valid under this level of system uncertainties. The calculation of FIS reachable sets under normal and faulty cases are discussed in section 7.3.3.

7.3.2 Robust threshold selection

The threshold is selected to evaluate the FIS and consequently a Boolean decision– normal or faulty is produced. In the absence of system uncertainties, the threshold

can be easily set to be zero since the state estimation error and consequently FIS approaches to zero in the steady-state under normal case. However, one can see from (7.2.5) that the state estimate error and consequently fault estimates are subjected to the effect of system uncertainties $\triangle\tilde{A}\tilde{x}$ and sensor noise Nn, which means the fault estimates are not zero even under normal conditions. So a threshold should be carefully designed such that it is robust against the system uncertainties.

The commonly used robust threshold selection approach is approximating all the uncertainties using unknown input with limited bounds or a bounding function [114]. There are two problems within this approach. Firstly, it is not an easy task to find an appropriate unknown input to cover the uncertainties due to the time-varying and unknown nature of state x. Secondly, it is pointed out in [114] (see, pp. 251) this approach will lead to a conservative threshold, since valuable information about the structure of the model uncertainties has not been taken into account.

To this end, the robust threshold is chosen by analysing the FIS reachable sets under normal case and a selected of faulty cases as discussed in Section. 7.3.1. Based on these two reachable sets, two objectives can be achieved. Firstly, a robust threshold can be chosen based on the calculated normal reachable set, which means if the fault estimate lies in the normal reachable set, it is concluded that no fault appears, while if the fault estimate deviates from the normal reachable set then it can be concluded that the corresponding fault has occurred. Secondly, by comparing the normal reachable set and faulty reachable set, the level of fault that can be detected by the observer based fault diagnosis system can also be determined. When the intersection of these two sets is empty, it can be concluded that the fault diagnosis algorithm can effectively detect the presence of fault, while if the intersection of these two sets is not empty (e.g., the amplitude of fault is too small), then the fault diagnosis algorithm fails to detect that particular type of fault. The principle of the proposed robust threshold selection for fault estimate based diagnosis approach is shown in Fig. 7.5.

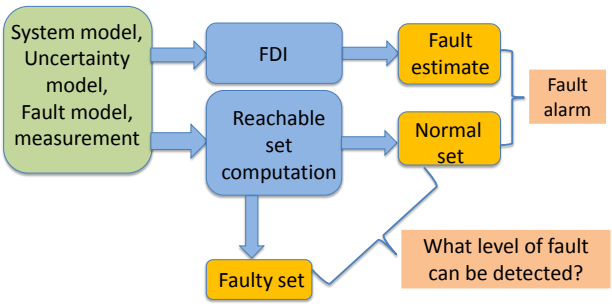

Figure 7.5. Overall diagram of fault diagnosis system with robust threshold.

7.3.3 FIS reachable set computation

In this section, the FIS reachable set computation is discussed under normal case and a selected of faulty cases. The aforementioned FIS reachable set computation problem is transformed into the problem of two state reachable set computation such that the existing tool on reachability analysis introduced in Section. 7.2.2 can be applied.

To facilitate analysing the effect of $\triangle\bar{A}\bar{x}$ and sensor noises Nn on the augmented state $\hat{\bar{x}}$ and consequently fault estimates, the dynamic of $\hat{\bar{x}}$ is derived and put into the format of (7.2.6) such that the technique of reachable set computation can be used.

On the one hand, from $e = \bar{x} - \hat{\bar{x}}$, the state estimation error dynamic (7.2.5) can be put into the following form

$$\dot{e} = (\bar{A} - \bar{K}_o\bar{C})e + \triangle\bar{A}(e + \hat{\bar{x}}) - \bar{K}_oNn. \tag{7.3.1}$$

On the other hand, one can see from (7.2.4) that the time-varying input $u = -K_cy_m + K_dy_d$ and y_m are involved in derivation of $\hat{\bar{x}}$, which will make the reachable set computation complicated. To simplify the problem, the control input u and measurement y_m are substituted into (7.2.4), such that the $\hat{\bar{x}}$ dynamics are given by

$$\begin{aligned}\dot{\hat{\bar{x}}} &= \bar{A}\hat{\bar{x}} + \bar{B}[-K_c(\bar{C}\bar{x} + Nn) + K_dy_d] + \bar{D}y_d + \bar{K}_o(\bar{C}\bar{x} + Nn - C\hat{\bar{x}}) \\ &= (\bar{A} - \bar{B}K_c\bar{C})\hat{\bar{x}} + (\bar{K}_o\bar{C} - \bar{B}K_c\bar{C})e + (\bar{D} + \bar{B}K_d)y_d + (\bar{K}_o - \bar{B}K_c)Nn.\end{aligned} \tag{7.3.2}$$

Combing (7.3.1) and (7.3.2), one can obtain the following composite dynamics including extended state estimate error e and extended state estimate $\hat{\bar{x}}$,

$$\begin{aligned}\underbrace{\begin{bmatrix}\dot{e}\\ \dot{\hat{\bar{x}}}\end{bmatrix}}_{\dot{\chi}} &= \underbrace{\begin{bmatrix}\bar{A} - \bar{K}_o\bar{C} + \triangle\bar{A} & \triangle\bar{A}\\ \bar{K}_o\bar{C} - \bar{B}K_c\bar{C} & \bar{A} - \bar{B}K_c\bar{C}\end{bmatrix}}_{\mathcal{A}}\underbrace{\begin{bmatrix}e\\ \hat{\bar{x}}\end{bmatrix}}_{\chi} \\ &\quad + \underbrace{\begin{bmatrix}O\\ \bar{D} + \bar{B}K_d\end{bmatrix}}_{u_c}y_d + \underbrace{\begin{bmatrix}-\bar{K}_o\\ \bar{K}_o - \bar{B}K_c\end{bmatrix}}_{u(t)}Nn\,.\end{aligned} \tag{7.3.3}$$

Using the under-brace notations in (7.3.3), the composite dynamic (7.3.3) can be put into a compact form, given by

$$\dot{\chi} = \mathcal{A}\chi + u_c \oplus u(t), \tag{7.3.4}$$

where $\chi = [e^T, \hat{\bar{x}}^T]^T$, $\mathcal{A}$ is the uncertain system matrix, u_c is the known input and

$u(t)$ is the uncertain input. One can see that (7.3.4) falls into the same format as that of the uncertain system (7.2.6) in Section. 7.2.2, which means the standard reachable set computation tool in Section. 7.2.2 can be applied. Then one can obtain the reachable set of χ and consequently FIS reachable sets under normal case and a selected of faulty cases, since the FIS are chosen as the fault estimates in fault estimation based diagnosis approach which are the elements of χ.

Remark: One can see from (7.3.3) that the distribution matrices of known input y_d and uncertain input n are different. To make the reachable set computation problem of system (7.3.3) solvable based on the existing tool (i.e., putting (7.3.3) into (7.3.4)), the original uncertain input n has been transformed into $u(t)$. This process will result in conservativeness in reachable set computation due to the fact that the dimension of uncertain input has been increased and consequently the single-use-expressions [118] of interval computation can not be achieved. However, future work can be done to handle this problem and consequently attenuate the conservativeness.

7.4 Simulations

In this section, the actuator and sensor fault diagnosis problem of a motor system using fault estimation based approach will be used to illustrate the principle of the proposed approach. The overall diagram of motor fault diagnosis system is shown in Fig. 7.6 where the closed-loop control system using state space feedback with

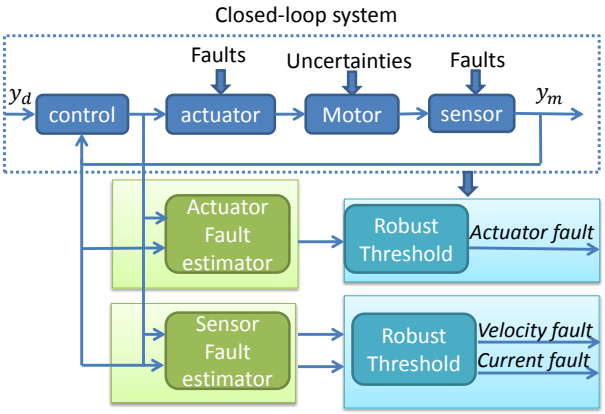

Figure 7.6. Overall diagram of motor fault diagnosis system.

integral action is introduced in Section. 7.4.1, the actuator fault estimator and sensor fault estimator and their corresponding robust threshold selection are given in Section. 7.4.2 and 7.4.3 respectively.

7.4.1 Motor system

A linear model of the motor system with actuator and sensor faults can be represented in the state-space model (7.2.2) where $x = [x_1, x_2, x_3, x_4]^T = [\theta, \omega, I, \int(\theta - \theta_d)dt]^T$ are the system states (the state $x_4 = \int(\theta - \theta_d)dt$ is introduced such that an integral control can be designed to remove the steady state tracking error), u is the control voltage, which is designed as

$$\begin{aligned} u &= -k_\theta(\theta_m - \theta_d) - k_{ei}x_4 - k_\omega\omega_m - k_i i_m \\ &= -K_c y_m + K_d\theta_d \end{aligned} \tag{7.4.1}$$

where θ_m, ω_m and i_m are the measurement value of position, velocity and current, respectively. The parameters $K_c = [k_\theta, k_\omega, k_i, k_{ei}]$ are the control parameters to be designed (see Appendix A.4) and $K_d := k_\theta$. $y_d = \theta_d$ is the desired output position, Γ_d the unknown load, y_m the measurement output, f_a the actuator fault, $f_s = \begin{bmatrix} f_{sv} \\ f_{sc} \end{bmatrix}$, where f_{sv} is the velocity sensor fault, f_{sc} is the current sensor fault, respectively. System matrix A, control input matrix B, desired output matrix D, load matrix Γ, measurement matrix C_m are given as follows:

$$A = \begin{bmatrix} 0 & 1 & 0 & 0 \\ 0 & -\frac{k_d}{J} & \frac{k_T}{J} & 0 \\ 0 & -\frac{k_e}{L} & -\frac{R}{L} & 0 \\ 1 & 0 & 0 & 0 \end{bmatrix},\ B = \begin{bmatrix} 0 \\ 0 \\ \frac{1}{L} \\ 0 \end{bmatrix},\ D = \begin{bmatrix} 0 \\ 0 \\ 0 \\ -1 \end{bmatrix}\ \Gamma = \begin{bmatrix} 0 \\ -\frac{1}{J} \\ 0 \\ 0 \end{bmatrix},\ S = \begin{bmatrix} 0 & 0 \\ 1 & 0 \\ 0 & 1 \\ 0 & 0 \end{bmatrix},$$

$$N = \begin{bmatrix} I_3 \\ \text{zeros}(3,1) \end{bmatrix},\ C_m = I_{4\times 4}.$$

The meaning of the aforementioned parameters and their corresponding normal values are referred to Appendix A.4. $\triangle A$ denotes the system parameter uncertainties and suppose that there are four key parameters with uncertainties, i.e., k_d, k_T, k_e and resistance R. The uncertainty levels are given as follows: $k_d \in [k_{dn} - 4\%k_{dn}, k_{dn} + 4\%k_{dn}]$, $k_T \in [k_{Tn} - 2\%k_{Tn}, k_{Tn} + 2\%k_{Tn}]$, $k_e \in [k_{en} - 2\%k_{en}, k_{en} + 2\%k_{en}]$ and $R \in [R_n - 5\%R_n, R_n + 5\%R_n]$, where $k_{dn}, k_{Tn}, k_{en}, R_n$ denote the normal parameter values. Without loss of generality, suppose that the sensor noises n_p, n_v, n_i lie in a bounded interval $\in [-0.01, 0.01]$.

7.4.2 Actuator fault diagnosis

In this section, the fault estimation based diagnosis approach is applied to the problem of actuator fault diagnosis. In this scenario, suppose that no sensor fault occurs to satisfy the observer observability and consequently only the actuator fault

and unknown load are treated as the additional states when designing the generalized state observer, i.e., $\bar{x}_1 = (x, f_a, \Gamma_d)$. The fault diagnosis observer is designed as

$$\begin{cases} \dot{\hat{\bar{x}}}_1 = \bar{A}_1\hat{\bar{x}}_1 + \bar{B}_1 u + \bar{D}_1 y_d + \bar{K}_{o1}(y - \hat{y}), \\ \hat{y} = \bar{C}_1\hat{\bar{x}}_1 \end{cases}$$

where the system matrices are given by $\bar{A}_1 = \begin{bmatrix} A & B & \Gamma \\ O & O & O \end{bmatrix}$, $\bar{B}_1 = \begin{bmatrix} B \\ O \end{bmatrix}$, $\bar{D}_1 = \begin{bmatrix} D \\ O \end{bmatrix}$ and $\bar{C}_1 = \begin{bmatrix} C & O & O \end{bmatrix}$. The observer gain $\bar{K}_{o1}$ can be found in Appendix A.4.

The reference position is chosen as a step signal at 0 sec with amplitude of $1rad$, while the unknown load Γ_d is given by the following function,

$$\Gamma_d = \begin{cases} 1\ Nm, & \mathrm{t} \in [0, 3] \\ 0.5\ Nm, & \mathrm{t} \in (3, 10] \end{cases}$$

The initial state of both the control system and observer system are supposed to be zero vector of appropriate dimension. The actuator fault with different amplitude $f_a = 1V$ and $f_a = 0.1V$ are supposed to occur at 6 sec respectively. The reachable set computation results for both normal case and actuator faulty cases are shown in Fig. 7.7 and 7.8, where the black lines are the stochastic simulations of the actuator fault estimate.

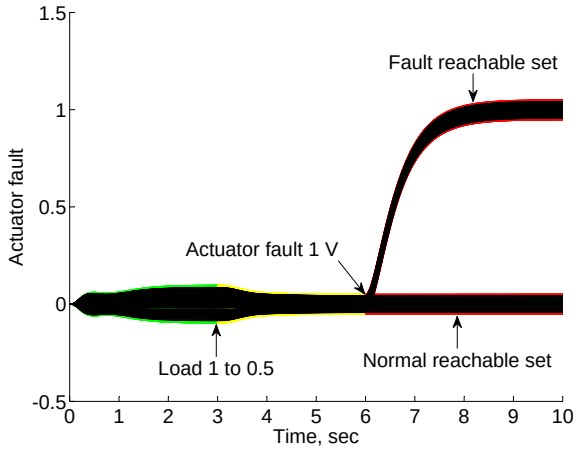

Figure 7.7. Reachable set of actuator fault estimate under normal case and actuator fault $f_a = 1$: green area (no fault under $\Gamma_d = 1$), yellow area (no fault under $\Gamma_d = 0.5$), red area (with and without fault under $\Gamma_d = 0.5$).

One can see from Figs. 7.7 and 7.8 that reachable set computation can effectively capture the dynamic of the fault estimates, since all the stochastic simulated fault estimates lie in the computed reachable set for both normal case and faulty case.

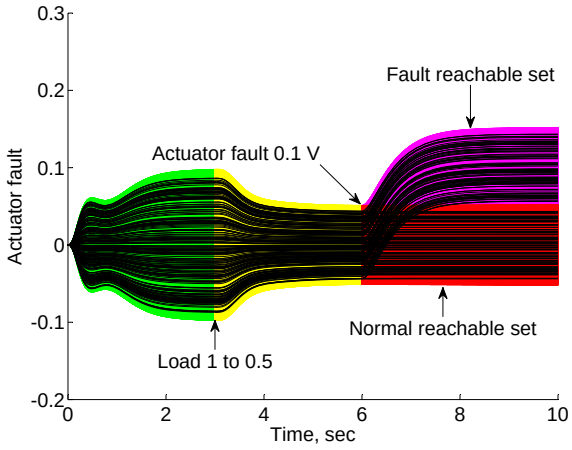

Figure 7.8. Reachable set of actuator fault estimate under normal case and actuator fault $f_a = 0.1$: green area (no fault under $\Gamma_d = 1$), yellow area (no fault under $\Gamma_d = 0.5$), red area (no fault under $\Gamma_d = 0.5$); pink area (with fault under $\Gamma_d = 0.5$). There are some overlaps between pink area and red area due to the effect of uncertainties.

When the unknown load is changed from 1 to 0.5 at 3 sec, the amplitude of reachable set reduces accordingly. This is due to the fact that when the load amplitude is reduced the state amplitude and also the effect of parameter uncertainties $\triangle Ax$ on the fault estimate will also be reduced.

Firstly, based on the two reachable sets in Fig. 7.7, one can qualitatively verify that the fault estimation based diagnosis algorithm is valid in the presence of given system uncertainties and sensor noises, since the FIS reachable set under normal case is close to zero and FIS reachable set under faulty case is substantially different from the one under normal case. Besides, based on the principle of the proposed threshold selection approach, the threshold can be chosen as the upper and lower bounds of the normal reachable set.

Secondly, one can see from Fig. 7.7 that in case of actuator fault $f_a = 1$, the fault reachable set (after 6 sec) does not intersect with the normal reachable set (after 6 sec) and so the fault diagnosis algorithm can effectively detect the presence of fault. While in case of actuator fault with a smaller amplitude $f_a = 0.1$, the fault reachable set intersect with the normal reachable set and so the fault diagnosis algorithm fails to detect the presence of the actuator fault with this particular amplitude. This phenomenon is reasonable since when the fault amplitude is too small, its effect on the fault estimate is limited and can not be distinguished from the effect of system uncertainties. So based on the proposed approach, one can determine the minimal fault amplitude that can be detected by a given fault diagnosis algorithm under a given scenario.

Remark: The reachable set computation is achieved in Matlab using the algorithm in Section. 7.2.2 in conjunction with the existing toolboxes including "INTerval LABoratory " [3] and Multi-Parametric Toolbox [4]. The step-size of reachable set computation is chosen as $i = 0.0015$ and the order of zonotope ρ is 600. To further improve the computation precision, one can reduce the step-size or increase the order of zonotope, however, it will result in longer computation time.

7.4.3 Sensor fault diagnosis

In this section, the problem of sensor fault diagnosis is further considered, where both velocity sensor fault and current sensor fault are considered. To satisfy the observability, it is supposed that no actuator fault occurs and so only the speed velocity fault, current sensor fault and unknown load are treated as the additional states when designing the extended state observer, i.e., $\bar{x}_2 = (x, f_s, \Gamma_d)$. The fault diagnosis observer is given as follows:

$$\begin{cases} \dot{\hat{\bar{x}}}_2 = \bar{A}_2\hat{\bar{x}}_2 + \bar{B}_2 u + \bar{D}_2 y_d + \bar{K}_{o2}(y - \hat{y}), \\ \hat{y} = \bar{C}_2\hat{\bar{x}} \end{cases}$$

where the system matrices are given by $\bar{A}_2 = \begin{bmatrix} A & O & \Gamma \\ O & O & O \end{bmatrix}$, $\bar{B}_2 = \begin{bmatrix} B \\ O \end{bmatrix}$, $\bar{D}_2 = \begin{bmatrix} D \\ O \end{bmatrix}$ and $\bar{C}_2 = \begin{bmatrix} C & S & O \end{bmatrix}$ and the observer gain matrix $\bar{K}_{o2}$ is referred to Appendix A.4.

The fault profile is given by the following function,

$$f_{sv} = \begin{cases} 0 \text{ rad/s}, & \text{t} \in [0, 5] \\ 0.5 \text{ rad/s}, & \text{t} \in (5, 10] \end{cases} \qquad f_{sc} = \begin{cases} 0 \text{ A}, & \text{t} \in [0, 7] \\ 0.5 \text{ A}, & \text{t} \in (7, 10] \end{cases}$$

The rest of simulation scenario is the same as that of Section 7.4.2. The reachable set computation results for speed sensor fault estimate and current sensor fault estimate are shown in Fig. 7.9 and 7.10 respectively, where the black lines are the stochastic simulations of the sensor fault estimate.

Similar to the case of actuator fault diagnosis, one can see from Figs. 7.9 and 7.10 that all the stochastic simulations lie the calculated FIS reachable sets, which verifies the effectiveness of reachable set computation algorithm. Besides, at 3 sec, the load amplitude is reduced and consequently the effect of uncertainties on FIS is reduced, i.e., the width of reachable set becomes smaller. Due to the presence of current

[3] i.e., Intlab, see the software via http://www.ti3.tu-harburg.de/rump/intlab/
[4] i.e., MPT, see the software via http://people.ee.ethz.ch/ mpt/3/

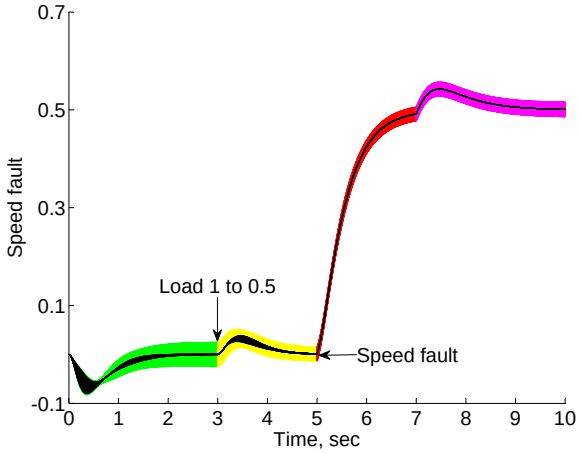

Figure 7.9. Reachable set of speed sensor fault estimate and stochastic simulations: green area (load with amplitude 1); yellow area (load with amplitude 0.5); red area (the presence of speed sensor fault); pink area (the presence of both speed and current sensor faults).

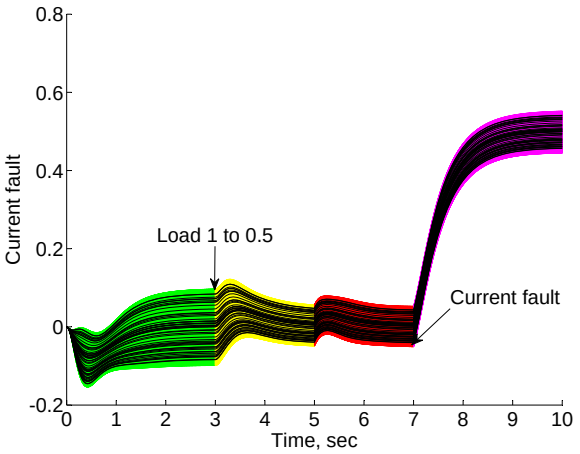

Figure 7.10. Reachable set of current sensor fault estimate and stochastic simulations: green area (load with amplitude 1); yellow area (load with amplitude 0.5); red area (the presence of speed sensor fault); pink area (the presence of both speed and current sensor faults).

sensor fault at 7 sec, there is a jump in the reachable set of speed fault estimate, this is due to the fact that the fault estimates for velocity sensor fault and current sensor fault are coupled with each other. Based on the calculated FIS reachable sets under normal case and faulty case, one can easily choose the threshold similar to the case of actuator fault diagnosis. Besides, one can also roughly determine the minimum detectable fault as that of actuator fault diagnosis.

7.5 Summary

In this Chapter, the problem of fault diagnosis system verification and robust threshold selection is considered for a typical model based fault diagnosis algorithm, i.e., fault estimation based approach. Due to the presence of system uncertainties and sensor noises, the fault indicating signals deviate from zero even under normal condition. To this end, the reachable set computation tool is drawn to calculate the fault indicating signal reachable set under normal case and a selected of faulty cases. Based on the calculated two reachable sets, a candidate fault diagnosis system can be qualitatively determined where it is still valid under all kinds of uncertainties. Besides, a robust threshold can be quantitatively selected which is robust to system uncertainties and consequently false alarm rate can be substantially reduced. In addition, by comparing those two reachable set, one can also determine what level of fault that can be detected by a given fault estimate algorithm. Actuator and sensor fault diagnosis of a motor system is given to illustrate the principle of the proposed approach.

This Chapter mainly focuses on the idea of fault diagnosis algorithm verification and robust threshold selection. The reachable set computation tool used may not be the latest one and the results may not be perfect now. But with more advanced reachable set computation tool and increasing computation power, the results in this Chapter can be substantially improved. Besides, the method in this Chapter can also be applied to the case of algorithm verification and robust threshold selection for other model based approach such as residual based and parameter estimation based fault diagnosis approach.

Chapter 8

COMPARISON VERIFICATION

8.1 Introduction

In Chapter 7, the framework of fault diagnosis system verification and robust threshold selection was proposed. In Chapter 2, a comparison analysis between the residual based and fault estimation based fault diagnosis approach was made in a qualitative way along with simple simulation comparison study. In this Chapter, however, the framework proposed in Chapter 7 is applied to the quantitative comparison analysis between the residual based and fault estimation based diagnosis approaches, which can shed light on the application scope of different fault diagnosis approaches. The sensor fault diagnosis problem of vehicle lateral dynamics is chosen as a case study. The relationship of this Chapter with previous Chapters is illustrated in Fig. 8.1.

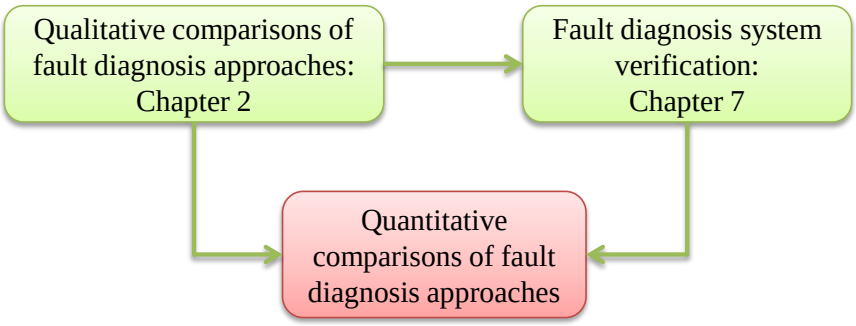

Figure 8.1. The relationship between this Chapter and previous Chapters.

8.2 Vehicle lateral dynamics

In model based fault diagnosis system design, the first step is to derive an appropriate model describing the system dynamics under consideration. To this end, in this section, vehicle lateral dynamics are introduced, where the standard one-track model is utilized, since it is one of the most widely used models for the purpose of vehicle lateral control and fault diagnosis system design [119–122] due to its availability for

on-line application (i.e., with low system order) and ability to well describe vehicle behaviour with lateral acceleration under 0.4 g (g denotes the acceleration of gravity) on normal dry asphalt roads [119–121]. The diagram of one-track model for vehicle lateral dynamics is shown in Fig. 8.2, where $\int r_c$ denotes the yaw angle and the rest of notations are explained whenever needed.

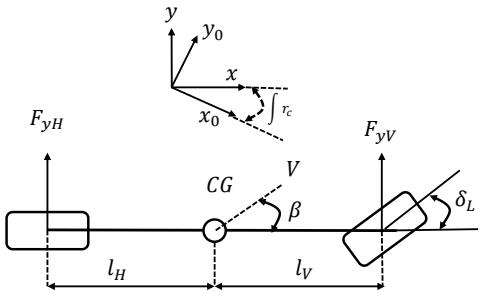

Figure 8.2. The diagram of a one-track model for vehicle lateral dynamics.

Assuming a constant vehicle velocity (see, Chapter 2 of [119] or pp. 79 of [121] for other assumptions), taking vehicle side slip angle β and yaw rate r_c as state variables, and the front wheel steering angle δ_L as input signal, vehicle lateral dynamics can be described by differential equations [119]

$$\begin{cases} mv(\dot{\beta} + \dot{r}_c) = F_{yV} + F_{yH} \\ I_z \dot{r}_c = l_V F_{yV} - l_H F_{yH} \end{cases}, \tag{8.2.1}$$

where m, v are the vehicle mass and longitudinal velocity, F_{yV}, F_{yH} are front and rear tire forces, I_z is the yaw moment of inertia, and l_V, l_H denote the distances from Centre of Gravity (CG) to front and rear tires, respectively.

Moreover, for small tire slip angles, lateral tire forces are usually approximated as a linear function of tire slip angles, which are defined by

$$\begin{cases} F_{yV} = c_{\alpha V}(\delta_c - \beta - l_V r_c/v) \\ F_{yH} = c_{\alpha_H}(-\beta + l_H r_c/v) \end{cases}, \tag{8.2.2}$$

where $c_{\alpha V}$ and $c_{\alpha H}$ are cornering stiffness of front and rear tires. The values of all the parameters are given in Appendix A.5.

Define vehicle state $x = [\beta; r_c]$ and control input $u = \delta_L$, substituting (8.2.2) into (8.2.1), one can obtain the state-space model of vehicle lateral dynamics, given

by

$$\dot{x} = \underbrace{\begin{bmatrix} -\dfrac{c_{\alpha V}+c_{\alpha H}}{mv} & \dfrac{l_H c_{\alpha H}-l_V c_{\alpha V}}{mv^2}-1 \\ \dfrac{l_H c_{\alpha H}-l_V c_{\alpha V}}{I_z} & -\dfrac{l_V^2 c_{\alpha V}+l_H^2 c_{\alpha H}}{I_z v} \end{bmatrix}}_{A_{un}} x + \underbrace{\begin{bmatrix} \dfrac{c_{\alpha V}}{mv} \\ \dfrac{l_V c_{\alpha V}}{I_z} \end{bmatrix}}_{B_{un}} u. \tag{8.2.3}$$

The variables that can be directly measured are the lateral acceleration signal α_y through accelerometer and the yaw rate signal r_c through gyrometer, i.e., $y = [\alpha_y; r_c]$ and consequently the measurement model is given by

$$y = \underbrace{\begin{bmatrix} -\dfrac{c_{\alpha V}+c_{\alpha H}}{m} & \dfrac{l_H c_{\alpha H}-l_V c_{\alpha V}}{mv} \\ 0 & 1 \end{bmatrix}}_{C_{un}} x + \underbrace{\begin{bmatrix} \dfrac{c_{\alpha V}}{m} \\ 0 \end{bmatrix}}_{D_{un}} u. \tag{8.2.4}$$

In practical applications, the system parameters in system model (8.2.3) and measurement model (8.2.4) inevitably have certain variations. As a result, rather than being a point, the elements of system matrices will fall into different intervals. That means the system matrices $A_{un}, B_{un}, C_{un}, D_{un}$ also fall into interval matrices (note: interval matrix denotes a matrix whose elements take values within intervals) according to the range of each parameters. For example, $A_{un} \in \mathcal{A}$, where $\mathcal{A} = [\underline{A}, \bar{A}]$ is a interval matrix with $\underline{A}$ and $\bar{A}$ being the lower and upper bound matrices element-wisely. The interval matrix $\mathcal{A}$ can also be equivalently represented by $\mathcal{A} = A + \Delta A$, where A is the normal matrix and ΔA can be seen as the radius matrix element-wisely. As a result, the vehicle lateral dynamics with uncertainties and sensor faults can be represented by the following generic systems

$$\begin{cases} \dot{x} = (A + \Delta A)x + (B + \Delta B)u \\ y = (C + \Delta C)x + (D + \Delta D)u + Ff \end{cases}. \tag{8.2.5}$$

In this model, the effect of sensor faults is also modelled through introducing fault variables $f = [f_a; f_y]$ (i.e., accelerometer fault f_a and gyrometer fault f_y) and their distribution matrix F (i.e., identity matrix for simultaneous accelerometer and gyrometer fault detection).

The objective of FD is to detect the presence of faults f_a and f_y (i.e., fault detection) and isolate which fault has occurred when a fault is detected (i.e., fault isolation). The comparison between two different types of model-based FD approaches are considered including residual based and fault estimate based approaches. Each approach contains a fault diagnosis observer for residual generation and a robust threshold for residual evaluation. The diagram of the overall fault diagnosis system

is shown in Fig. 8.3.

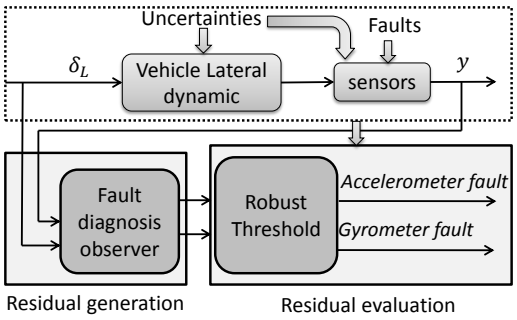

Figure 8.3. The diagram of fault diagnosis system for vehicle lateral dynamics including fault diagnosis observer and robust threshold selection.

8.3 Main results

In this section, the main results are presented. Specifically, the model-based FD observer design for residuals (fault estimates) generation is firstly discussed including conventional residual based and recent fault estimation based approaches, whose role in the overall FD system is shown in Fig. 8.3. The residual is chosen to indicate the presence of fault, and consequently it is expected to be close to zero in fault-free case and deviate from zero in the presence of faults [13]. However, due to the presence of inevitable uncertainties in practice, the residuals (or fault estimates) are not zero under normal condition. Then the problem of verification and robust threshold selection for the aforementioned model-based FD systems are further investigated, where both of them are transformed into the problem of reachable set computation for uncertain systems.

8.3.1 Residual based approach

In residual based FD, a set of FD observers are usually needed to isolate different faults, where each observer is designed to be only sensitive to one particular fault [6, 21]. The diagram of the residual based FD for vehicle lateral dynamics is shown in Fig. 8.4.

The i^{th} residual based FD observer for system (8.2.5), which is only sensitive to i^{th} sensor fault, takes the following form

$$\begin{cases} \dot{\hat{x}}_i = A\hat{x}_i + Bu + K_i^r(y_i - \hat{y}_i) \\ \hat{y}_i = C_i\hat{x}_i + D_i u \end{cases}, \tag{8.3.1}$$

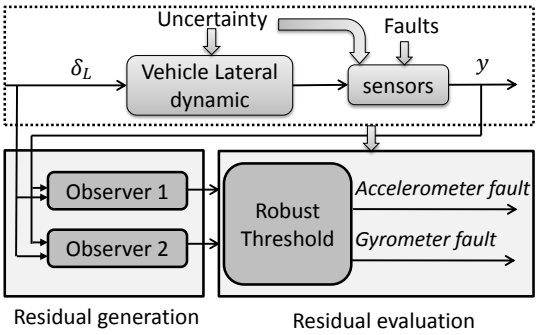

Figure 8.4. The diagram of residual based FD system for vehicle lateral dynamics including two FD observers and robust threshold.

where the subscript i means the i^{th} observer. y_i, the sub-vector of the original measurement vector y, is chosen in such a way that the i^{th} observer is only sensitive to i^{th} sensor fault (see, [5,6] for details). C_i, D_i are the normal matrices corresponding to y_i. K_i^r is the observer gain matrix, which can be designed based on H_∞ theory or simply pole assignment technique under the observability of the matrix pair (A, C_i).

The output estimation errors $r_i = y_i - \hat{y}_i$ or their functions in the case of y_i with high dimension are usually chosen as the residual signal. The residual r_i can be put into the following form

$$r_i = y_i - \hat{y}_i = C_i e_i + \Delta C_i x + \Delta D_i u + F_i f, \tag{8.3.2}$$

where $e_i = x - \hat{x}_i$. One can further obtain from Eqs. (8.2.5) and (8.3.1) that the error dynamics satisfy

$$\begin{aligned} \dot{e}_i = (A - K_i^r C_i)e_i + (\Delta A - K_i^r \Delta C_i)x \\ + (\Delta B - K_i^r \Delta D_i)u - K_i^r F_i f \end{aligned} \tag{8.3.3}$$

Substituting Eq. (8.3.2) into Eq. (8.3.1), the state estimate can be put into an equivalent form, given by

$$\dot{\hat{x}}_i = A\hat{x}_i + Bu + K_i^r C_i e_i + K_i^r \Delta C x + \Delta D_i u + K_i^r F f. \tag{8.3.4}$$

From Eqs. (8.3.2) and (8.3.3), one can see that the residuals r_i is sensitive to fault $F_i f$. *However, it is also subject to the effect of system uncertainties* $\Delta A, \Delta B, \Delta C, \Delta D$, *and state* x *and control input* u. *This will bring many challenges to the FD verification and threshold selection, since the uncertainties take values in intervals and result in infinite combinations.*

Verification and threshold

The verification and threshold selection results in Chapter (7) is directly applied. From $e_i = x_i - \hat{x}_i$, one can obtain $x_i = e_i + \hat{x}_i$. Substituting it into Eqs. (8.3.3) and (8.3.4), one can obtain the following composite system

$$\underbrace{\begin{bmatrix}\dot{e}_i\\ \dot{\hat{x}}_i\end{bmatrix}}_{\dot{\chi}} = \underbrace{\begin{bmatrix}A - K_i^r C_i + \Delta A - K_i^r \Delta C_i & \Delta A - K_i^r \Delta C_i\\ K_i^r C_i + K_i^r \Delta C_i & A + K_i^r \Delta C_i\end{bmatrix}}_{\mathcal{A}} \underbrace{\begin{bmatrix}e_i\\ \hat{x}_i\end{bmatrix}}_{\chi} + \underbrace{\begin{bmatrix}\Delta B - K_i^r \Delta D_i\\ B + \Delta D_i\end{bmatrix} u + \begin{bmatrix}-K_i^r F_i\\ K_i^r F_i\end{bmatrix} f}_{\mathcal{BU}}. \tag{8.3.5}$$

Using the under-brace notation, system (8.3.5) can be put into the following compact format

$$\dot{\chi} = \mathcal{A}\chi + \mathcal{BU}. \tag{8.3.6}$$

where $\chi, \mathcal{A}, \mathcal{B}$ and $\mathcal{U}$ are all interval variables.

Following the same procedure, the residual Eq. (8.3.2) can be put into the following form,

$$r_i = [C_i + \Delta C_i,\ \Delta C_i] \begin{bmatrix} e_i \\ \hat{x}_i \end{bmatrix} + \Delta D_i u + F_i f \tag{8.3.7}$$

As a result, after the reachable set of system (8.3.6) or equivalently (8.3.5) is calculated, the reachable set of r_i in (8.3.7) can be further calculated through set transformation.

8.3.2 Fault estimation based approach

The fault estimation based approach [6, 122] is further considered; different from residual based approach, the fault estimates directly serve as the residuals for fault detection and isolation, which can simplify the fault detection and isolation logic [6].

Considering that the common sensor faults are bias, drift, scaling with unknown amplitude and occurring time, a linear model can effectively describe their dynamics [122]. Without loss of generality, the state augmentation approach is used for fault estimate, where a first-order model is chosen (see [122] for second-order models and [7] for high order models). In this approach, faults are augmented as additional states and can be estimated along with the original system states [6]. Taking $\bar{x} = (x, f)$, system (8.2.5) can be equivalently represented by the following extended

system

$$\begin{cases} \dot{\bar{x}} = (\bar{A} + \Delta\bar{A})\bar{x} + (\bar{B} + \Delta\bar{B})u \\ y = (\bar{C} + \Delta\bar{C})\bar{x} + (D + \Delta D)u \end{cases}, \tag{8.3.8}$$

where $\bar{A} = \begin{bmatrix} A & O \\ O & O \end{bmatrix}$, $\bar{B} = \begin{bmatrix} B \\ O \end{bmatrix}$ and $\bar{C} = \begin{bmatrix} C & F \end{bmatrix}$.

Then a FD observer can be designed for system (8.3.8) using the normal matrices under the observability of the pair $(\bar{A}, \bar{C})$, as follows

$$\begin{cases} \dot{\hat{\bar{x}}} = \bar{A}\hat{\bar{x}} + \bar{B}u + \bar{K}_o(y - \hat{y}) \\ \hat{y} = \bar{C}\hat{\bar{x}} + Du \\ \hat{f} = P\hat{\bar{x}} \end{cases}, \tag{8.3.9}$$

where the gain matrix $\bar{K}_o$ is the observer gain matrix to be designed (e.g., pole assignment of the pair $(\bar{A}, \bar{C})$) and P is the projection matrix to obtain fault estimate from the augmented state estimate. Then fault estimates $\hat{f}$ directly indicate the status of the sensors.

Verification and threshold

Similar to the case of residual based approach, the verification and threshold selection problem is formulated into the sate reachable set computation problem for uncertain systems.

Combing (8.3.8) and (8.3.9), the error dynamic $e = \bar{x} - \hat{\bar{x}}$ can be obtained

$$\dot{e} = (\bar{A} - \bar{K}_o\bar{C})e + (\Delta\bar{A} - \bar{K}_o\Delta\bar{C})\bar{x} + (\Delta\bar{B} - \bar{K}_o\Delta D)u. \tag{8.3.10}$$

In addition, substituting measurement $y = (\bar{C} + \Delta\bar{C})\bar{x} + (D + \Delta D)u$ of (8.3.8) into system (8.3.9), one can obtain

$$\begin{aligned} \dot{\hat{\bar{x}}} &= \bar{A}\hat{\bar{x}} + \bar{B}u + \bar{K}_o(y - \hat{y}) \\ &= \bar{A}\hat{\bar{x}} + \bar{B}u + \bar{K}_o(\bar{C}e + \Delta\bar{C}\bar{x} + \Delta Du) \end{aligned}. \tag{8.3.11}$$

Both system (8.3.10) and (8.3.11) involve unknown state variables $\bar{x}$, to make the reachability analysis feasible, it is eliminated through the relationship $\bar{x} = e + \hat{\bar{x}}$. Substituting $\bar{x} = e + \hat{\bar{x}}$ into (8.3.10) and (8.3.11) and putting them together, one

can obtain

$$\underbrace{\begin{bmatrix}\dot{e}\\ \dot{\hat{x}}\end{bmatrix}}_{\dot{\chi}} = \underbrace{\begin{bmatrix}\bar{A}-\bar{K}_o\bar{C}+\Delta\bar{A}-\bar{K}_o\Delta\bar{C} & \Delta\bar{A}-\bar{K}_o\Delta\bar{C}\\ \bar{K}_o\bar{C}+\bar{K}_o\Delta\bar{C} & \bar{A}+\bar{K}_o\Delta\bar{C}\end{bmatrix}}_{\mathcal{A}}\underbrace{\begin{bmatrix}e\\ \hat{\hat{x}}\end{bmatrix}}_{\chi} + \underbrace{\begin{bmatrix}\Delta\bar{B}-\bar{K}_o\Delta D\\ \bar{B}+\bar{K}_o\Delta D\end{bmatrix}u}_{\mathcal{B}\mathcal{U}}. \tag{8.3.12}$$

Similar to the case of residual based approach, using the under-brace notations in (8.3.12), Eq. (8.3.12) can be put into a compact form similar to Eq. (8.3.6). Consequently, if the reachable set of the system (8.3.12) can be calculated, then the reachable set of the fault estimates $\hat{f}$ can thus be obtained.

Now the problem of residuals (or fault estimates) reachable set calculation under normal case and a selected faulty cases has been transformed into the state reachability analysis of uncertain system (8.3.6), the implementation issue of which has been discussed in Chapter 7.

8.4 Application study

In this section, the results will be demonstrated through the case study of sensor fault diagnosis problem for vehicle lateral dynamics given in Section. 8.2. Both the verification and threshold selection problem for residual based and fault estimation based FD approaches discussed in Section. 8.3 are considered. The accelerometer fault and gyrometer fault of vehicle lateral dynamics are considered simultaneously. The simulation scenario including initial state interval, uncertain parameter intervals and steering control input is given as follows.

Without loss of generality, assume that the uncertainty appears in the vehicle velocity v, since it is the main uncertainty source [123] due to sensor measurement errors (other parameter uncertainties can be similarly considered). The vehicle velocity is assumed to be within a bounded interval $v \in [19, 21]$ m/sec, then following the procedure of [123], system matrices A_{un} and B_{un} in can be calculated as interval matrices $A_{un} \in A + [-1, 1] \times \Delta A, B_{un} \in B + [-1, 1] \times \Delta B$, with $A, \Delta A, B$ and ΔB given by

$$A = \begin{bmatrix}-4.2832 & -0.9275\\ 23.6162 & -5.8513\end{bmatrix}, \Delta A = \begin{bmatrix}-0.2142 & -0.0073\\ 0 & -0.2926\end{bmatrix},$$
$$B = \begin{bmatrix}1.7662 & 33.2580\end{bmatrix}, \Delta B = \begin{bmatrix}0.0883 & 0\end{bmatrix}.$$

where A is a stable matrix with complex poles.

The initial values of slip angle and yaw rate are within a bounded interval vector $([-0.02, 0.02]; [0.03, 0.07])$. The known steering angle input $u_c(t)$ is a step input with amplitude 0.05 rad at 1 sec (in this case, the lateral acceleration is guaranteed to be less than 0.4 g such that the one-track mode can well describe the vehicle lateral dynamics). The accelerometer sensor fault f_a and gyrometer fault f_y will given where needed and will be plotted in the following figures directly. The sensor faults with different amplitudes are considered to evaluate the FD algorithms.

8.4.1 Residual based approach

The residual based approach in Section. 8.3.1 is first considered. The observer gain matrices $K_i^r, i = 1, 2$ in (8.3.1) are designed using pole assignment of the normal system matrix pair (A, C_i) such that the poles of matrix $A - K_i^r C_i$ are $[-8; -7]$; the results are $K_1^r = [-0.0607, -0.2256]$ and $K_2^r = [-0.4999,\ 4.8655]$. Since the initial system states $x(0) = [0; 0.05]$ can not be known exactly due to measurement errors, the initial states of the FD observer are supposed to lie in a bounded interval, given by $\hat{x}_i(0) = \Big[\ (-0.02, 0.02),\ \ (0.03, 0.07)\ \Big]$.

Given the uncertain parameters, the interval matrices in Eq. (8.3.6) can be calculated using INTerval LABoratory (INTLAB) software. Now the initial state uncertainties, system matrix uncertainties in (8.3.6) are all available, the reachability analysis tool can be applied to calculate the reachable sets of the residuals. The step-size for reachability analysis is chosen as 0.01 and the order of zonotope ρ is 800 (the calculation accuracy can be further increased by reducing step-size and increasing zonotope order, which will require longer computation time), under which configuration the computation time for each observer is about 1.5 sec using Matlab 2012 with Intel Core i5-3570 CUP @ 3.40 GHz. The reachable sets of the residuals (grey areas) and 200 exemplary trajectories (blacks lines) using stochastic Monte Carlo Simulations are shown Figs. 8.5 and 8.6 respectively.

It can be observed from Figs. 8.5 and 8.6 that *all the exemplary trajectories fall into the calculated reachable sets* and the reachable sets are not conservative, i.e., the trajectories are not far away from the boundaries of the reachable sets, which again verifies the effectiveness of the reachability analysis tool.

During 0 to 1 sec where no steering control input is given, one can see that the effect of initial state uncertainties and parameter uncertainties on residuals will gradually decrease. This is because in the absence of control input, the system states of vehicle lateral dynamics and consequently the effect of uncertainties will converge to zero in steady-state due to the system convergence (i.e., the real parts of the

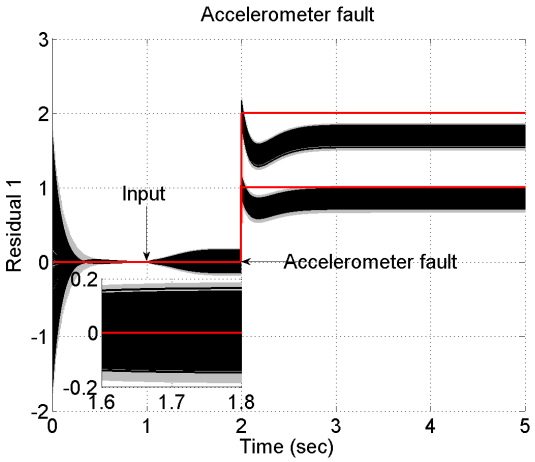

Figure 8.5. Accelerometer fault profile (red lines); the reachable set of residual 1 sensitive to accelerometer fault (grey areas) with its zoom-in plot from 1.6 sec–1.8 sec and their stochastic simulated trajectories (black lines).

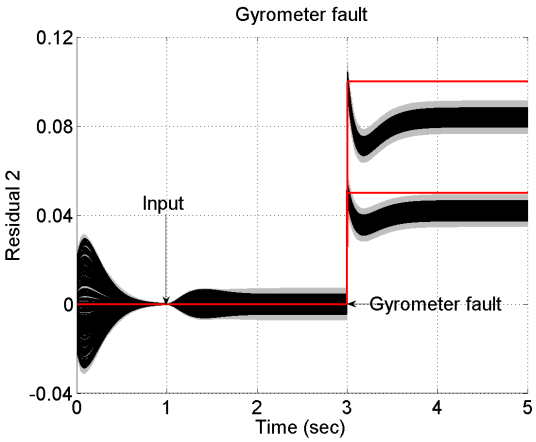

Figure 8.6. Gyrometer fault profile (red lines); the reachable set of residual 2 sensitive to gyrometer fault (grey areas) and their stochastic simulated trajectories (black lines).

eigenvalues of A_{un} are negative). After 1 sec, steering control input $u = 0.05$ rad is executed on the system, as a result, the system states of the vehicle lateral dynamics and consequently the effect of system uncertainties on residuals will no long be zero.

One can see from Figs. 8.5 and 8.6, that in the presence of accelerometer fault at 2 sec (or gyrometer fault at 3 sec), the residual 1 sensitive to accelerometer fault (or residual 2 sensitive to gyrometer fault) substantially deviates from its normal reachable set before 2 sec (or 3 sec), which verifies the effectiveness of the residual based FD algorithm.

After the FD observer converges, *one can choose the upper and lower bound of the residual reachable set as the interval threshold, which is* $[-0.2, 0.2]$ *for accelerometer*

fault detection and $[-0.01, 0.01]$ *for gyrometer fault detection. Residuals that deviate from the interval threshold indicate the presence of fault.* By iteratively decreasing the fault amplitude and performing reachable set calculation such that the upper bound of residual under normal case and lower bound of residual under faulty case are equal, one can find the minimum fault amplitude that can be detected by the residual based FD algorithm under described uncertainties; that is 0.55 m/s^2 for accelerometer fault and 0.05 *rad* for gyrometer fault.

8.4.2 Fault estimation based approach

The fault estimation based approach in Section. 8.3.2 is then considered. The observer gain matrix $\bar{K}_o$ in (8.3.9) is designed using pole assignment of the normal system matrix pair $(\bar{A}, \bar{C})$ such that the poles of matrix $\bar{A} - \bar{K}_o\bar{C}$ are $[-10; -9; -4; -3]$. Similarly, the initial states are supposed to be lie in a bounded interval $\hat{\bar{x}}_0 = \Big[\ (-0.02, 0.02),\ (0.03, 0.07),\ 0,\ 0\ \Big]$.

Similar to the case of residual based approach in Section. 8.4.1, the interval matrices $\mathcal{A}$ and $\mathcal{B}$ in (8.3.12) can be calculated. Consequently, the reachability analysis tool can be applied to calculate the reachable sets of the accelerometer and gyrometer fault estimates. The setting for the reachable set computation tool is the same as that in Section. 8.4.1, and the computation time is about 3 sec. The reachable sets of accelerometer and gyrometer fault estimates (grey areas) and 200 exemplary trajectories (black lines) using stochastic Monte Carlo Simulations are shown Figs. 8.7 and 8.8 respectively.

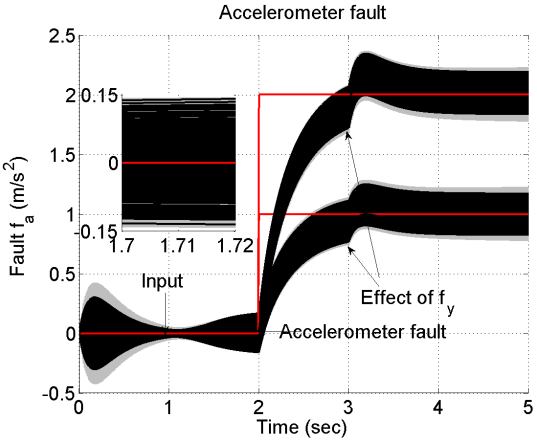

Figure 8.7. Accelerometer fault profile (red lines); the reachable set of the accelerometer fault estimate (grey areas) with its zoom-in plot from 1.7 sec to 1.72 sec and stochastic simulated trajectories (black lines).

From Figs. 8.7 and 8.8, similar conclusion (to the case of residual based ap-

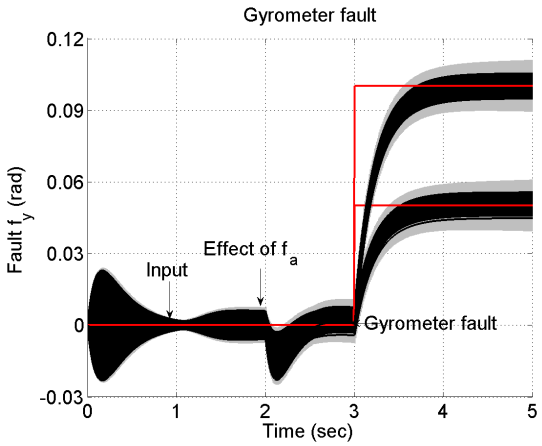

Figure 8.8. Gyrometer fault profile (red lines); the reachable set of the gyrometer fault estimate (grey areas) and stochastic simulated trajectories (black lines).

proach) can be drawn about the effect of initial state uncertainties and control input on fault estimates. One can see from Figs. 8.7 and 8.8, that in the presence of accelerometer fault at 2 sec (or gyrometer sensor fault at 3 sec), the reachable set of the accelerometer fault estimate (or gyrometer fault estimate) substantially deviates from its normal reachable set before 2 sec (before 3 sec for gyrometer fault), which verifies the effectiveness of fault estimation based FD algorithm. One can also see the effect of gyrometer fault on accelerometer fault reachable set at 3 sec (or the effect of accelerometer fault on reachable set of gyrometer fault estimate at 2 sec); this is due to the fact that they are coupled with each other in the FD observer design.

Based on the threshold selection principle, the interval threshold is chosen $[-0.16, 0.16]$ for accelerometer fault detection and $[-0.012, 0.012]$ for gyrometer fault detection. One can also find the minimum fault amplitude that can be detected by fault estimation based FD algorithm under described uncertainties; that is 0.4 m/s^2 for accelerometer fault and 0.02 rad for gyrometer fault.

8.4.3 Comparisons

Although both residual based and fault estimation based FD approaches have been verified to be effective for sensor fault diagnosis (for fault with large enough amplitude) using the case study of accelerometer and gyrometer fault diagnosis for vehicle lateral dynamics. There exist many differences in terms of fault diagnosis logic, sources of false alarm, application scope. A comparison between them has been made and summarized in Table. 8.1

Table 8.1. Parameters in longitudinal dynamics of the missile

Approach	Residual	Fault estimation
Observer number	Multiple	Single
Fault decoupled	Yes	No
Source of false alarm	initial uncertainties	fault coupling
Detectable accelerometer fault	0.55 m/s^2	0.4 m/s^2
Detectable gyrometer fault	0.05 rad	0.02 rad

Some observations from Table. 8.1 are given as follows:

- Residual based FD requires multiple observer to achieve fault isolation, while fault estimation based one only requires one observer;
- Residual based approach can achieve fault decoupling, while fault estimation based approach fails to decouple different faults;
- The initial uncertainties have more effect on the performance of residual based approach than fault estimation based one;
- Fault estimation based approach can detect sensor faults (accelerometer and gyrometer sensor faults) with smaller amplitude than residual based one.

8.5 Summary

In this Chapter, the quantitative comparison analysis between residual based and fault estimation based diagnosis approach is made using the fault diagnosis verification and robust threshold selection tool proposed in Chapter 7. The sensor fault diagnosis problem of vehicle lateral dynamics is chosen as the case study. The effectiveness of residual based and fault estimation based diagnosis approaches are summarized and compared in an quantitative way.

Chapter 9

SUMMARY AND FUTURE WORK

In this Chapter, the contributions of this thesis are summarized. Furthermore, a discussion on possible future work is also included.

9.1 Summary

This thesis is mainly on practically-motivated theoretical research on fault estimation algorithms: design and verification. The overall objectives are threefold:

- Compare residual based and fault estimation based fault diagnosis approaches both qualitatively and quantitatively;
- Propose a set of disturbance estimation algorithms for the purpose of fault estimate according to different specifications;
- Provide a new perspective to the problem of fault diagnosis system verification and robust threshold selection.

To this end, the fault diagnosis algorithms are first reviewed, where emphasis is put on model based fault diagnosis algorithms (e.g., the residual based and fault estimation based approaches). The disturbance estimation algorithms are also reviewed and categorized according to the different state information used for the derivation of disturbance estimate. On this basis, a comparison analysis between the traditional residual based and fault estimation based fault diagnosis approaches is made, from which it is discovered that the fault estimation based approach provides a simple fault diagnosis logic (especially for fault isolation) and also the fault severity information.

Then a set of disturbance observer algorithms (for the purpose of fault estimation) are proposed. Specifically, the properties of a unified Kalman filter are first

investigated including existence, optimality and asymptotic stability. The results can provide a unified existence condition accommodating the classical Kalman filter and Unknown input observer as its special cases. On this basis, the results are applied to the problem of simultaneous state and disturbance estimation, termed full order disturbance observer design since all the state information is needed in the derivation of disturbance estimate.

Noting that not all the state information is needed to derive the disturbance estimate, reduced-order disturbance observer design is then considered. A reduced disturbance observer is first proposed for discrete-time linear systems where a slowly time-varying disturbance model is assumed, which can unify both the full order and reduced order disturbance observer on this topic (i.e., disturbance observer design with a slowly time-varying disturbance model). And more importantly, an easily verified existence condition is provided thorough two matrix rank equality conditions.

To improve the disturbance estimate performance for the case where poor prior disturbance model information is available, another reduced-order disturbance observer is designed for discrete-time linear stochastic system with easily-checked existence condition. This is achieved by using a functional observer structure in conjunction with minimum-variance-unbiased-estimation technique.

Following this line of thought, attention is then turned to the relationship between time-domain disturbance observer and frequency-domain disturbance observer. It is rigorously shown that these two complete different disturbance observer design principles share the same structure in transfer function format. The main differences between them are also identified such as disturbance observer order. Then a time-domain disturbance observer is proposed based on the functional observer design to reduce the disturbance observer order.

In practical applications, however, there are always some mismatches between the real pant and the mathematical model used to describe it. This phenomenon will bring two challenging issues for model based fault diagnosis. On the one hand, it is challenging to verify a fault diagnosis algorithm, i.e., answering the question that under what condition (e.g., level of uncertainties) a given fault diagnosis algorithm is valid. On the other hand, it is hard to choose an appropriate threshold to evaluate the fault indicating signals.

To this end, the rest of the thesis focuses on these two challenging issues. They are formulated as the reachability analysis problem for uncertain systems. The basic philosophy of the proposed approach is to quantitatively evaluate the effect of uncertainties and faults on fault indicating signals. Two practical illustrating

examples including actuator and sensor fault diagnosis for a direct motor system, and sensor fault diagnosis for vehicle lateral dynamics are presented to demonstrate the main idea of the proposed approach. Particularly, a quantitative comparison between the residual based and fault estimation based fault diagnosis approaches are further made based on the newly proposed approach.

9.2 Future Work

Based on the research outcome in this thesis, the future work (or research challenges to be more exact) involved are provided below in conjunction with the possible solutions. They are categorized in terms of algorithm design (see, Section. 9.2.1) and application verification (see, Section. 9.2.2).

9.2.1 Algorithm design

The future work on algorithm design can mainly be categorised into algorithm design for disturbance observer and algorithm design for system verification and robust threshold generation.

Disturbance observer design

Disturbance observer design for linear systems is relatively mature and in the stage of practical application. However, the disturbance observer for nonlinear systems (see, [50, 62, 124] among many others) assumes that the full states are directly measurable or the system nonlinear terms satisfy some assumptions (e.g., Lipschitz). Consequently, the disturbance observer design for generic nonlinear systems should be further developed. A Bayesian inference approach (particle filter for discrete-time stochastic system to be more exact) may provide a solution. Two examples are taken as follows:

The first example is about unknown input estimation in input channel (i.e., for actuator fault estimation). Consider the following generic nonlinear system in the presence of fault (or disturbance) in input channel:

$$\begin{cases} \dot{x} = f(x) + g_1(x)u + g_2(x)d \\ y = h(x) \end{cases}, \tag{9.2.1}$$

The fault d can be modelled (or approximately represented) by a linear system with unknown initial values

$$\dot{w} = Ww,\ d = Vw\ . \tag{9.2.2}$$

Then systems (9.2.1) and (9.2.2) can be combined to obtain a composite system, given by

$$\begin{cases} \begin{bmatrix} \dot{x} \\ \dot{w} \end{bmatrix} = \begin{bmatrix} f(x) + g_2(x)Vw \\ Ww \end{bmatrix} + \begin{bmatrix} g_1(x) \\ 0 \end{bmatrix} u \\ y = h(x) \end{cases}, \tag{9.2.3}$$

Putting the aforementioned system into the corresponding discrete-time counterpart, the particle filtering can be drawn to solve the problem of augmented state estimation problem, considering that particle filter can handle generic nonlinear system.

The second example is about unknown input estimation in measurement channel (for sensor fault estimation). Consider the following generic nonlinear system in the presence of fault (or disturbance) in measurement channel:

$$\begin{cases} \dot{x} = f(x) + g_1(x)u \\ y = h(x) + Dd \end{cases}, \tag{9.2.4}$$

Combing systems (9.2.4) and (9.2.2) results in a composite system, given by

$$\begin{cases} \begin{bmatrix} \dot{x} \\ \dot{w} \end{bmatrix} = \begin{bmatrix} f(x) \\ Ww \end{bmatrix} + \begin{bmatrix} g_1(x) \\ 0 \end{bmatrix} u \\ y = h(x) + DVw \end{cases}, \tag{9.2.5}$$

Similar to the case of example 1, after transforming the systems into the discrete-time counterpart, the particle filtering can be drawn to solve the problem of augmented state estimation problem. *Particularly, given system states x, the remaining systems are conditionally linear system and marginalized particle filtering can be used to derive the state and fault estimation in a more efficient way.*

The disturbance observer design should also accommodate some practical issues, which may lead to new research challenges. Some examples are given as follows:

- How to design a disturbance observer based control for uncertain systems using saturated actuator, since in practical applications input saturation is prevalent due to the limited capabilities of actuator. The mechanism of anti-windup control can be integrated with disturbance observer based control.

- How to design a disturbance observer accommodating the effects of sensor noises, since they are inevitable in practical applications and may degrade performance if not being handled properly. The classical Kalman filter and disturbance observer can be fused together to reduce the effect of noises.

It is demonstrated in Chapter. 3 that by incorporating certain prior information on disturbances, both state estimation and disturbance estimation performance can be enhanced. The prior information in Chapter. 3 is still limited, more types of prior information should be exploited, particularly the prior information learned from history data. Machine learning algorithms can be drawn to learn and build the prior information in large amount of history data.

Verification and robust threshold generation

In Chapters 7 and 8, the problem of fault diagnosis system verification and robust threshold generation is formulated into reachability analysis for uncertain systems. The effectiveness of the algorithm is also verified using different examples.

However, the examples therein are linear systems. Although there is no such assumption in the proposed approach, the fault diagnosis system verification and robust threshold selection for uncertain nonlinear systems have not been considered and is more challenging in comparison with the linear one. For the verification problem of nonlinear system fault diagnosis, more advanced reachable set computation algorithms should be drawn to compute the reachable set. Besides, in practical applications, the reference inputs may be time-varying. Consequently, effective reachability analysis algorithms for uncertain systems with time-varying inputs should also be developed.

Exact reachability analysis is only possible for a limited type of linear systems. For generic linear systems and nonlinear systems, approximation is usually used to obtain an over-approximation of the true reachable set. How to obtain a tight approximation for true reachable set is also an open and challenging question to be answered.

9.2.2 Experimental validation

Most of the results in this thesis are verified using numerical examples, experimental verification and validation is necessary and may pose new research challenges. The future work on experimental validation will mainly be focused on the following three aspects including application validation of the comparison analysis between the residual based and fault estimation based fault diagnosis approaches in Chapter 2, different kinds of disturbance estimation algorithms proposed in Chapters 3–6 and the validation of verification and threshold generation algorithm based reachable set computation in Chapter 7.

Appendix A

SUPPLEMENTARY MATERIALS

A.1 Appendix for Chapter 2

In this section, the motor driver system for electric A/C is introduced, which serves as the case study in Section. 2.3 of Chapter 2.

A.1.1 Principe of motor systems

The whole model of a motor system can be divided into two subsystems including an electrical model and a mechanical model.

Electrical subsystem: According to Kirchhoff's law, one can obtain the equation of the electrical model as

$$L\dot{I} + RI = V - k_e\omega \tag{A.1.1}$$

Mechanical subsystem: The equation for the mechanical subsystem can be derived based on the torque balance as follows:

$$J\dot{\omega} = k_T I - k_d\omega - \Gamma_d \tag{A.1.2}$$

The meanings of all the aforementioned notations and their corresponding values for simulation study are referred to [125], which are summarized in Table A.1.

A.1.2 Controller design

To eliminate steady-state position control error under external load and system uncertainties, an integral action is usually introduced when designing a controller. To this end, the integral of the output error is augmented as an extra state, i.e., $x_4 = \int(y_o - y_d)dt$, where y_o is the system output and $y_d = \theta_d$ is the reference position. Since all of the state variables are very easy to measure (a potentiometer for position, a tachometer for speed and an ammeter for current), one can design a full-state feedback controller without a state observer. In this paper, the control

Table A.1. Meanings of Notations

Notation	Significance	Value
L	Armature inductance	170E-3 (H)
I	Armature current	A
k_e	Back-EMF constant	14.7E-3
R	Armature resistance	4.67 Ohms
V	Input voltage	V
J	Motor inertia	42.6E-6 Kg·m^2
ω	Rotor rotation speed	rad/s
k_T	Motor electrical constant	14.7E-3
k_d	Mechanical dumping constant	47.3E-6
Γ_d	Load torque	N·m

scheme is designed as

$$u = -k_\theta(\theta_m - \theta_d) - k_e x_4 - k_\omega \omega_m - k_i i_m \tag{A.1.3}$$

where θ_m, ω_m and i_m are the measurement value of position, velocity and current, respectively. The parameters k_θ, k_e, k_ω and k_i are the control parameters to be designed. The aforementioned systems can be put into state space model, which is discussed in the following section.

A.1.3 State space model

Based on the aforementioned two subsystems (A.1.1) and (A.1.2), a linear model of the motor system can be obtained as follows:

$$\begin{cases} \dot{x} = Ax + Bu + Dy_d + \Gamma\Gamma_d, \\ y_m = C_m x, \\ y_o = c_o x \end{cases} \tag{A.1.4}$$

where $x = [x_1, x_2, x_3, x_4]^T = [\theta, \omega, I, \int(\theta - \theta_d)dt]^T$ is the system state, $u = V$ the control voltage, $y_d = \theta_d$ the desired output position, Γ_d the load, y_m the measurement output and y_o the controlled output. System matrix A, control input matrix B, desired output matrix D, load matrix Γ, measurement matrix C_m and output matrix c_o are given as follows:

$$A = \begin{bmatrix} 0 & 1 & 0 & 0 \\ 0 & -\frac{k_d}{J} & \frac{k_T}{J} & 0 \\ 0 & -\frac{k_e}{L} & -\frac{R}{L} & 0 \\ 1 & 0 & 0 & 0 \end{bmatrix}, \; B = \begin{bmatrix} 0 \\ 0 \\ \frac{1}{L} \\ 0 \end{bmatrix}, \; D = \begin{bmatrix} 0 \\ 0 \\ 0 \\ -1 \end{bmatrix} \; \Gamma = \begin{bmatrix} 0 \\ -\frac{1}{J} \\ 0 \\ 0 \end{bmatrix}, \; C_m = I_{4\times 4},$$

$c_o = \begin{bmatrix} 1 & 0 & 0 & 0 \end{bmatrix}$.

A.2 Appendix for Chapter 3

A.2.1 Proof of Lemma 1

$$rank(\begin{bmatrix} zI_n - A_k & -G_k \\ C_{k+1} & O \\ O & D_k \end{bmatrix}) = rank(\begin{bmatrix} zI_n - A_k & -G_k \\ C_{k+1} & O \\ O & D_k \end{bmatrix} \begin{bmatrix} I_n & O \\ O & [F_{0k}\ D_k^T] \end{bmatrix})$$

$$= rank(\begin{bmatrix} zI_n - A_k & -G_kF_{0k} & -G_kD_k^T \\ C_{k+1} & O & O \\ O & D_kF_{0k} & D_kD_k^T \end{bmatrix}) = rank(\begin{bmatrix} zI_n - A_k & -F_k \\ C_{k+1} & O \end{bmatrix}) + rank(D_kD_k^T).$$

A.2.2 Proof of Theorem 4

Inspired by the approaches in [72,79], the proof of Theorem 4 is organized as follows. First, it will be shown that $P_{k|k}$ is monotonically increasing and converges to a fixed point $\bar{P}$ for the zero initial covariance matrix $P_{0|0} = 0$. Next, the asymptotic stability of the proposed filter is proved. Finally, one can demonstrate that the convergence of $P_{k|k}$ and the asymptotic stability of the filter still hold for any arbitrary initial covariance $P_{0|0} \geq 0$.

Monotonicity

First, one can show by induction that $P_{k|k}$ is monotonically increasing for initial covariance $P_{0|0} = 0$. Define a matrix function

$$\begin{aligned} \phi(K, X) = &(A - KCA)X(A - KCA)^T \\ &+(I - KC)Q(I - KC)^T + KRK^T, \end{aligned}$$

and define $f(X) = \phi(K^*, X)$, where K^* is the gain matrix (3.4.3) of the filter that corresponds to the covariance matrix X. Note that for any $0 \leq X \leq Y$, one has

$$f(X) = \phi(K_X^*, X) \leq \phi(K_Y^*, X) \leq \phi(K_Y^*, Y) = f(Y), \tag{A.2.1}$$

where the first inequality can be obtained from Theorem 3 and the second inequality is immediate from the definition of $\phi(K, X)$.

Clearly one has $P_{0|0} \leq P_{1|1}$ for $P_{0|0} = 0$. Now suppose $P_{k-1|k-1} \leq P_{k|k}$ holds

for step k. Then noting that $P_{k|k} = f(P_{k-1|k-1})$ and $P_{k+1|k+1} = f(P_{k|k})$, one can obtain $P_{k|k} \leq P_{k+1|k+1}$ based on Eq. (A.2.1). By induction, $P_{k|k}$ is monotonically increasing for all k when initial covariance $P_{0|0} = 0$.

From the monotonicity of $P_{k|k}$ and in conjunction with the boundedness of $P_{k|k}$ shown in Lemma 3, one can conclude that $P_{k|k}$ converges to a unique fixed point for zero initial covariance $P_{0|0}$.

Asymptotic stability

Let $\bar{P}$ be a solution of the steady-state version of the error covariance equation in Eq. (3.5.1), i.e. $\bar{P} = \phi(\bar{K}, \bar{P})$, where $\bar{K}$ is the corresponding gain matrix. Note that the fixed point obtained previously also satisfies this equation.

Suppose the asymptotic stability of the time-invariant filter does not hold, i.e. there exist some $|\lambda| \geqslant 1$ and the corresponding eigenvector $\omega \neq 0$ such that

$$(A - \bar{K}CA)^T\omega = \lambda\omega. \tag{A.2.2}$$

From $\bar{P} = \phi(\bar{K}, \bar{P})$, one can have

$$(1 - |\lambda|^2)\omega^*\bar{P}\omega = \omega^*(I - \bar{K}C)Q(I - \bar{K}C)^T\omega + \omega^*\bar{K}R\bar{K}^T\omega,$$

where the superscript $*$ denotes the complex conjugation. Since $|\lambda| \geqslant 1$, the above equation indicates that both sides of the equation are equal to zero since the right-hand side is nonnegative. Hence one has

$$[(I - \bar{K}C)Q^{\frac{1}{2}}]^T\omega = 0 \quad \text{and} \quad \bar{K}^T\omega = 0. \tag{A.2.3}$$

Then one can obtain from Eq. (A.2.3) that

$$(Q^{\frac{1}{2}})^T\omega = 0. \tag{A.2.4}$$

In addition, from the second equality of (A.2.3) and Eq. (A.2.2), one can obtain

$$A^T w = \lambda w. \tag{A.2.5}$$

Eqs. (A.2.4) and (A.2.5) implies that $(A, Q^{\frac{1}{2}})$ is not stabilizable. This contradiction disproves the assumption that the time-invariant filter is unstable.

Non-zero initial covariance

It is now demonstrated that $P_{k|k}$ approaches to $\bar{P}$ for any non-negative initial covariance $P_{0|0}$. First, note that

$$\begin{aligned} P_{k|k} - \bar{P} &= \phi(K_k, P_{k-1|k-1}) - \phi(\bar{K}, \bar{P}) \\ &\leq \phi(\bar{K}, P_{k-1|k-1}) - \phi(\bar{K}, \bar{P}) \\ &= (A - \bar{K}CA)(P_{k-1|k-1} - \bar{P})(A - \bar{K}CA)^T, \end{aligned}$$

where the inequality holds due to Theorem 3, and $\bar{K}$ and $\bar{P}$ are a solution of $P = \phi(\bar{K}, \bar{P})$.Since $(A - \bar{K}CA)$ is stable, the right-hand side of the above equation will approaches to 0 as k tends to $+\infty$. Hence one can obtain $P_{k|k} \leq \bar{P}$ for large k.

Now let $P^0_{k|k}$ denote the covariance matrix corresponding to the initial covariance $P_{0|0} = 0$. Then from $0 = P^0_{0|0} \leq P_{0|0}$ and applying (A.2.1), one can obtain $P^0_{1|1} \leq P_{1|1}$. By induction, it can be easily verified that the inequality in the initial covariance matrixes propagates for all k, i.e. $P^0_{k|k} \leq P_{k|k}$ for all k. Since

$$\bar{P} = \lim_{k\to\infty} P^0_{k|k} \leq \lim_{k\to\infty} P_{k|k} \leq \bar{P}\,,$$

One can conclude that $P_{k|k}$ will converge to a unique $\bar{P}$. This completes the proof of Theorem 4.

A.2.3 Proof of Eq. (3.6.7)

First, one can obtain the inverse of M_k as follows

$$M_k^{-1} = [G_k,\ G_k^{\perp}] \begin{bmatrix} (I - F_{0k}F_{0k}^T)D_k^T(D_kD_k^T)^{-1} & O & F_{0k} \\ O & I & O \end{bmatrix}.$$

Then Eq. (3.6.7) can be obtained:

$$\begin{aligned} D_k\hat{d}_k &= D_k(G_k^TG_k)^{-1}G_k^TM_k^{-1}\begin{bmatrix} r_k \\ O \\ O \end{bmatrix} + D_k(G_k^TG_k)^{-1}G_k^TM_k^{-1}\begin{bmatrix} O \\ O \\ I \end{bmatrix}\hat{\delta}_k \\ &= D_k(G_k^TG_k)^{-1}G_k^TG_k(I - F_{0k}F_{0k}^T)D_k^T(D_kD_k^T)^{-1}r_k \\ &\quad + D_k(G_k^TG_k)^{-1}G_k^TG_kF_{0k}\hat{\delta}_k = r_k. \end{aligned}$$

A.2.4 Proof of Eq. (3.6.8)

Define $M_{k-1}^P = P_{k|k}\bar{M}_{k-1}^T(\bar{M}_{k-1}P_{k|k-1}\bar{M}_{k-1}^T)^{-1}$. Then one has

$$\begin{aligned}
&M_{k-1}^{-1}\tilde{r}_{k-1} - K_kC_kM_{k-1}^{-1}\tilde{r}_{k-1}\\
&= (I - K_kC_k)M_{k-1}^{-1}\tilde{r}_{k-1}\\
&= M_{k-1}^P\bar{M}_{k-1}M_{k-1}^{-1}\tilde{r}_{k-1}\\
&= M_{k-1}^P\bar{M}_{k-1}G_{k-1}D_{k-1}^T(D_{k-1}D_{k-1}^T)^{-1}D_{k-1}d_{k-1}\\
&= M_{k-1}^P\begin{bmatrix} D_{k-1} & O\\ O & I\end{bmatrix}[G_{k-1},\ G_{k-1}^\perp]^{-1}\times G_{k-1}D_{k-1}^T(D_{k-1}D_{k-1}^T)^{-1}D_{k-1}d_{k-1}\\
&= M_{k-1}^P\begin{bmatrix} r_{k-1}\\ O\end{bmatrix} = M_{k-1}^P\bar{M}_{k-1}G_{k-1}d_{k-1}\\
&= P_{k|k}\bar{M}_{k-1}^T(\bar{M}_{k-1}P_{k|k-1}\bar{M}_{k-1}^T)^{-1}\bar{r}_{k-1},
\end{aligned}$$

where in the above derivation, the following identities have been used:

$$M_{k-1}^{-1}\tilde{r}_{k-1} = G_{k-1}D_{k-1}^T(D_{k-1}D_{k-1}^T)^{-1}D_{k-1}d_{k-1}, \tag{A.2.6}$$

$$I - K_kC_k = M_{k-1}^P\bar{M}_{k-1}. \tag{A.2.7}$$

Now one can show Eq. (A.2.7):

$$\begin{aligned}
&I - K_kC_k - M_{k-1}^p\bar{M}_{k-1}\\
&= I - K_kC_k - P_{k|k}\bar{M}_{k-1}^T(\bar{M}_{k-1}P_{k|k-1}\bar{M}_{k-1}^T)^{-1}\bar{M}_{k-1}\\
&= I - P_{k|k}C_k^TR_k^{-1}C_k - P_{k|k}[\bar{M}_{k-1}^T(\bar{M}_{k-1}P_{k|k-1}\bar{M}_{k-1}^T)^{-1}\\
&\quad\times\bar{M}_{k-1} + C_k^TR_k^{-1}C_k - C_k^TR_k^{-1}C_k]\\
&= I - P_{k|k}C_k^TR_k^{-1}C_k - [I - P_{k|k}C_k^TR_k^{-1}C_k]\\
&= O,
\end{aligned}$$

where $\bar{M}_k = \begin{bmatrix} D_k & O\\ O & I\end{bmatrix}[G_k,\ G_k^\perp]^{-1}$.

A.3 Appendix for Chapter 6

A.3.1 Proof of Theorem 13

First consider transfer function $G_{u\hat{d}}$. From the identity $A^{-1} = adj(A)/det(A)$, one can obtain:

$$\begin{aligned}
G_{u\hat{d}} &= -H\tilde{C}[sI - (\bar{A} - K\bar{C})]^{-1}\bar{B}\\
&= \frac{-[O, H]adj(sI - (\bar{A} - K\bar{C}))\bar{B}}{det(sI - (\bar{A} - K\bar{C}))}.
\end{aligned} \tag{A.3.1}$$

In addition, for SISO system (A, B, C), the following property holds,

$$Cadj(sI - A)B = \begin{vmatrix} sI - A & B \\ -C & 0 \end{vmatrix}. \tag{A.3.2}$$

Partitioning the gain matrix K into $K = [K_1^T, K_2^T]^T$ in conjunction with (A.3.2), the numerator of (A.3.1) is

$$\begin{aligned} &-[O, H]adj[sI - (\bar{A} - K\bar{C})]\bar{B} \\ &= -\begin{vmatrix} sI - A + K_1C & -DH & B \\ K_2C & sI - S & O \\ O & -H & 0 \end{vmatrix} = -\begin{vmatrix} I & -DH & -K_1 \\ O & sI - S & -K_2 \\ O & -H & 0 \end{vmatrix} \begin{vmatrix} sI - A & O & B \\ O & I & O \\ -C & O & 0 \end{vmatrix} \\ &= -\begin{vmatrix} sI - S & -K_2 \\ -H & 0 \end{vmatrix} \begin{vmatrix} sI - A & B \\ -C & 0 \end{vmatrix} = Hadj(sI - S)K_2Cadj(sI - A)B. \end{aligned} \tag{A.3.3}$$

Then consider transfer function $G_{y\hat{d}}$. Similar to (A.3.1) and (A.3.3), one can obtain the following two identities,

$$\begin{aligned} G_{y\hat{d}} &= H\tilde{C}[sI - (\bar{A} - K\bar{C})]^{-1}K \\ &= \frac{[O, H]adj[sI - (\bar{A} - K\bar{C})]K}{det(sI - (\bar{A} - K\bar{C}))}. \end{aligned} \tag{A.3.4}$$

and

$$\begin{aligned} &[O, H]adj[sI - (\bar{A} - K\bar{C})]K \\ &= \begin{vmatrix} sI - A + K_1C & -DH & K_1 \\ K_2C & sI - S & K_2 \\ O & -H & 0 \end{vmatrix} = -\begin{vmatrix} I & -DH & -K_1 \\ O & sI - S & -K_2 \\ O & -H & 0 \end{vmatrix} \begin{vmatrix} sI - A & O & O \\ O & I & O \\ -C & O & 1 \end{vmatrix} \\ &= -\begin{vmatrix} sI - S & -K_2 \\ -H & 0 \end{vmatrix} det(sI - A) = Hadj(sI - S)K_2det(sI - A). \end{aligned} \tag{A.3.5}$$

Substituting (A.3.3) into (A.3.1) and (A.3.5) into (A.3.4) ends the proof.

A.3.2 Proof of Eq. (6.3.6)

To prove $G_{u\hat{d}}(0) = 1$, one only needs to prove the subtraction of the denominator and numerator of (A.3.1) is zero at $s = 0$, which is given as follows:

$$\begin{aligned} &\begin{vmatrix} -A + K_1C & -DH & B \\ K_2C & -S & O \\ O & -H & 0 \end{vmatrix} + \begin{vmatrix} -A + K_1C & -DH \\ K_2C & -S \end{vmatrix} \\ &= \begin{vmatrix} -A + K_1C & -DH & B \\ K_2C & -S & O \\ O & -H & 0 \end{vmatrix} + \begin{vmatrix} -A + K_1C & -DH & O \\ K_2C & -S & O \\ O & -H & 1 \end{vmatrix} \end{aligned}$$

$$
\begin{aligned}
&= \begin{vmatrix} -A+K_1C & -DH & B \\ K_2C & -S & O \\ O & -H & 1 \end{vmatrix} = \begin{vmatrix} -A+K_1C & -DH & D \\ K_2C & -S & O \\ O & -H & 1 \end{vmatrix} \\
&= \begin{vmatrix} -A+K_1C & O & D \\ K_2C & -S & O \\ O & O & 1 \end{vmatrix} = \begin{vmatrix} -A+K_1C & O \\ K_2C & -S \end{vmatrix} \\
&= det(-A+K_1C)det(-S),
\end{aligned}
$$

where the identity $D = B$ has been used in the third equality. The proof ends since $det(S) = 0$.

A.3.3 Proof of Eq. (6.3.7)

From (A.3.1), one can obtain the denominator of $1/(1 - G_{u\hat{d}})$, given by

$$
\begin{aligned}
&det(sI - (\bar{A} - K\bar{C})) + [O, H]adj(sI - (\bar{A} - K\bar{C}))\bar{B} \\
&= \begin{vmatrix} sI - A + K_1C & -DH & O \\ K_2C & sI - S & O \\ O & -H & 1 \end{vmatrix} + \begin{vmatrix} sI - A + K_1C & -DH & B \\ K_2C & sI - S & O \\ O & -H & 0 \end{vmatrix} \\
&= \begin{vmatrix} sI - A + K_1C & -DH & B \\ K_2C & sI - S & O \\ O & -H & 1 \end{vmatrix} = \begin{vmatrix} sI - A + K_1C & O & B \\ K_2C & sI - S & O \\ O & O & 1 \end{vmatrix} \\
&= det(sI - A + K_1C)det(sI - S),
\end{aligned}
$$

where in the third equality $D = B$ has been used.

A.3.4 Proof of Theorem 14

Without loss of generality, suppose $C = [1, O_{1\times n-1}]$ (this assumption can always be satisfied for SISO system (6.2.2) through some non-singular linear transformation). Partitioning $\begin{bmatrix} J & K \end{bmatrix}$ into $\begin{bmatrix} J_1 & K_1 \\ J_2 & K_2 \end{bmatrix}$ and taking the specific structure of L into account, the matrix F can be put into the following form:

$$
\begin{aligned}
F &= L\bar{A}L^+ - [J, K]\begin{bmatrix} \bar{C}\bar{A}L^+ \\ \bar{C}L^+ \end{bmatrix} \\
&= \begin{bmatrix} L_0 & O \\ O & I \end{bmatrix}\begin{bmatrix} A & DH \\ O & S \end{bmatrix}\begin{bmatrix} L_0^+ & O \\ O & I \end{bmatrix} - \begin{bmatrix} J_1 & K_1 \\ J_2 & K_2 \end{bmatrix}\begin{bmatrix} CAL_0^+ & CDH \\ CL_0^+ & O \end{bmatrix} \qquad \text{(A.3.6)} \\
&= \begin{bmatrix} L_0AL_0^+ - J_1CAL_0^+ - K_1CL_0^+ & L_0DH - J_1CDH \\ -J_2CAL_0^+ - K_2CL_0^+ & S - J_2CDH \end{bmatrix}.
\end{aligned}
$$

Noticing that $L_0 = [O, I]$ has a full-row rank and so $L_0^+ = L_0^T$ and matrix

A, B can be partitioned into $\begin{bmatrix} A_1 & A_1 \\ A_3 & A_4 \end{bmatrix}$ and $\begin{bmatrix} B_1 \\ B_2 \end{bmatrix}$, respectively, one can obtain the following matrix equalities:

$$\begin{aligned} &L_0AL_0^+ = A_4,\ CAL_0^+ = A_2, \\ &CL_0^+ = 0,\ L_0B = B_2,\ CB = B_1. \end{aligned} \tag{A.3.7}$$

First consider $G_{u\hat{d}}$. Similar to the proof of Theorem 13, one can obtain the following identity.

$$G_{u\hat{d}} = -H\tilde{C}(sI - F)^{-1}T = \frac{-H\tilde{C}adj(sI - F)T}{det(sI - F)}. \tag{A.3.8}$$

Based on (A.3.7) in conjunction with the definition of F in (A.3.6), the numerator of (A.3.8) is governed by

$$\begin{aligned} &H\tilde{C}adj(sI - F)T \\ &= -\begin{vmatrix} sI - A_4 + J_1A_2 & -L_0DH + J_1CDH & B_2 - J_1B_1 \\ J_2A_2 & sI - S + J_2CDH & -J_2B_1 \\ O & -H & O \end{vmatrix} \\ &= -\begin{vmatrix} sI - A_4 + J_1A_2 & O & B_2 - J_1B_1 \\ J_2A_2 & sI - S & -J_2B_1 \\ O & -H & O \end{vmatrix} \\ &= -\begin{vmatrix} I & -J_1 & O \\ O & -J_2 & -(sI - S) \\ O & O & H \end{vmatrix} \begin{vmatrix} sI - A_4 & O & B_2 \\ -A_2 & O & B_1 \\ O & -I & O \end{vmatrix} \\ &= -\begin{vmatrix} -J_2 & -(sI - S) \\ O & H \end{vmatrix} \begin{vmatrix} O & -A_2 & B_1 \\ O & sI - A_4 & B_2 \\ -I & O & O \end{vmatrix} \\ &= -(-1)^q \begin{vmatrix} -(sI - S) & -J_2 \\ H & O \end{vmatrix} \begin{vmatrix} O & -A_2 & B_1 \\ -A_3 & sI - A_4 & B_2 \\ -I & O & O \end{vmatrix} \\ &= (-1)^{2q} \begin{vmatrix} (sI - S) & J_2 \\ -H & O \end{vmatrix} \begin{vmatrix} sI - A_1 & -A_2 & B_1 \\ -A_3 & sI - A_4 & B_2 \\ -I & O & O \end{vmatrix} \\ &= Hadj(sI - S)J_2Cadj(sI - A)B. \end{aligned} \tag{A.3.9}$$

Secondly, consider $G_{y\hat{d}}$. Similar to the proof of Theorem 13, one can obtain the following identity,

$$\begin{aligned} G_{y\hat{d}} &= H\tilde{C}[(sI - F)^{-1}G + J] \\ &= \frac{H\tilde{C}adj(sI - F)G}{det(sI - F)} + \frac{H\tilde{C}Jdet(sI - F)}{det(sI - F)}, \end{aligned} \tag{A.3.10}$$

the numerator of which is as follows:

$$
\begin{aligned}
&H\tilde{C}adj(sI-F)G + H\tilde{C}Jdet(sI-F) \\
&= \begin{vmatrix} sI-F & G \\ -H\tilde{C} & O \end{vmatrix} + \begin{vmatrix} sI-F & O \\ -H\tilde{C} & H\tilde{C}J \end{vmatrix} = \begin{vmatrix} sI-F & G \\ -H\tilde{C} & H\tilde{C}J \end{vmatrix} \\
&= \begin{vmatrix} sI-F & sJ-FJ+G \\ -H\tilde{C} & O \end{vmatrix} = \begin{vmatrix} sI-F & sJ+K \\ -H\tilde{C} & O \end{vmatrix} \\
&= \begin{vmatrix} sI-A_4+J_1A_2 & -L_0DH+J_1CDH & sJ_1+K_1 \\ J_2A_2 & sI-S+J_2CDH & sJ_2+K_2 \\ O & -H & O \end{vmatrix} \\
&= \begin{vmatrix} sI-A_4+J_1A_2 & O & sJ_1+K_1 \\ J_2A_2 & sI-S & sJ_2+K_2 \\ O & -H & O \end{vmatrix}.
\end{aligned}
\tag{A.3.11}
$$

At this stage, suppose the following identities hold (its proof will be given later):

$$
\begin{cases} K_1 = -J_1A_1 + A_3, \\ K_2 = -J_2A_1. \end{cases}
\tag{A.3.12}
$$

Substituting (A.3.12) into (A.3.11) gives

$$
\begin{aligned}
&H\tilde{C}adj(sI-F)G + H\tilde{C}Jdet(sI-F) \\
&= \begin{vmatrix} sI-A_4+J_1A_2 & O & sJ_1-J_1A_1+A_3 \\ J_2A_2 & sI-S & sJ_2+-J_2A_1 \\ O & -H & O \end{vmatrix} \\
&= \begin{vmatrix} I & O & -J_1 \\ O & sI-S & -J_2 \\ O & -H & O \end{vmatrix} \begin{vmatrix} sI-A_4 & O & A_3 \\ O & I & O \\ -A_2 & O & -sI+A_1 \end{vmatrix} \\
&= \begin{vmatrix} sI-S & -J_2 \\ -H & O \end{vmatrix} \begin{vmatrix} sI-A_4 & A_3 \\ -A_2 & -sI+A_1 \end{vmatrix} \\
&= Hadj(sI-S)J_2det(sI-A).
\end{aligned}
\tag{A.3.13}
$$

Substituting (A.3.9) into (A.3.8), and (A.3.13) into (A.3.10) ends the proof.

Then the proof of (A.3.12) is given, which is based on the Sylvester equation in (6.4.3). From the Sylvester equation, one can obtain

$$
G\bar{C} = W\bar{A} - FW. \tag{A.3.14}
$$

Taking the structure of $\bar{C}$ and W into consideration, (A.3.14) is equivalent to

$$
\begin{aligned}
\begin{bmatrix} G_1 & O & O \\ G_2 & O & O \end{bmatrix} &= \begin{bmatrix} (L_0-J_1C)A & (L_0-J_1C)DH \\ -J_2CA & S-J_2CDH \end{bmatrix} \\
&- \begin{bmatrix} A_4-J_1A_2 & (L_0-J_1C)DH \\ -J_2A_2 & S-J_2CDH \end{bmatrix} \begin{bmatrix} L_0-J_1C & O \\ -J_2C & I \end{bmatrix},
\end{aligned}
$$

based on which in conjunction with $[L_0 - J_1C] = [-J_1, I]$, one can obtain

$$\begin{cases} G_1 = A_3 - A_1J_1 + (A_4 - J_1A_2)J_1 \\ \qquad\quad + (L_0DH - J_1CDH)J_2, \\ G_2 = -J_2A_1 - J_2A_2J_1 + (S - J_2CDH)J_2 \end{cases}$$

From $K = G - FG$, one can obtain

$$\begin{cases} K_1 = G_1 - F_1J_1 - F_2J_2 = A_3 - A_1J_1, \\ K_2 = G_2 - F_3J_1 - F_4J_2 = -J_2A_1. \end{cases}$$

This ends the proof.

A.3.5 Proof of Eq. (6.4.17)

To prove $G_{u\hat{d}}(0) = 1$, one only needs to prove the subtraction of the numerator and denominator of (A.3.8) is zero at $s = 0$, which is given as follows:

From (A.3.9), the denominator minus the numerator is

$$\begin{vmatrix} -A_4 + J_1A_2 & O & B_2 - J_1B_1 \\ J_2A_2 & -S & -J_2B_1 \\ O & -H & O \end{vmatrix} + \begin{vmatrix} -A_4 + J_1A_2 & -L_0DH + J_1CDH & O \\ J_2A_2 & -S + J_2CDH & O \\ O & -H & I \end{vmatrix}$$

$$= \begin{vmatrix} -A_4 + J_1A_2 & O & B_2 - J_1B_1 \\ J_2A_2 & -S & -J_2B_1 \\ O & -H & O \end{vmatrix} + \begin{vmatrix} -A_4 + J_1A_2 & O & -L_0D + J_1CD \\ J_2A_2 & -S & J_2CD \\ O & -H & I \end{vmatrix}.$$

When $D = B$ and consequently $J_2CD = J_2B_1$ and $-L_0D + J_1CD = -B_2 + J_1B_1$, the above equation can be further calculated as

$$\begin{vmatrix} -A_4 + J_1A_2 & O & O \\ J_2A_2 & -S & O \\ O & -H & I \end{vmatrix} = \begin{vmatrix} -A_4 + J_1A_2 & O \\ J_2A_2 & -S \end{vmatrix}$$

$$= det(-A_4 + J_1A_2)det(-S).$$

The proof ends since $det(S) = 0$.

A.4 Appendix for Chapter 7

The meanings of the motor system parameters and its corresponding normal values for simulation study are summarized in Table A.2.

The controller gain matrix is designed as $K_c = [8, 1.3, 0.2, 12.6]$ and $k_\theta = 8$. The observer gain $\bar{K}_{o1}$ for actuator fault diagnosis is based on pole assignment, where the poles are selected as $[-8, -7, -6, -5, -2, -2.2]$. Similarly, the observer gain $\bar{K}_{o2}$ for sensor fault diagnosis is also based on pole assignment with poles $[-8, -7, -6, -5, -2, -2.2, -2.4]$.

Table A.2. The normal values of motor parameters

Notation	Significance	Value
L	Armature inductance	0.046 H
k_e	Back-EMF constant	0.57
R	Armature resistance	1 Ohms
J	Motor inertia	0.093 Kg·m^2
k_T	Motor electrical constant	0.57
k_d	Mechanical dumping constant	0.008

A.5 Appendix for Chapter 8

Table A.3. Parameters of vehicle lateral dynamics.

Notation	Value	Significance
m	1621 kg	vehicle total mass
l_V	1.15 m	distance from CG to front axle
l_H	1.38 m	distance from CG to rear axle
I_z	1975 Kg ·m^2	moment of inertia about the z-axis
$c_{\alpha V}$	57117 N/rad	front axle tire cornering stiffness
$c_{\alpha H}$	81396 N/rad	rear axle tire cornering stiffness

Appendix B

PUBLICATION LIST

B.1 Papers under review or in preparation

1. Dewei Yi, **Jinya Su***, Cunjia Liu, and Wen-Hua Chen (2016). Workload Recognition Using Machine Learning Algorithms. (in preparation)

2. **Jinya Su***, Cunjia Liu, and Wen-Hua Chen (2017). Disturbance Rejection Control for Uncertain Systems Using Saturated Actuator. (submitted to IFAC World Congress, Toulouse, France.)

3. Jean Smith*, **Jinya Su**, Cunjia Liu, Wen-Hua Chen (2016). Gust Alleviation of a small UAV Using Disturbance Observer Based Control with Anti-windup. (under review, Journal of Intelligent & Robotic Systems).

4. **Jinya Su***, Wen-Hua Chen, Further results on "Reduced order disturbance observer for discrete-time linear systems", *submitted to Automatica.*

5. **Jinya Su***, Wen-Hua Chen, "Verification and threshold selection for model-based fault diagnosis systems", *drafted, tentatively submitted to IET Control Theory and Application.*

6. **Jinya Su***, Dewei Yi, Cunjia Liu, Wen-Hua Chen. "Vehicle tracking in consideration of dependent behaviours", *drafted, tentatively submit to IEEE Transactions on Intelligent Transportation System.*

7. **Jinya Su***, Wen-Hua. Chen, "Fault diagnosis system verification and robust threshold selection using reachability analysis", *submitted to IEEE Transactions on Systems, Man and Cybernetics: Systems, under review.*

B.2 Published papers (chronologically)

1. Dewei Yi, **Jinya Su***, Cunjia Liu, Wen-Hua Chen. "A data-driven situation awareness algorithm for vehicle lane change", *19th IEEE Intelligent Transportation Systems Conference (ITSC), Brazil, November 1–4, 2016, accepted.*

2. Fanlin Meng, **Jinya Su**, Cunjia Liu, Wen-Hua Chen. "Dynamic decision making in lane change: game theory with receding horizon", *UKACC International Conference on Control, Belfast, 2016, accepted.*

3. **Jinya Su***, Wen-Hua Chen, Jun Yang. "On relationship between time-domain and frequency-domain disturbance observers and its applications", *ASME Journal of Dynamic Systems, Measurement, and Control*, 2016.

4. **Jinya Su**, Baibing Li*, Wen-Hua Chen, Jun Yang. "Reduced-order disturbance observer design for discrete-time linear stochastic system", *Transaction of the Institute of Measurement and Control*, 38(6), pp. 657–664, 2016.

5. **Jinya Su***, Wen-Hua Chen. "Fault diagnosis for vehicle lateral dynamics with robust threshold" *Proceeding of the 2016 International Conference on Industrial Technology*, Taipei, China, pp. 1777–1782, 2016.

6. **Jinya Su**, Baibing Li*, and Wen-Hua Chen. "On existence, optimality and asymptotic stability of the Kalman filter with partially observed inputs", *Automatica* 53: 149–154, 2015.

7. **Jinya Su**, Baibing Li*, Wen-Hua Chen. "Simultaneous state and input estimation with partial information on the inputs", *System science and control engineering*, 3(1): 445–452, 2015.

8. **Jinya Su***, Baibing Li, and Wen-Hua Chen. "Recursive filter with partial knowledge on inputs and outputs", *International Journal of Automation and Computing* 12(1): 35–42, 2015.

9. **Jinya Su***, Wen-Hua Chen, Baibing Li. "High order disturbance observer design for linear and nonlinear system", *Proceeding of the 2015 IEEE International Conference on Information and Automation*, Lijiang, China, 1893–1898, August 2015.

10. **Jinya Su***, Wen-Hua Chen, and Baibing Li. "Nonlinear State Estimation with Nonlinear Equality Constraints", *Proceedings of the 53th IEEE Control and Decision Conference (CDC)*, Los Angeles, USA, 2014.

11. **Jinya Su***, Wen-Hua Chen, and Baibing Li. "Disturbance observer based fault diagnosis", *Proceeding of IEEE 33rd Chinese Control Conference (CCC), pp. 3024–3029, Nanjing, China, 2014.*

12. Jun Yang, **Jinya Su**, Shihua Li*, and Xinghuo Yu. "High-order mismatched disturbance compensation for motion control systems via a continuous dynamic sliding-mode approach." *IEEE Transactions on Industrial Informatics*, 10 (1): 604–614, 2014.

13. **Jinya Su**, Jun Yang*, and Shihua Li. "Continuous finite-time anti-disturbance control for a class of uncertain nonlinear system." *Transactions of the Institute of Measurement and Control*, 36(3): 300–311, 2014.

14. **Jinya Su***, Baibing Li, and Wen-Hua Chen. "Bayesian recursive filtering with partially observed inputs and missing measurements", *Proceeding of 19th International Conference on Automation and Computing (ICAC)*, pp. 1–6, Brunel, U.K., 2013.

15. Jun Yang, Shihua Li*, **Jinya Su**, and Xinghuo Yu. "Continuous nonsingular terminal sliding mode control for systems with mismatched disturbances", *Automatica* 49(7): 2287–2291, 2013.

16. **Jinya Su**, Jun Yang*, and Shihua Li. "Finite-time disturbance rejection control for robotic manipulators based on sliding mode differentiator", *25th Chinese Control and Decision Conference (CCDC)*, pp. 3844–3849. IEEE, 2013.

BIBLIOGRAPHY

[1] K. Ohishi, M. Nakao, K. Ohnishi, and K. Miyachi, "Microprocessor-controlled dc motor for load-insensitive position servo system," *Industrial Electronics, IEEE Transactions on*, no. 1, pp. 44–49, 1987.

[2] S. Gillijns and B. De Moor, "Unbiased minimum-variance input and state estimation for linear discrete-time systems," *Automatica*, vol. 43, no. 1, pp. 111–116, 2007.

[3] B. Li, "State estimation with partially observed inputs: A unified kalman filtering approach," *Automatica*, vol. 49, no. 3, pp. 816–820, 2013.

[4] K.-S. Kim and K.-H. Rew, "Reduced order disturbance observer for discrete-time linear systems," *Automatica*, vol. 49, no. 4, pp. 968–975, 2013.

[5] R. V. Beard, "Failure accomodation in linear systems through self-reorganization." Ph.D. dissertation, Massachusetts Institute of Technology, 1971.

[6] J. Su, W.-H. Chen, and B. Li, "Disturbance observer based fault diagnosis," in *Control Conference (CCC), 2014 33rd Chinese*. IEEE, 2014, pp. 3024–3029.

[7] ——, "High order disturbance observer design for linear and nonlinear systems," in *Information and Automation, 2015 IEEE International Conference on*. IEEE, 2015, pp. 1893–1898.

[8] J. Su, B. Li, and W.-H. Chen, "On existence, optimality and asymptotic stability of the kalman filter with partially observed inputs," *Automatica*, vol. 53, pp. 149–154, 2015.

[9] J. Su, B. Li, W.-H. Chen, and Y. Jun, "Reduced-order disturbance observer design for discrete-time linear stochastic systems," *Transactions of the Institute of Measurement and Control*, 2016, accepted.

[10] J. Su, W.-H. Chen, and J. Yang, "On relationship between time-domain and frequency-domain disturbance observers and its applications," *Journal of Dynamic Systems, Measurement, and Control*, 2016.

[11] J. Su and W.-H. Chen, "Fault diagnosis for vehicle lateral dynamics with robust threshold," in *17th IEEE International Conference on Industrial Technology*. available online, IEEE, 2016.

[12] V. Venkatasubramanian, R. Rengaswamy, K. Yin, and S. N. Kavuri, "A review of process fault detection and diagnosis: Part i: Quantitative model-based methods," *Computers & chemical engineering*, vol. 27, no. 3, pp. 293–311, 2003.

[13] I. Hwang, S. Kim, Y. Kim, and C. E. Seah, "A survey of fault detection, isolation, and reconfiguration methods," *Control Systems Technology, IEEE Transactions on*, vol. 18, no. 3, pp. 636–653, 2010.

[14] J. Marzat, H. Piet-Lahanier, F. Damongeot, and E. Walter, "Model-based fault diagnosis for aerospace systems: a survey," *Proceedings of the Institution of Mechanical Engineers, Part G: Journal of Aerospace Engineering*, pp. 1329–1360, 2012.

[15] R. Schaefer, "Unmanned aerial vehicle reliability study," *Office of the Secretary of Defense, Washington, DC*, 2003.

[16] Z. Hameed, Y. Hong, Y. Cho, S. Ahn, and C. Song, "Condition monitoring and fault detection of wind turbines and related algorithms: A review," *Renewable and Sustainable energy reviews*, vol. 13, no. 1, pp. 1–39, 2009.

[17] A. Zolghadri, "Advanced model-based fdir techniques for aerospace systems: Today challenges and opportunities," *Progress in Aerospace Sciences*, vol. 53, pp. 18–29, 2012.

[18] N. Laouti, N. Sheibat-Othman, and S. Othman, "Support vector machines for fault detection in wind turbines," *IFAC Proceedings Volumes*, vol. 44, no. 1, pp. 7067–7072, 2011.

[19] S. Mahadevan and S. L. Shah, "Fault detection and diagnosis in process data using one-class support vector machines," *Journal of Process Control*, vol. 19, no. 10, pp. 1627–1639, 2009.

[20] H. L. Jones, "Failure detection in linear systems." Ph.D. dissertation, Massachusetts Institute of Technology, 1973.

[21] J. Chen and R. J. Patton, *Robust model-based fault diagnosis for dynamic systems.* Springer Publishing Company, Incorporated, 2012.

[22] R. Isermann, *Fault-diagnosis systems: an introduction from fault detection to fault tolerance.* Springer Science & Business Media, 2006.

[23] D. G. Luenberger, "Observers for multivariable systems," *Automatic Control, IEEE Transactions on*, vol. 11, no. 2, pp. 190–197, 1966.

[24] M. Zeitz, "The extended luenberger observer for nonlinear systems," *Systems & Control Letters*, vol. 9, no. 2, pp. 149–156, 1987.

[25] A. Xu and Q. Zhang, "Nonlinear system fault diagnosis based on adaptive estimation," *Automatica*, vol. 40, no. 7, pp. 1181–1193, 2004.

[26] X. Zhang, M. M. Polycarpou, and T. Parisini, "Fault diagnosis of a class of nonlinear uncertain systems with lipschitz nonlinearities using adaptive estimation," *Automatica*, vol. 46, no. 2, pp. 290–299, 2010.

[27] H. Hammouri, M. Kinnaert, and E. El Yaagoubi, "Observer-based approach to fault detection and isolation for nonlinear systems," *Automatic Control, IEEE Transactions on*, vol. 44, no. 10, pp. 1879–1884, 1999.

[28] G. Besançon, "High-gain observation with disturbance attenuation and application to robust fault detection," *Automatica*, vol. 39, no. 6, pp. 1095–1102, 2003.

[29] C. Edwards, S. K. Spurgeon, and R. J. Patton, "Sliding mode observers for fault detection and isolation," *Automatica*, vol. 36, no. 4, pp. 541–553, 2000.

[30] C. P. Tan and C. Edwards, "Sliding mode observers for robust detection and reconstruction of actuator and sensor faults," *International Journal of Robust and Nonlinear Control*, vol. 13, no. 5, pp. 443–463, 2003.

[31] R. E. Kalman, "A new approach to linear filtering and prediction problems," *Journal of Fluids Engineering*, vol. 82, no. 1, pp. 35–45, 1960.

[32] C.-T. Chang and J.-W. Chen, "Implementation issues concerning the ekf-based fault diagnosis techniques," *Chemical Engineering Science*, vol. 50, no. 18, pp. 2861–2882, 1995.

[33] S. J. Julier and J. K. Uhlmann, "Unscented filtering and nonlinear estimation," *Proceedings of the IEEE*, vol. 92, no. 3, pp. 401–422, 2004.

[34] C. Andrieu, A. Doucet, S. S. Singh, and V. B. Tadic, "Particle methods for change detection, system identification, and control," *Proceedings of the IEEE*, vol. 92, no. 3, pp. 423–438, 2004.

[35] V. Puig, J. Quevedo, T. Escobet, and S. de las Heras, "Passive robust fault detection approaches using interval models," in *Proceedings of the 15th IFAC world congress, Barcelona, Spain*, vol. 1, 2002, pp. 1–2.

[36] S.-A. Raka and C. Combastel, "Fault detection based on robust adaptive thresholds: A dynamic interval approach," *Annual Reviews in Control*, vol. 37, no. 1, pp. 119–128, 2013.

[37] J. Armengol, L. Travé-Massuyès, J. Vehi, and J. L. de la Rosa, "A survey on interval model simulators and their properties related to fault detection," *Annual reviews in control*, vol. 24, pp. 31–39, 2000.

[38] V. Puig, A. Stancu, T. Escobet, F. Nejjari, J. Quevedo, and R. J. Patton, "Passive robust fault detection using interval observers: Application to the damadics benchmark problem," *Control engineering practice*, vol. 14, no. 6, pp. 621–633, 2006.

[39] V. Puig, J. Saludes, and J. Quevedo, "Worst-case simulation of discrete linear time-invariant interval dynamic systems," *Reliable Computing*, vol. 9, no. 4, pp. 251–290, 2003.

[40] I. Fagarasan, S. Ploix, and S. Gentil, "Causal fault detection and isolation based on a set-membership approach," *Automatica*, vol. 40, no. 12, pp. 2099–2110, 2004.

[41] A. Hashemi and P. Pisu, "Adaptive threshold-based fault detection and isolation for automotive electrical systems," in *Intelligent Control and Automation (WCICA), 2011 9th World Congress on.* IEEE, 2011, pp. 1013–1018.

[42] L. M. Ho, "Application of adaptive thresholds in robust fault detection of an electromechanical single-wheel steering actuator," in *8th IFAC Symposium on Fault Detection, Supervision and Safety of Technical Processes (SAFEPROCESS)*, 2012.

[43] T. Raïssi, G. Videau, and A. Zolghadri, "Interval observer design for consistency checks of nonlinear continuous-time systems," *Automatica*, vol. 46, no. 3, pp. 518–527, 2010.

[44] F. Mazenc and O. Bernard, "Asymptotically stable interval observers for planar systems with complex poles," *Automatic Control, IEEE Transactions on*, vol. 55, no. 2, pp. 523–527, 2010.

[45] C. Combastel, "Stable interval observers in for linear systems with time-varying input bounds," *Automatic Control, IEEE Transactions on*, vol. 58, no. 2, pp. 481–487, 2013.

[46] T. Raissi, D. Efimov, and A. Zolghadri, "Interval state estimation for a class of nonlinear systems," *Automatic Control, IEEE Transactions on*, vol. 57, no. 1, pp. 260–265, 2012.

[47] D. Efimov, T. Raïssi, S. Chebotarev, and A. Zolghadri, "Interval state observer for nonlinear time varying systems," *Automatica*, vol. 49, no. 1, pp. 200–205, 2013.

[48] C. Johnson, "Optimal control of the linear regulator with constant disturbances," *Automatic Control, IEEE Transactions on*, vol. 13, no. 4, pp. 416–421, 1968.

[49] J. Han, "From pid to active disturbance rejection control," *Industrial Electronics, IEEE transactions on*, vol. 56, no. 3, pp. 900–906, 2009.

[50] W.-H. Chen, D. J. Ballance, P. J. Gawthrop, and J. O'Reilly, "A nonlinear disturbance observer for robotic manipulators," *Industrial Electronics, IEEE Transactions on*, vol. 47, no. 4, pp. 932–938, 2000.

[51] S. Li, J. Yang, W.-h. Chen, and X. Chen, *Disturbance observer-based control: methods and applications*. CRC Press, 2014.

[52] E. Schrijver and J. Van Dijk, "Disturbance observers for rigid mechanical systems: equivalence, stability, and design," *Journal of Dynamic Systems, Measurement, and Control*, vol. 124, no. 4, pp. 539–548, 2002.

[53] Y. Choi, K. Yang, W. K. Chung, H. R. Kim, and I. H. Suh, "On the robustness and performance of disturbance observers for second-order systems," *IEEE Transactions on Automatic Control*, vol. 48, no. 2, pp. 315–320, 2003.

[54] L. Guo and S. Cao, *Anti-disturbance control for systems with multiple disturbances*. CRC Press, 2013.

[55] W.-H. Chen, J. Yang, L. Guo, and S. Li, "Disturbance-observer-based control and related methodsan overview," *IEEE Transactions on Industrial Electronics*, vol. 63, no. 2, pp. 1083–1095, 2016.

[56] A. Radke and Z. Gao, "A survey of state and disturbance observers for practitioners," in *American Control Conference, 2006*. IEEE, 2006, pp. 6–pp.

[57] K.-S. Kim, K.-H. Rew, and S. Kim, "Disturbance observer for estimating higher order disturbances in time series expansion," *Automatic Control, IEEE Transactions on*, vol. 55, no. 8, pp. 1905–1911, 2010.

[58] J.-L. Chang, "Applying discrete-time proportional integral observers for state and disturbance estimations," *Automatic Control, IEEE Transactions on*, vol. 51, no. 5, pp. 814–818, 2006.

[59] H. Fang, R. A. De Callafon, and J. Cortés, "Simultaneous input and state estimation for nonlinear systems with applications to flow field estimation," *Automatica*, vol. 49, no. 9, pp. 2805–2812, 2013.

[60] F. J. Bejarano, "Partial unknown input reconstruction for linear systems," *Automatica*, vol. 47, no. 8, pp. 1751–1756, 2011.

[61] Y. Xiong and M. Saif, "Unknown disturbance inputs estimation based on a state functional observer design," *Automatica*, vol. 39, no. 8, pp. 1389–1398, 2003.

[62] W.-H. Chen, "Disturbance observer based control for nonlinear systems," *Mechatronics, IEEE/ASME Transactions on*, vol. 9, no. 4, pp. 706–710, 2004.

[63] C. D. Johnson, "Further study of the linear regulator with disturbances–the case of vector disturbances satisfying a linear differential equation," *Automatic Control, IEEE Transactions on*, vol. 15, no. 2, pp. 222–228, 1970.

[64] L. B. Freidovich and H. K. Khalil, "Performance recovery of feedback-linearization-based designs," *Automatic Control, IEEE Transactions on*, vol. 53, no. 10, pp. 2324–2334, 2008.

[65] R. Clark, "Instrument fault detection," *IEEE Transactions on Aerospace Electronic Systems*, vol. 14, pp. 456–465, 1978.

[66] S. Li, J. Yang, W.-H. Chen, and X. Chen, "Generalized extended state observer based control for systems with mismatched uncertainties," *Industrial Electronics, IEEE Transactions on*, vol. 59, no. 12, pp. 4792–4802, 2012.

[67] P. K. Kitanidis, "Unbiased minimum-variance linear state estimation," *Automatica*, vol. 23, no. 6, pp. 775–778, 1987.

[68] M. Darouach, M. Zasadzinski, and S. J. Xu, "Full-order observers for linear systems with unknown inputs," *IEEE transactions on automatic control*, vol. 39, no. 3, pp. 606–609, 1994.

[69] M. Darouach and M. Zasadzinski, "Unbiased minimum variance estimation for systems with unknown exogenous inputs," *Automatica*, vol. 33, no. 4, pp. 717–719, 1997.

[70] C.-S. Hsieh, "Robust two-stage kalman filters for systems with unknown inputs," *Automatic Control, IEEE Transactions on*, vol. 45, no. 12, pp. 2374–2378, 2000.

[71] Y. Cheng, H. Ye, Y. Wang, and D. Zhou, "Unbiased minimum-variance state estimation for linear systems with unknown input," *Automatica*, vol. 45, no. 2, pp. 485–491, 2009.

[72] H. Fang and R. A. De Callafon, "On the asymptotic stability of minimum-variance unbiased input and state estimation," *Automatica*, vol. 48, no. 12, pp. 3183–3186, 2012.

[73] G. Mann and I. Hwang, "State estimation and fault detection and identification for constrained stochastic linear hybrid systems," *Control Theory & Applications, IET*, vol. 7, no. 1, pp. 1–15, 2013.

[74] D. Simon, *Optimal state estimation: Kalman, H infinity, and nonlinear approaches*. John Wiley & Sons, 2006.

[75] M. Hou and P. Muller, "Design of observers for linear systems with unknown inputs," *Automatic Control, IEEE Transactions on*, vol. 37, no. 6, pp. 871–875, 1992.

[76] M. Corless and J. Tu, "State and input estimation for a class of uncertain systems," *Automatica*, vol. 34, no. 6, pp. 757–764, 1998.

[77] F. J. Bejarano, T. Floquet, W. Perruquetti, and G. Zheng, "Observability and detectability of singular linear systems with unknown inputs," *Automatica*, vol. 49, no. 3, pp. 793–800, 2013.

[78] B. Li, "A non-gaussian kalman filter with application to the estimation of vehicular speed," *Technometrics*, vol. 51, no. 2, pp. 162–172, 2009.

[79] B. D. Anderson and J. B. Moore, *Optimal filtering*. Courier Corporation, 2012.

[80] J. Su, B. Li, and W.-H. Chen, "Bayesian recursive filtering with partially observed inputs and missing measurements," in *Automation and Computing (ICAC), 2013 19th International Conference on*. IEEE, 2013, pp. 1–6.

[81] F. J. Bejarano, L. Fridman, and A. Poznyak, "Unknown input and state estimation for unobservable systems," *SIAM Journal on Control and Optimization*, vol. 48, no. 2, pp. 1155–1178, 2009.

[82] H. Kimura, "Deadbeat function observers for discrete-time linear systems," *SIAM Journal on Control and Optimization*, vol. 16, no. 6, pp. 880–894, 1978.

[83] M. Darouach, "Existence and design of functional observers for linear systems," *Automatic Control, IEEE Transactions on*, vol. 45, no. 5, pp. 940–943, 2000.

[84] T. L. Fernando, L. S. Jennings, and H. M. Trinh, "Generality of functional observer structures," in *Decision and Control and European Control Conference (CDC-ECC), 2011 50th IEEE Conference on.* IEEE, 2011, pp. 4000–4004.

[85] J. L. Crassidis and J. L. Junkins, *Optimal estimation of dynamic systems.* CRC press, 2011.

[86] M. S. Phatak and N. Viswanadham, "Actuator fault detection and isolation in linear systems," 1988.

[87] H. Jingqing, "The" extended state observer" of a class of uncertain systems [j]," *Control and Decision*, vol. 1, 1995.

[88] T. Umeno and Y. Hori, "Robust speed control of dc servomotors using modern two degrees-of-freedom controller design," *Industrial Electronics, IEEE Transactions on*, vol. 38, no. 5, pp. 363–368, 1991.

[89] N. H. Jo, Y. Joo, and H. Shim, "A study of disturbance observers with unknown relative degree of the plant," *Automatica*, vol. 50, no. 6, pp. 1730–1734, 2014.

[90] E. Sariyildiz and K. Ohnishi, "A guide to design disturbance observer," *Journal of Dynamic Systems, Measurement, and Control*, vol. 136, no. 2, p. 021011, 2014.

[91] H. Shim and N. H. Jo, "An almost necessary and sufficient condition for robust stability of closed-loop systems with disturbance observer," *Automatica*, vol. 45, no. 1, pp. 296–299, 2009.

[92] S.-S. Yeh and P.-L. Hsu, "Perfectly matched feedback control and its integrated design for multiaxis motion systems," *ASME Journal of Dynamic Systems, Measurement and Control*, vol. 126, no. 3, pp. 547–557, 2004.

[93] J. Yang, S. Li, J. Su, and X. Yu, "Continuous nonsingular terminal sliding mode control for systems with mismatched disturbances," *Automatica*, vol. 49, no. 7, pp. 2287–2291, 2013.

[94] K. Yamada, S. Komada, M. Ishida, and T. Hori, "Characteristics of servo system using high order disturbance observer," in *Decision and Control, 1996., Proceedings of the 35th IEEE Conference on*, vol. 3. IEEE, 1996, pp. 3252–3257.

[95] R. Miklosovic, A. Radke, and Z. Gao, "Discrete implementation and generalization of the extended state observer," in *American Control Conference, 2006.* IEEE, 2006, pp. 6–pp.

[96] G.-P. Jiang, S.-P. Wang, and W.-Z. Song, "Design of observer with integrators for linear systems with unknown input disturbances," *Electronics Letters*, vol. 36, no. 13, pp. 1168–1169, 2000.

[97] M. Darouach and H. S. Ali, "Optimal unbiased functional filtering in the frequency domain," *Systems Science & Control Engineering: An Open Access Journal*, vol. 2, no. 1, pp. 308–315, 2014.

[98] J. Su, J. Yang, and S. Li, "Continuous finite-time anti-disturbance control for a class of uncertain nonlinear system," *Transactions of the Institute of Measurement and Control*, vol. 36, no. 3, pp. 300–311, 2013.

[99] J. Yang, J. Su, S. Li, and X. Yu, "High-order mismatched disturbance compensation for motion control systems via a continuous dynamic sliding-mode approach," *Industrial Informatics, IEEE Transactions on*, vol. 10, no. 1, pp. 604–614, 2014.

[100] L. Wang, C. T. Freeman, E. Rogers, and D. H. Owens, "Experimentally validated continuous-time repetitive control of non-minimum phase plants with a prescribed degree of stability," *Control Engineering Practice*, vol. 18, no. 10, pp. 1158–1165, 2010.

[101] D. Zhou, X. He, Z. Wang, G.-P. Liu, and Y. Ji, "Leakage fault diagnosis for an internet-based three-tank system: an experimental study," *Control Systems Technology, IEEE Transactions on*, vol. 20, no. 4, pp. 857–870, 2012.

[102] S. Yin, H. Luo, and S. X. Ding, "Real-time implementation of fault-tolerant control systems with performance optimization," *Industrial Electronics, IEEE Transactions on*, vol. 61, no. 5, pp. 2402–2411, 2014.

[103] S. Dey, P. Pisu, and B. Ayalew, "A comparative study of three fault diagnosis schemes for wind turbines," *Control Systems Technology, IEEE Transactions on.*

[104] Z. Gao and S. X. Ding, "Actuator fault robust estimation and fault-tolerant control for a class of nonlinear descriptor systems," *Automatica*, vol. 43, no. 5, pp. 912–920, 2007.

[105] R. Seliger and P. M. Frank, "Fault-diagnosis by disturbance decoupled nonlinear observers," in *Decision and Control, 1991., Proceedings of the 30th IEEE Conference on*. IEEE, 1991, pp. 2248–2253.

[106] C. Keliris, M. M. Polycarpou, and T. Parisini, "A distributed fault detection filtering approach for a class of interconnected continuous-time nonlinear systems," *Automatic Control, IEEE Transactions on*, vol. 58, no. 8, pp. 2032–2047, 2013.

[107] B. Jiang and F. N. Chowdhury, "Fault estimation and accommodation for linear mimo discrete-time systems," *Control Systems Technology, IEEE Transactions on*, vol. 13, no. 3, pp. 493–499, 2005.

[108] Z. Zhang and I. M. Jaimoukha, "On-line fault detection and isolation for linear discrete-time uncertain systems," *Automatica*, vol. 50, no. 2, pp. 513–518, 2014.

[109] V. Puig, J. Quevedo, T. Escobet, F. Nejjari, and S. De Las Heras, "Passive robust fault detection of dynamic processes using interval models," *Control Systems Technology, IEEE Transactions on*, vol. 16, no. 5, pp. 1083–1089, 2008.

[110] R. J. Patton, R. N. Clark, and P. M. Frank, *Issues of fault diagnosis for dynamic systems*. Springer Science & Business Media, 2000.

[111] S. Ding, T. Jeinsch, P. Frank, and E. Ding, "A unified approach to the optimization of fault detection systems," *International journal of adaptive control and signal processing*, vol. 14, no. 7, pp. 725–745, 2000.

[112] M. Zhong, S. X. Ding, J. Lam, and H. Wang, "An lmi approach to design robust fault detection filter for uncertain lti systems," *Automatica*, vol. 39, no. 3, pp. 543–550, 2003.

[113] M. Althoff, "Formal and compositional analysis of power systems using reachable sets," 2014.

[114] S. X. Ding, *Model-based fault diagnosis techniques: design schemes, algorithms, and tools*. Springer Science & Business Media, 2008.

[115] X. Zhang, L. Tang, and J. Decastro, "Robust fault diagnosis of aircraft engines: A nonlinear adaptive estimation-based approach," *Control Systems Technology, IEEE Transactions on*, vol. 21, no. 3, pp. 861–868, 2013.

[116] A. Abdullah and M. Zribi, "Sensor-fault-tolerant control for a class of linear parameter varying systems with practical examples," *Industrial Electronics, IEEE Transactions on*, vol. 60, no. 11, pp. 5239–5251, 2013.

[117] M. Althoff, "Reachability analysis and its application to the safety assessment of autonomous cars," *Technische Universitt Mnchen*, 2010.

[118] M. Althoff, O. Stursberg, and M. Buss, "Reachability analysis of linear systems with uncertain parameters and inputs," in *Decision and Control, 2007 46th IEEE Conference on*. IEEE, 2007, pp. 726–732.

[119] R. Rajamani, *Vehicle dynamics and control*. Springer Science & Business Media, 2011.

[120] S. Varrier, D. Koenig, and J. J. Martinez, "Robust fault detection for uncertain unknown inputs lpv system," *Control Engineering Practice*, vol. 22, pp. 125–134, 2014.

[121] M. El-ghatwary, "Robust fuzzy observer-based fault detection for nonlinear systems," Ph.D. dissertation, Universität Duisburg-Essen, Fakultät für, 2007.

[122] Z. Gao, S. X. Ding, and Y. Ma, "Robust fault estimation approach and its application in vehicle lateral dynamic systems," *Optimal Control Applications and Methods*, vol. 28, no. 3, pp. 143–156, 2007.

[123] M. Althoff, D. Althoff, D. Wollherr, and M. Buss, "Safety verification of autonomous vehicles for coordinated evasive maneuvers," in *Intelligent vehicles symposium (IV), 2010 IEEE*. IEEE, 2010, pp. 1078–1083.

[124] L. Guo and W.-H. Chen, "Disturbance attenuation and rejection for systems with nonlinearity via dobc approach," *International Journal of Robust and Nonlinear Control*, vol. 15, no. 3, pp. 109–125, 2005.

[125] M. Sharifian, R. Rahnavard, and H. Delavari, "Velocity control of dc motor based intelligent methods and optimal integral state feedback controller," *International Journal of Computer theory and engineering*, vol. 1, no. 1, pp. 1793–1801, 2009.